

Distribution Agreement

In presenting this thesis or dissertation as a partial fulfillment of the requirements for an advanced degree from Emory University, I hereby grant to Emory University and its agents the non-exclusive license to archive, make accessible, and display my thesis or dissertation in whole or in part in all forms of media, now or hereafter known, including display on the world wide web. I understand that I may select some access restrictions as part of the online submission of this thesis or dissertation. I retain all ownership rights to the copyright of the thesis or dissertation. I also retain the right to use in future works (such as articles or books) all or part of this thesis or dissertation.

Signature:

Michael A. Christopher

Date

LSD1 Continuously Protects the Differentiated State of Neurons

By

Michael A. Christopher

Doctor of Philosophy

Graduate Division of Biological and Biomedical Sciences
Genetics and Molecular Biology

David Katz, Ph.D.
Advisor

Allan Levey, M.D., Ph.D.
Committee Member

Xiaodong Cheng, Ph.D.
Committee Member

Gary Bassell, Ph.D.
Committee Member

Paula Vertino, Ph.D.
Committee Member

Accepted:

Lisa A. Tedesco, Ph.D.
Dean of the James T. Laney School of Graduate Studies

Date

LSD1 Continuously Protects the Differentiated State of Neurons

By

Michael A. Christopher

B.S., Georgia College and State University, 2011

Advisor: David Katz, Ph.D.

An abstract of

A dissertation submitted to the Faculty of the

James T. Laney School of Graduate Studies of Emory University

in partial fulfillment of the requirements for the degree of

Doctor of Philosophy

in the Graduate Division of Biological and Biomedical Sciences

Genetics and Molecular Biology

2016

ABSTRACT

LSD1 Continuously Protects the Differentiated State of Neurons

by Michael A. Christopher

Epigenetic regulation of transcription is carried out by a plethora of enzymes that read and modify the state of chromatin. One facet of this regulation takes place by the addition and removal of posttranslational modifications on the tails of the histone proteins to which the DNA is wrapped around. One of the many types of modifications is methylation of different lysine residues. Histone methylation can be associated with either active or repressed transcription, and the specificity is determined by which histone, and lysine residue it is found on. These modifications are dynamic and regulated by methyltransferases and demethylases. One of these is lysine specific demethylase 1 (LSD1/KDM1a). LSD1 has primarily been studied in the context of cell fate transitions, and little is known about its role in differentiated cells, specifically neurons of the brain. To investigate the role of LSD1 in differentiated cells types, we inducibly deleted *Lsd1* in adult mice and assayed various tissues for detrimental effects. We find that ubiquitous deletion of *Lsd1* in adult mice results in paralysis accompanied by hippocampal and cortical neurodegeneration. Further, we find that genome-wide transcriptional changes that occur in human dementia take place in mice in the absence of LSD1. These data suggest that deletion of *Lsd1* is sufficient to recapitulate human neurodegeneration in mice. In addition, degenerating neurons lacking LSD1 display ectopic reactivation of stem cell genes. This suggests a new paradigm, where differentiated cells are continuously required to repress transcription of other cell fates and may not be fully committed to the differentiated fate. Finally, the mechanism by which the accumulation of pathological protein aggregates in human dementias leads to neuronal cell death is unknown. We find that LSD1 is mislocalized with cytoplasmic pTau in Alzheimer's Disease and pTDP-43 in Frontotemporal Dementia, suggesting its nuclear function could be compromised. Together with the observation that loss of LSD1 in adult mice is sufficient to cause neurodegeneration, my findings suggest a model of human neurodegeneration where LSD1 nuclear activity is inhibited by its sequestration in the cytoplasm by pathological protein aggregates, leading to neuronal cell death by misregulation LSD1 transcriptional targets.

LSD1 Continuously Protects the Differentiated State of Neurons

By

Michael A. Christopher

B.S., Georgia College and State University, 2011

Advisor: David Katz, Ph.D.

A dissertation submitted to the Faculty of the
James T. Laney School of Graduate Studies of Emory University
in partial fulfillment of the requirements for the degree of
Doctor of Philosophy
in the Graduate Division of Biological and Biomedical Sciences
Genetics and Molecular Biology

2016

ACKNOWLEDGEMENTS

First, I owe Dave the highest and most sincere thank you. By some miracle, he let me rotate in his lab despite all my efforts to dissuade him from doing so. Our first meeting to discuss a potential rotation consisted of me saying absolutely nothing while he spoke of all the wonderful science that was going on in his lab. Why would I do such a thing, you ask? Surely I had a single thought to contribute to the conversation. In fact, my head was swimming with things to say, but during that conversation I had a realization that I was in PRIMETIME now. No longer was I at Georgia College & State University, where I was the big fish in a little pond. No sir, I was in the office of an up and coming scientist on the verge of amazing discoveries. I was so terrified that I did not belong here. So I didn't say anything. What could I possibly add? Ask so dumb question, hell no. But, as luck would have it, Dave let me rotate anyway and the rest is history. Since then, he has been the best mentor I could ask for. He always puts my best interests at the forefront of decisions that affect me and gives me a push when I sitting still. He taught me to think better as a scientist and be a better person in the world, and for that I am forever grateful.

Second, I have to thank Ellen France for not letting me prevent her from mentoring me as well. We met in my undergraduate Genetics course where I promptly tried to get out taking a test. You see, she was returning from pregnancy leave and I thought I could pull a fast one and get out of taking a test I missed with the interim professor while I was sick. She ultimately conceded, but saw something in a punk kid that led her to asking me to try working in her lab. This is where the magic happened. She helped me fall in love with benchwork and figure out what I wanted to do with the rest of my life. Her guidance at such a fragile time was a key moment in my life. I mean, I wanted to go to medical school! I will always look back fondly on those days and marvel at their importance.

My thesis committee has also been a solid rock of support the last four years: Paula Vertino, Allan Levey, Gary Bassell and Xiaodong Cheng. Before my first committee meeting, Dave told me to make sure I “control my committee”, meaning, don't let them suggest a bunch of experiments I don't want to do. What he should have told me is to make sure I control him during my committee meetings!

My committee helped me keep him in check and also provided great advice on experiments and career decisions. It was also wildly entertaining to watch Xiaodong grab his own bag of potato chips for chromatin club!

I managed to beat the odds by meeting and marrying the most wonderful person in the world while completing my degree. Rebekah is my best friend and the anchor of my sanity when everything seems to be crashing down around me. She is not only a scientist herself, but likes to do the fun/stupid/nerdy things I like as well. At the time of this writing, she is in Los Angeles by herself, in a city where she knows no one for six weeks, waiting for me to move there. She did this for me. Only a person that loves you would do such a thing. I am truly the luckiest boy in the world.

I also have the best group of friends both at Emory and elsewhere. Shenanigans abound whenever I'm with these guys, mostly of the inebriated variety, but also ones of heartfelt conversation about the meaning of the universe, discussing what controls are necessary for ChIP, debating whether there is a penis in a picture, risking our lives on white water rapids, and explaining what exactly happens at a Magic tournament. My friends have been an incredible support system and provided some much needed escapism.

Finally, my growing family has helped remember where I came from. My mother and father bought me a telescope when I was like six or so, and my wonder of the universe has never ceased since. They have always given me the encouragement I needed, the patience I sometimes don't deserve, and the cash dollars when things are hairy. Elsewise, I have a sister, stepsister, stepmother, stepfather, brother-in-law and niece that make me laugh and listen to all my stories of life in the big city. But most of all they love me unconditionally, which all I could ever ask for.

TABLE OF CONTENTS

CHAPTER 1: INTRODUCTION	1
1.1 Introduction to epigenetics.....	2
1.2 Epigenetics modifications and their regulators.....	3
1.2.1 DNA Methylation	3
1.2.2 Histone Modifications.....	6
1.2.3 RNAs that regulate chromatin.....	7
1.3 MeCP2 regulates long gene expression in neurons.....	8
1.4 REST colocalizes with protein aggregates in neurodegenerative diseases	11
1.5 FMR1 mRNA induces epigenetic silencing of the locus	15
1.6 A possible role for LSD1 in neurological disease.....	16
Scope of the dissertation	19
1.7 Figures	20
CHAPTER 2: METHODS	22
2.1 Solutions and Buffers.....	23
2.2 Mouse work	24
2.2.1 Mouse lines	24
2.2.2 Mouse genotyping by PCR	25
2.2.3 Tamoxifen injections.....	25
2.2.4 Quantification of <i>Lsd1</i> deletion.....	26
2.2.5 Morris Water Maze	26
2.2.6 Fear Conditioning	27

2.2.7 Mouse Tissue Fixation	27
2.3 Staining	28
2.3.1 Immunofluorescence - Mouse	28
2.3.2 Immunohistochemistry – Mouse	28
2.3.3 Immunohistochemistry - Human	29
2.3.4 Immunofluorescence – Human	30
2.3.5 Quantification of LSD1 Colocalization with pTau and pTDP-43.....	31
2.3.6 TUNEL Assay.....	31
2.4 RNA Sequencing	32
2.4.1 RNA isolation	32
2.4.2 Sequencing library preparation	32
2.4.3 RNA sequencing Analysis	32
2.4.4 Comparison to Human Gene Expression Data.....	33
 CHAPTER 3: LSD1 PROTECTS AGAINST HIPPOCAMPAL AND CORTICAL NEURODEGENERATION.....	
3.1 Abstract.....	37
3.2 Introduction.....	37
3.3 Results.....	39
3.3.1 LSD1 is continuously required to prevent neurodegeneration.....	39
3.3.2 Loss of LSD1 results in learning and memory defects	43
3.3.3 LSD1 inhibits reactivation of stem cell transcription	44
3.3.4 Loss of LSD1 induces common neurodegeneration pathways	45

3.3.5 <i>Lsd1</i> ^{CAGG} gene expression changes correlate with expression changes in AD and FTD cases ..	46
3.3.7 LSD1 is mislocalized in human dementias	49
3.3.8 <i>Lsd1</i> ^{CAGG} mice do not have protein aggregates	50
3.3.9 Increased stem cell gene expression in AD and FTD patients	51
3.4 Discussion	51
3.5 Figures	54
CHAPTER 4: DISCUSSION.....	88
4.1 LSD1 is Neuroprotective	89
4.2 Interaction of LSD1 and pTau	94
4.3 LSD1 Continuously Maintains the Differentiated State of Neurons	99
4.4 Conclusions and Future Directions	102
4.5 Figures	104
REFERENCES	108

List of Tables

Table 2-1	Genotyping Primers	34
Table 2-2	Primary Antibodies	35

List of Figures

Figure 1-1	Chromatin modifications and their associated factors	21
Figure 3-1	Neurodegeneration in <i>Lsd1^{CAGG}</i> mice.	54
Figure 3-2	Absence of spinal cord motor neuron and muscle defects in <i>Lsd1^{CAGG}</i> Mice.	56
Figure 3-3	Neurodegeneration in <i>Lsd1^{CAGG}</i> mice.	58
Figure 3-4	LSD1 expression in adult murine hippocampal and cortical neurons.	60
Figure 3-5	Absence of neurodegeneration in the <i>Lsd1^{CAGG}</i> cerebellum.	62
Figure 3-6	LSD1 is not required for kidney and liver cell viability.	64
Figure 3-7	Loss of LSD1 results in learning and memory deficits.	66
Figure 3-8	<i>Lsd1^{CAGG}</i> mice have learning and memory deficits.	68
Figure 3-9	Differential expression of genes in <i>Lsd1^{CAGG}</i> hippocampus.	70
Figure 3-10	Ectopic activation of stem cell genes in <i>Lsd1^{CAGG}</i> mice.	72
Figure 3-11	Neural stem cell gene expression in <i>Lsd1^{CAGG}</i> mice.	74
Figure 3-12	Loss of LSD1 induces common neurodegeneration pathways.	76
Figure 3-13	Expression changes in <i>Lsd1^{CAGG}</i> mice correlate with those in AD and FTD.	78
Figure 3-14	LSD1 co-localization with pTau and pTDP-43 aggregates in AD and FTD.	80
Figure 3-15	LSD1 mislocalization is specific to AD and FTD.	82
Figure 3-16	Absence of pathological protein aggregates in <i>Lsd1^{CAGG}</i> mice.	84
Figure 3-17	Stem cell gene expression in human dementia.	86
Figure 4-1	Model of LSD1-mediated human neurodegeneration	104
Figure 4-2	New model Waddington's epigenetic landscape	106

CHAPTER 1: INTRODUCTION

Portions of this chapter appear in a review article in preparation:

Christopher and Katz (2016). The epigenetics of neurological disease.

1.1 Introduction to epigenetics

Advances in molecular biology and genomics have allowed researchers to uncover roles for epigenetic regulation in a diversity of biological processes. Epigenetic mechanisms have been discovered for many phenotypes that were previously unexplained by classical genetics. These mechanisms are found in the variety of modifications and states that can occur in chromatin. One of the most studied chromatin modifications is the methylation of DNA at cytosine residues and, as recently discovered, on adenine residues. Methylation of cytosines is correlated with repressed transcription, while methylation on adenines appears to be correlated with active transcription. Histone modifications add another layer of epigenetic control by modifying the three-dimensional structure of the chromatin. DNA is wrapped around a histone octamer to produce the fundamental unit of chromatin, the nucleosome. Nucleosomes can be tightly packaged into condensed heterochromatin that prevents transcription of genes packaged in this manner. They can also be loosened to form euchromatin that allows access of the transcriptional machinery to genes that should be expressed. Regulation of the chromatin state is governed by the pattern of post-translational modifications on histones, primarily methylation and acetylation of lysine and arginine residues. This pattern is established by “writers”, enzymes such as histone methyltransferases and acetyltransferases; removed by “erasers”, histone demethylases and deacetylases; and “readers”, enzymes like chromatin remodelers that recognize certain modifications to manipulate chromatin.

The majority of epigenetic research has focused on its role in cellular transitions and how it allows for the passage of information across cell divisions and through the germline. For example, considerable attention has been paid to the contributions of epigenetic aberrations during oncogenesis. In fact, epigenetic changes have been designated as one of the hallmarks of cancer (Hanahan and Weinberg, 2011). Transgenerational inheritance of phenotypes has also been of interest. These phenotypes arise when an insult or a mutation in an epigenetic pathway

creates heritable epigenetic information that is passed to subsequent generations. In each of these cases, cellular division acts as a vector for the passage of epigenetic information. However, mature neurons no longer undergo mitosis, and thus do not have an inheritance paradigm. This makes the developed nervous system an interesting system to study epigenetic regulation. What epigenetic regulation is required in post mitotic neurons and how is it established and maintained? Are there consequences for misregulation of these processes that manifests in human disease? This chapter will highlight recent stories documenting examples of epigenetic regulators necessary to establish and maintain proper neuron physiology and how they could be the underlying mechanisms of neurological disease.

1.2 Epigenetics modifications and their regulators

1.2.1 DNA Methylation

One layer of gene regulation occurs at the DNA level by methylation of cytosine residues. Cytosine methylation occurs by the addition of a methyl group to the fifth position of the cytosine base (5mC) and is donated by *S*-adenosylmethionine. This reaction is carried out by the DNA methyltransferase enzymes. DNMT3a and DNMT3b can methylate cytosines *de novo*, without the context of other methylated residues (Okano et al., 1999). DNMT1, the maintenance methyltransferase, recognizes palindromic hemimethylated CpG dinucleotides and adds a methyl group to the unmethylated cytosine on the opposite strand (Leonhardt et al., 1992). Through this action of DNMT1, DNA methylation can be inherited through DNA replication and thus a cell division.

However, this paradigm is challenged in the context of a post mitotic neuron. Do neurons require active maintenance of an epigenetic mark thought to play a hereditary role in the absence of cell division? Fan and colleagues provided evidence this is true. The researchers showed that in when both *Dnmt1* and *Dnmt3a* are deleted in excitatory neurons, mice display learning and

memory deficits without neuronal loss (Feng et al., 2010). This phenotype only occurred in double mutant mice, and not in either single mutant. This suggests these enzymes are redundant in adult excitatory neurons and play a role in neuronal processes. Indeed, double mutant mice hippocampi displayed abnormal long term potentiation following stimulation, suggesting the learning deficits are due to neuronal plasticity errors. Expression of genes involved in plasticity was also misregulated in double mutant mice brains. Together, this demonstrates that the DNA methyltransferases play redundant roles in post mitotic neurons by regulating gene expression associated with learning and memory. This is in contrast to the paradigm of cellular differentiation, brings to light a requirement for dynamic epigenetic regulation in a static cell (Feng et al., 2010).

Initially, methylated cytosines in the CpG context were thought to be the only form of DNA methylation, and serve as a form of heritable gene silencing through heterochromatin formation. Cytosine methylation has been extensively studied in the context of CpG islands, genomic regions containing a higher rate of CpG dinucleotides than the rest of the genome. These regions are thought to be evolutionarily conserved, as CpGs are underrepresented in the genome due to spontaneous deamination of methylcytosine into thymine, which is not detected as a mutation by DNA repair pathways (Coulondre et al., 1978). More recently, it has been shown that DNA methylation is much more complicated. 5mC can be oxidized to form 5-hydroxymethylcytosine (5hmC), 5-formylcytosine (5fC), and 5-carboxylcytosine (5caC). This set of reactions is carried out by the ten-eleven translocase (TET) family of enzymes (Ito et al., 2011; Tahiliani et al., 2009). This series of oxidation reactions is part of an active demethylation reaction that does not require cell division to simply dilute 5mC through replication. 5hmC appears to be stable in the genome, and may function to influence chromatin state (Pastor et al., 2011). In the brain, 5hmC occurs exclusively in the CpG context and is enriched in the gene bodies of highly expressed genes (Lister et al., 2013). 5fC and 5caC are found at extremely low

levels in the embryonic stem cell genome (at major satellite repeats), but accumulate in regulatory regions when thymine-DNA glycosylase (TDG) is depleted (Shen et al., 2013). TDG removes the 5caC base to allow for base excision repair enzymes to replace the abasic site with an unmethylated cytosine (He et al., 2011). This suggests there is dynamic demethylation of cytosines occurring in embryonic stem cells at regulatory regions. This could mean that 5fC and 5caC are simply reaction intermediates that can be captured, but are normally found at low levels at specific loci. Currently, their epigenetic role is unclear.

Additionally, cytosine methylation does not occur exclusively in the CpG context. The first single-base pair resolution mapping of DNA methylation found that it also widely occurs in a non CpG context (Lister et al., 2009) (termed 5mCH, where H is an A, T, or C). The highest levels of 5mCH are found in embryonic stem cells, followed by neurons and neural progenitors (Hon et al., 2013; Schultz et al., 2015). This enrichment of 5mCH in these cell types suggests it may have cell type specific roles. Interestingly, the 5mCH found in neurons appears to be gained during development. 5mCH is lost during embryonic stem cell differentiation (Lister et al., 2009), and then reacquired by neurons during neurogenesis (Lister et al., 2013). Furthermore, 5mCH plays a critical role in the specification of neuronal subtypes. Recent work from Ecker, Nathans, and colleagues describes how the DNA methylome predicts current and previous cell type gene expression (Mo et al., 2015). Using the INTACT method for nuclei purification (Deal and Henikoff, 2010), they isolated three different neuron subtypes (excitatory pyramidal neurons, Parvalbumin interneurons and Vasoactive intestinal peptide interneurons) and performed RNA-seq along with MethylC-seq. This allowed for generation of matching transcriptome and DNA methylome datasets from the different neuronal subtypes. They find that gene body 5mCH (which is associated with repressed transcription) is the most correlated pattern of DNA methylation with gene expression across all three neuronal subtypes (compared to 5mCH and 5mCG in promoters, and 5mCG in gene bodies). This suggests that gene body 5mCH is closer linked transcriptional

control than other contexts of DNA methylation in neurons and is part of the epigenetic program that defines neuron subtype specification (Mo et al., 2015). This implies that aberrations to DNA methylation in neurons during development could have dramatic alterations to neuronal behavior and thus organismal phenotypic outcomes. This raises another set of questions: can these outcomes manifest in neurological disease and what are the other players could contribute to these phenotypes?

1.2.2 Histone Modifications

Other factors that could contribute to neurological disease are writers and erasers of histone modifications. Histones are highly conserved set of proteins that assemble in an octamer composed of pairs of H2A, H2B, H3, and H4. This octamer is then wrapped around by DNA forming a nucleosome. The N-terminal tails of histones are less structured than the core of the octamer and are free to interact with DNA or other nucleosomes (Ausio et al., 1989; Whitlock and Simpson, 1977). Because of this, they can be posttranslationally modified without disrupting the structure core structure of the nucleosome. Importantly, these modifications are reversible, allowing for dynamic regulation. This language of histone modifications and their influence on chromatin has been termed the “histone code” (Jenuwein and Allis, 2001). A wide-range of modifications has been described. Phosphorylation appears to result from signal transduction pathways. For example, phosphorylation of serine 10 on histone 3 (H3S10p) is acquired in genes after response to stimulation such as growth factors (Mahadevan et al., 1991), suggesting it is linked to transcriptional activation. Acetylation of lysine residues is thought promote euchromatin formation by reducing the positive charge of lysine side chains, thereby disrupting the electrochemical attraction of the positively charged histones to the negatively charged backbone of the DNA. This can be functionally seen by the disruption of the 30nm fiber (a proposed higher order structure of chromatin) by H4K16 acetylation (Ausio et al., 1989).

Methylation of specific lysine residues influences chromatin depending on the residue that is modified in a more complex manner. One of the most highly studied is H3K4 methylation, which is associated with active transcription. H3K4me is established by the MLL and SET family of enzymes (Dou et al., 2005; Hughes et al., 2004; Lee and Skalnik, 2005; Nakamura et al., 2002). H3K4 can be mono-, di-, or tri-methylated. H3K4me3 is found primarily in the promoters of active genes, H3K4me2 is found in the gene bodies of active genes, and H3K4me1 is found in enhancers that associated with active genes (Greer and Shi, 2012). Mono- and dimethylation of H3K4 are removed by the amine oxidase containing lysine specific demethylase 1 (LSD1), but it is incapable of removing trimethylation. This is accomplished by a set of Jumonji domain (Jmj) containing set of demethylases JARID1 and JARID1b (Seward et al., 2007; Xiang et al., 2007b). H3K9me is established by several methyltransferases, including G9a and SETDB1 (Schultz et al., 2002; Tachibana et al., 2002) . H3K9 is primarily found di- and tri-methylated and is concurrent with DNA methylation in the genome. It has been proposed that they can be inherited together through cell division (Nady et al., 2011; Rothbart et al., 2013). It is erased by the Jmj domain containing JHDM2A (Yamane et al., 2006). H3K27 is primarily found in the form of tri-methylation and is established by EZH2 of the Polycomb repressive complex 2 (PRC2) (Laible et al., 1997) and is erased by the Jmj containing enzymes UTX and JMJD3 (Lee et al., 2007; Xiang et al., 2007a). DNA methylation and H3K27me3 are mutually exclusive in the genome, but the significance of this relationship is unclear (Rose and Klose, 2014). Many other lysine residues of histones are modified via methylation and contribute to epigenetic regulation. These examples highlight the complex interplay between histone methylation and other epigenetic regulators.

1.2.3 RNAs that regulate chromatin

In addition to histone modifications and DNA methylation, there is growing evidence that a further layer of epigenetic regulation exists at the level of RNA-mediated establishment and regulation of chromatin states. The first evidence in mouse that RNA influences chromatin state

is that of the X-inactive-specific-transcript (*Xist*) long-noncoding RNA (Brockdorff et al., 1992; Brown et al., 1992). The transcript is specifically expressed from the inactive X chromosome leading to multiple copies of the transcript coating the chromosome *in cis* (Clemson et al., 1996). The *Xist* transcripts bind to and recruit the heterochromatin-forming Polycomb repressive complex 2 (PRC2) (Zhao et al., 2008) and YY1 protein (Jeon and Lee, 2011). Other long-noncoding RNAs have been shown to regulate chromatin in a similar manner. The HOTAIR transcript serves as a scaffolding molecule between the PRC2 complex and LSD1-CoREST complex (Tsai et al., 2010). Coupling these complexes, there can be a targeted simultaneous removal of active H3K4me by LSD1 and deposition of repressive H3K27me, serving as an epigenetic switch from on to off. Additionally, Piwi-interacting RNAs (piRNAs) are short RNAs that interact with the PIWI family of proteins and are thought to target the complex to transposon sites in the germline in order to facilitate silencing (Weick and Miska, 2014). In all of these cases, a noncoding RNA serves as a trigger or guide for other molecules in the maintenance of the chromatin, adding another layer of complex epigenetic regulation.

Together, these many different facets of epigenetic regulation influence the state of chromatin. Recruitment of various factors to different loci determines whether a permissive euchromatic state exists, allowing for transcription to occur, or whether a repressive state exists that silences expression through the formation of heterochromatin. These states are dynamic, allowing for fine tuning of transcriptional programs that establish different cell fates (Figure 1-1).

1.3 MeCP2 regulates long gene expression in neurons

One protein that could play a role in epigenetic-mediated neurological disease is methyl-CpG-binding protein 2 (MeCP2). It was first identified as a methylated DNA binding protein (Lewis et al., 1992). MeCP2 showed a much higher affinity for oligonucleotides containing methylated cytosines than the previously described MeCP1. While MeCP1 required at least 12 methylated cytosines per oligonucleotide, MeCP2 showed binding capabilities with just a single

methylated cytosine. This robust affinity for methylated cytosine suggested MeCP2 could link DNA cytosine methylation with transcriptional repression by binding methylated DNA and inhibiting transcription (Lewis et al., 1992). It was later shown the transcriptional repressor domain (TRD) of MeCP2 associates with Sin3a, a transcriptional repressor (Hassig et al., 1997; Laherty et al., 1997; Nagy et al., 1997), and histone deacetylases (HDACs), which facilitate chromatin compaction. Transcriptional repression associated with MeCP2 is relieved by treatment the HDAC inhibitor trichostatin A, suggesting recruitment of HDACs to genomic regions containing DNA by MeCP2 is a critical step in MeCP2-mediated repression (Nan et al., 1998).

MeCP2 is expressed in all vertebrates, but has yet to be detected in invertebrates. It is found in a variety of tissues, but most highly expressed in the brain, with levels comparable to histone octamers (Skene et al., 2010). During neurogenesis, its expression starts low then increases until it plateaus at neuronal maturation where it remains highly expressed in neurons, but not glia, throughout the life of organism (Kishi and Macklis, 2004). Interestingly this expression pattern mirrors the acquisition of 5mCH in neurons (Lister et al., 2013). Its genetic locus was shown to contain causative mutations for Rett syndrome (RTT) (Amir et al., 1999), an autism spectrum disorder. The mutations were observed in the methyl binding domain and transcriptional repressor domains of MeCP2, suggesting transcriptional repression by MeCP2 was being inhibited in the patients. RTT primarily affects females, and males with mutations in MeCP2 die within the first two years of life (Schule et al., 2008). Patients display neurodevelopmental degeneration, starting off with normal development, but then quickly declining between 6-18 months of age. These phenotypes follow the expression pattern of MeCP2 being highly expressed after neurogenesis. They also display a characteristic hand clenching, along with intellectual disability and autism spectrum behavior (Hagberg et al., 1983).

Despite this obvious role for MeCP2 in RTT, there was still no clear mechanism as to how MeCP2 dysfunction could lead to RTT. However, recent data suggest that in absence of MeCP2, long genes (>100 kb) in neurons are inappropriately derepressed (Gabel et al., 2015). The authors showed that in brains of RTT patients and in mouse models of RTT, there is a genome-wide length-dependent increase in gene expression. Long genes are normally bound by MeCP2 and have higher levels of 5mCA in their gene bodies, suggesting that MeCP2 binds 5mCA residues to repress transcription. These long genes are associated with neuronal processes, suggesting their expression must be tightly regulated in neurons by MeCP2. Consistent with this model, the authors find that disruption of DNMT3a leads to a length-dependent increase in expression of these genes, presumably through loss of 5mCA. This role for MeCP2 as a regulator of long genes appears to be a neuron-specific phenomenon, as other tissues do not display this misregulation of long gene expression. The authors suggest that MeCP2 tempers the expression of these long genes to prevent their over expression which could disrupt neuronal physiology (Gabel et al., 2015).

Given the pattern of gene body 5mCH in neurons (Lister et al., 2013; Mo et al., 2015) and this role for MeCP2-mediated repression of long genes, a model for RTT emerges. As neurodevelopment takes place, neuronal subtypes are specified and gene body 5mCA is acquired at genes where expression needs to either be repressed or tightly regulated. Normally, this gene body methylation is established by DNMT3a/b and controlled by MeCP2 and associated factors. However, in the absence of MeCP2, this finely tuned regulation is lost and derepression of neuronal genes occurs. Alternatively, a perturbation to DNMT3a/b could lead to aberrant 5mCA and thus MeCP2 binding. In both of these scenarios, there is inappropriate expression can then lead inappropriate transcriptional regulation of neuronal genes occurs, causing neuronal dysfunction which manifests in autism like phenotypes.

1.4 REST colocalizes with protein aggregates in neurodegenerative diseases

Alzheimer's Disease (AD) is the most common form of dementia worldwide, accounting for about 60-70% of cases (Rademakers and Rovelet-Lecrux, 2009). Patients present with memory loss and require years of care following cognitive decline. There is a global reduction in brain mass during the course of the disease, primarily driven by loss of synaptic connectivity and neuronal processes. Neuronal loss does take place, but is mostly confined to excitatory neurons of the entorhinal cortex and CA1 of the hippocampus. Loss of synaptic connectivity has a greater correlation with cognitive decline than neuronal loss, suggesting it may play a greater role in the development of AD (Palop et al., 2006). Improper neural network activity also takes place. Hippocampal hyperactivity has also been observed, which is correlated with reduced hippocampal volume (Putchu et al., 2011; Sperling et al., 2010). Together, the combination of neuronal loss, neuronal hyperactivity and synaptic loss leads to cognitive dysfunction resulting in the dementia phenotype.

During the course of the disease, there is an accumulation of pathological protein aggregates in the brain. Two distinct structures occur: senile plaques containing amyloid beta ($A\beta$) and phosphorylated tau containing neurofibrillary tangles. (Glenner and Wong, 1984; Masters et al., 1985). $A\beta$ plaques are composed of a peptide derived from amyloid precursor protein (APP) (Masters et al., 1985). APP is a constitutively expressed transmembrane protein found in many cell types (Kang et al., 1987). As part of normal neuron physiology, APP is cleaved by a series of secretases, α -secretase, β -secretase (BACE), and γ -secretase (Presenilin 1 and 2) (Esch et al., 1990; Vassar et al., 1999; Wolfe et al., 1999). Different combinations of cleavage result in different peptide products. Of these, cleavage by BACE then by the Presenilins results the 42 amino acid peptide product ($A\beta_{42}$) (Vetrivel et al., 2006). $A\beta_{42}$ has aggregation propensity and forms amyloid plaques. This product occurs normally and takes decades to aggregate. Unsurprisingly, mutations in this processing pathway are associated with familial

forms of AD. In these cases, individuals develop early-onset AD, presumably due to a shift in APP cleavage that produces more A β 42.

Another gene with associations to AD is *ApoE*. ApoE is an apolipoprotein with three major allelic isoforms: ϵ 2, ϵ 3, and ϵ 4. The isoforms arise from single amino acid substitutions. Individuals with the ApoE4 allele have a greater than 90% chance of developing late-onset AD (Corder et al., 1993). This high incidence of AD in individuals with the mutation strongly suggests the ApoE protein has a role in the development of the disease. However, no clear role has been defined yet. Astrocytes appear to be the primary source of ApoE in the brain and the different isoforms display distinct binding capabilities of A β , suggesting it could play a role in clearance of A β aggregation (Huang, 2006). Despite these clear genetic links with AD, identified genetic associations account for only a small fraction of susceptibility to AD (Lambert and Amouyel, 2007). This suggests that other factors contribute to the development of AD.

The microtubule associated protein Tau is the protein most highly implicated in AD that does not have a genetic mutation associated with the disease. Tau is normally found in the dendrites of neurons and facilitates the polymerization of microtubules (Drechsel et al., 1992). During the course of AD, Tau protein becomes hyperphosphorylated and acetylated (Bramblett et al., 1993; Cohen et al., 2011). This results in aggregation of the protein into filamentous neurofibrillary tangles (NFTs). Formation of NFTs is thought to occur secondarily to accumulation of A β , as mutations in APP and Presenilins are sufficient to induce formation of both A β plaques and NFTs (Bertram et al., 2010). NFTs accumulate intracellularly and were originally thought to contribute to the disease by reducing the available pool of Tau to perform its normal function with microtubules, thereby disrupting cytoskeletal physiology (Morris et al., 2011). This view has recently been challenged, by the observation that the pathogenic form accumulates in dendrites and can disrupt synaptic transmission. Although Tau aggregation appears to occur as a consequence of A β aggregation, its presence in demented brains has a

higher correlation with cognitive decline than the presence A β plaques, suggesting Tau burden could be more tightly linked to the pathogenicity of the disease (Arriagada et al., 1992).

Despite our understanding of which molecules aggregate and how it occurs, there is still a gap in understanding of how these aggregates cause neuronal cell death. Numerous models for the connection between protein aggregates and neuronal cell death have been suggested, including neuroinflammation in response to protein aggregates mediated by microglia and the complement cascade (Wisniewski and Wegiel, 1991; Zhang et al., 2013), cell cycle reactivation and DNA replication (Busser et al., 1998) and loss of mitochondria and generation of reactive oxygen species (Lin and Beal, 2006). Additionally, there have been several attempts to identify other agents using genetic approaches, but only loci associated with production of protein aggregates have been found (Baker et al., 2006; Cruts et al., 2006; Lambert and Amouyel, 2007). Because of this, doubts about the amyloid hypothesis have been raised. These doubts are supported by the observation that some healthy elderly individuals have buildups of protein aggregates, but do not show signs of cognitive impairment (Price and Morris, 1999). This suggests that these aggregates are not entirely sufficient to cause neurodegeneration. Thus, finding alternative mechanisms for neurodegeneration in AD is of utmost importance.

The RE-1 silencing transcription factor (REST) was recently shown to be neuroprotective and aberrantly associated with protein aggregates during the course of neurodegenerative diseases, and could thus, possibly be a missing piece in the AD puzzle (Lu et al., 2014). REST, also known as neural restrictive silencing factor (NRSF), is a repressive transcription factor that binds to the canonical RE-1 recognition motif sequence and with the help of a set of co-repressors silences transcription of neuronal genes in non-neuronal lineages (Chong et al., 1995; Schoenherr and Anderson, 1995). This silencing is achieved through the recruitment of HDACs and repressive histone methyltransferases, such as G9a the H3K9 methyltransferase (Roopra et al., 2004). Other corepressors that have been reported to associate with REST include: CoREST,

LDS1, MeCP2, and the C-terminal binding protein (CtBP) (Ballas et al., 2005; Ooi and Wood, 2007). Despite its status as a master negative regulator of the neuronal cell fate, REST is expressed at low levels in neurons, suggesting it may still play a role in adult neurons.

However, its role in adults was largely unexplored. Yankner and colleagues recently showed that REST expression is reactivated in aging human neurons and gains neuroprotective properties by binding to and repressing apoptotic genes (Lu et al., 2014). They also showed that a mouse model of REST mutation develops age-related neurodegeneration, and *C. elegans* mutant for the REST orthologue (*spr-4*) are more susceptible to oxidative stress and A β toxicity, further demonstrating the conserved neuroprotective qualities of REST. Yankner and colleagues also showed that during the course of several age-related neurodegenerative diseases, such as AD, FTD, and dementia with Lewey-bodies (DLB) REST protein is sequestered away from neuronal nuclei into autophagosomes along with protein aggregates that develop during the course of the disease. When REST protein is absent from the nucleus, there is an increase in global H3K9 acetylation levels, suggesting epigenetic derepression occurs in the absence of REST. The degree of sequestration outside of the nucleus correlates with the severity of the cognitive impairment of the patient. These findings suggest that pathological protein aggregates cause the mislocalization of REST, leading to the loss of its neuroprotective properties and normal epigenetic regulation. These findings also demonstrate the necessity of proper epigenetic maintenance of transcriptional repression. In the absence of REST protein, pro-apoptotic REST targets could be inappropriately expressed and lead to neuronal cell death by activating apoptosis pathways. Presumably, in the absence of nuclear REST, other corepressors dependent upon REST for targeting to specific loci are no longer brought to their appropriate targets and fail to maintain proper epigenetic states of these loci. This potentially explains the dramatic phenotypes associated with nuclear REST depletion, as thousands of loci become dysregulated.

1.5 FMR1 mRNA induces epigenetic silencing of the locus

A role for RNA-mediated epigenetic regulation in neurological disease can be found in Fragile X Syndrome (FXS), the most common form of inherited intellectual disability. Patients have characteristic IQ scores below 70 and are commonly on the autism spectrum (Fisch et al., 2002). The disease is named for the appearance of bent X chromosomes on karyotypes of patients. This bend takes place at the Fragile X mental retardation 1 locus (FMR1), the causative gene of the syndrome (Ashley et al., 1993b). The disease is mostly observed in males because they are hemizygous for the gene and are therefore susceptible to mutations in their single allele. The protein encoded by the gene (FMRP) is an RNA binding protein that tightly regulates local translation in neurons by inhibiting translation presynaptically (Ashley et al., 1993a; Hanson and Madison, 2007). However, development of the disease occurs through an epigenetic silencing of the locus and consequential loss of the protein (Coffee et al., 2002; Coffee et al., 1999; Pieretti et al., 1991; Verheij et al., 1993). Patients always have an expansion of a CGG trinucleotide repeat in the 5' UTR of the FMR1 gene adjacent to the promoter that is more than 200 repeats, while individuals with fewer repeats are asymptomatic and considered to have a permutation (Fu et al., 1991). Because the expansion contains a CpG dinucleotide, it was hypothesized that CpG methylation could play a role in the silencing of the locus. Indeed, human embryonic stem cells with >200 CGG repeats express *Fmr1* in the undifferentiated state and lack chromatin modifications associated with silencing at the genetic locus. Like what is observed in FXS embryos, when the cells are cultured under differentiation conditions, there is a down regulation of the transcript, an acquisition of DNA CpG methylation, a loss of H3K9 acetylation, and a gain in H3K9 methylation at the *Fmr1* locus (Eiges et al., 2007). However, the factors that trigger silencing of the *Fmr1* locus are unknown.

Recent work from Jaffary and colleagues suggests that the *Fmr1* mRNA may initiate silencing of the locus (Colak et al., 2014). Human embryonic stem cells (hESC) derived from

FXS patients with a CGG expansion of at least 200 display *Fmr1* expression comparable to undifferentiated control cells, but the transcript is silenced when the hESC are differentiated into neurons. During silencing, H3K4me2 is lost and H3K9me2 is gained at the *Fmr1* locus. During differentiation, knockdown of the FMR1 transcript prevented the acquisition of heterochromatin marks at the locus, suggesting the transcript itself is necessary for the induction of heterochromatic silencing. The authors hypothesized that the CGG repeat in the transcript binds to the DNA to form a heteroduplex. Using chromatin isolation by RNA purification (ChIRP), which uses biotinylated oligonucleotides to immunoprecipitate RNA bound to chromatin, the authors showed that the *Fmr1* transcript binds to the *Fmr1* locus prior to heterochromatic silencing specifically in FXS cell lines. This interaction is most enriched when oligonucleotides are tiled next to the trinucleotide repeat of the transcript and when primer pairs closest to the trinucleotide repeat on the chromosome are used to amplify the precipitated DNA. This suggests the anchor point of the interaction takes place between the repeat regions of the DNA and RNA. Furthermore, the interaction is abolished when treated with RNaseH, which selectively degrades RNA-DNA heteroduplexes. These data suggest that the trinucleotide repeat in the 5'-UTR of the transcript binds to the trinucleotide repeat of the DNA prior to the heterochromatic silencing of the *Fmr1* gene and leads to its silencing (Colak et al., 2014). Future studies will likely focus on uncovering the machinery that responds to this RNA-DNA interaction to silence the locus, and whether abolishing this interaction could be a therapeutic target.

1.6 A possible role for LSD1 in neurological disease

As mentioned earlier, histone methylation is reversible, allowing it to serve as a dynamic regulator of transcription. Histone demethylases are responsible for the removal of histone methylation. One of these, LSD1 specifically demethylates mono- and di-methylation of lysine 4 on histone H3 (H3K4me1/2), but not H3K4me3 (Shi et al., 2004; You et al., 2001), and requires the corepressor Co-REST to demethylate H3K4 in the context of a nucleosome (Lee et al., 2005).

By demethylating H3K4, LSD1 acts as a transcriptional repressor by removing an active modification. Alternatively, when associated with the Androgen Receptor complex, LSD1 has been shown to demethylate H3K9me2 (Metzger et al., 2005), allowing it to also serve as a transcriptional activator by removing a repressive mark. A third specificity has recently been described: a neuronal specific isoform (LSD1n), which contains the additional exon 8a, can specifically demethylate the repressive H4K20me2 (Wang et al., 2015). It is proposed that this isoform demethylates H4K20me2 in neurons in response to stimulation to activate genes involved in neurotransmission.

The most studied role for LSD1 is that of a facilitator of cell fate transitions. This can be seen from knockouts in several organisms and systems. The *C. elegans* mutant for the LSD1 orthologue (*spr-5*) has transgenerational progressive sterility over the course of 30 generations. This sterility is thought to arise from the accumulation of H3K4me2 in spermatogenesis genes causing inappropriate expression of sperm genes in oocytes. This sterility phenotype has also been observed in *Drosophila* mutants for *Lsd1* (Di Stefano et al., 2007), although this occurs in the first generation. Together, these observations suggest that LSD1 functions in the reprogramming of epigenetic information between generations, likely by demethylating histones in oocytes to prevent transmission to the offspring. Because of this, H3K4me2 has been proposed to serve as an epigenetic memory of transcription, and its passage through cell division and the germline can influence gene expression in the daughter cells and zygotes. Thus, LSD1 is necessary for the proper passage of epigenetic cell fate information in *Drosophila* and *C. elegans*.

LSD1 is necessary for proper differentiation of mouse embryonic stem cells (mESCs) (Whyte et al., 2012). LSD1 binds to promoters and enhancers of critical embryonic stem cell genes in (mESCs), but does not actively demethylate the H3K4 methylation associated with these loci. However, when the mESCs are differentiated, LSD1 erases the H3K4 methylation associated with these loci. This is done in complex with the nucleosome remodeling and

deacetylase complex (NuRD complex), which contains HDAC1 and 2, as well as the ATPase remodeler Mi-2 β . When mESCs are differentiated in the presence of an LSD1 inhibitor there is retention of critical stem cell gene expression and the associated H3K4 methylation at their loci. This suggests that LSD1 is responsible for the demethylation of H3K4 methylation at stem cell genes during mESC differentiation, which enables proper repression of the loci (Whyte et al., 2012). As such LSD1 regulates the cell fate transition of mESCs.

Depletion of LSD1 causes phenotypes in mice, as well. *Lsd1* homozygous mutant mice arrest at embryonic day 5.5 and fail to properly elongate the egg cylinder, before being resorbed by embryonic day 7.5 (Wang et al., 2009; Wang et al., 2007). In addition, loss of LSD1 causes a wide range of phenotypes: mice have defects in olfactory receptor choice when deleted in developing telencephalon and circadian rhythm when a critical phosphorylation site is mutated; *in vitro*, researchers observe defects in plasma cell and hematopoietic cell differentiation from *Lsd1* knockdown; *in vivo*, deletion of *Lsd1* in pituitary tissue, hematopoietic stem cells, and trophoblast stem cells leads to differentiation defects, and deletion in the oocyte leads to maternal to zygotic transition failure (Kerenyi et al., 2013; Lyons et al., 2013; Nam et al., 2014; Saleque et al., 2007; Su et al., 2009; Wang et al., 2007; Wasson et al., 2016; Zhu et al., 2014). Therefore, the requirement of LSD1 to facilitate cell fate transitions is highly conserved and critical to many developmental processes.

Despite an understanding of LSD1's role as a facilitator of cell fate transitions, little is known about the requirement for LSD1 in differentiated cell types. Furthermore there has been no indication that LSD1 has a role in neurological disease, though there are a few lines of evidence hinting at a possible connection between LSD1 and neurodegenerative disease. LSD1 has been shown to be neuroprotective against oxygen glucose deprivation in rat cortical neurons, indicating it could be required in differentiated neurons (Dai et al., 2010). Additionally, the REST complex described earlier to be affected in AD (Lu et al., 2014), is a potential interactor with LSD1 in

neurons. LSD1 is commonly found complexed with Co-REST, which is a corepressor of REST. However, in the context of embryonic stem cells, LSD1 appears to be recruited to target genes independently of REST (Adamo et al., 2011). The potential link between neurodegeneration and an epigenetic regulator is also reinforced by the observation of defects in epigenetic silencing in the presence of pTau. Overexpression of mutant human Tau, associated with familial cases of FTD, results in loss of heterochromatin in *Drosophila* and mouse (Frost et al., 2014). Additionally, neurons containing NFTs display significant loss of heterochromatin in human AD and FTD cases (Frost et al., 2014). This suggests that factors that promote heterochromatin formation could be impaired in the presence of NFTs.

Scope of the dissertation

Given this possible connection between LSD1 and neurodegeneration, I have examined the requirement for LSD1 in neurons and looked for evidence of LSD1 dysfunction in human neurodegenerative disorders. In this study I examine the effect of deleting *Lsd1* in adult mice. Ubiquitous deletion of *Lsd1* is sufficient to cause neurodegeneration in mice that recapitulates that observed in human dementia. Thus, LSD1 is neuroprotective and critical to maintaining neurons. In addition to neuronal cell death, I describe how ectopic expression of stem cell genes occurs in adult neurons in the absence of LSD1. This suggests that differentiated cells continuously require repression of stem cell genes and loss this repression is correlated with LSD1-mediated neuronal cell death. I also propose that mislocalization of LSD1 with pathological protein aggregates in the cytoplasm contributes to the neurodegeneration observed in human dementia by sequestering LSD1 outside of the nucleus. Given that loss of LSD1 in adult mice is sufficient to cause neuronal cell death and other associated molecular signatures of the diseases, the loss of LSD1 from human neuronal nuclei is a potential contributor to the etiology of human dementia.

1.7 Figures

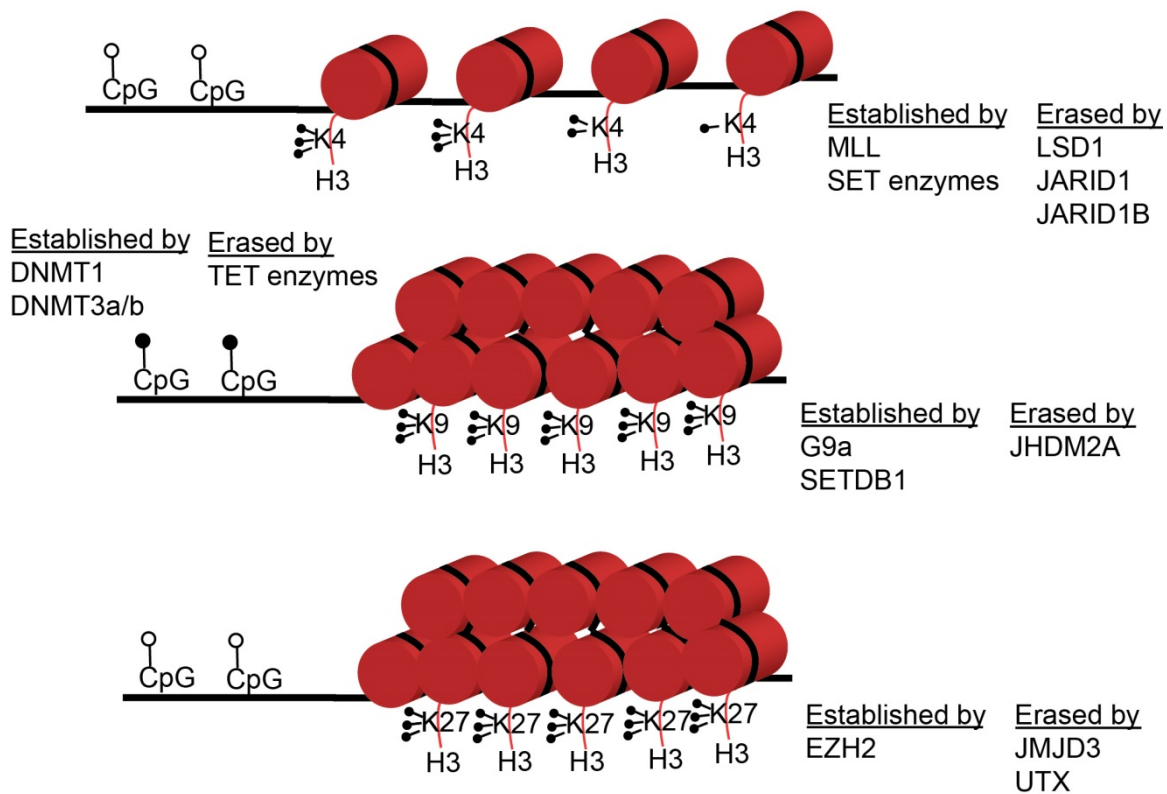


Figure 1-1 | Chromatin modifications and their associated factors

Transcriptionally permissive euchromatin is associated with the absence of DNA methylation (open lollipops) and the presence of H3K4me3/2/1. This mark is established by the MLL and SET family of enzymes and is found in genes actively undergoing transcription. H3K4me3 is found in the promoters, H3K4me2 is found in gene bodies, and H3K4me1 is found in the enhancers of active genes. These marks are erased by demethylases such as LSD1, JARID1 and JARID1b. One type of heterochromatin displays concurrent cytosine methylation (closed lollipops) and H3K9me3. Cytosine methylation is established by the DNA methyltransferases and erased by the TET family of enzymes. H3K9me3 is established by G9a and SETDB1 and erased by JHDM2A. A second type of heterochromatin contains H3K27me3 and no cytosine methylation (open lollipops). H3K27me3 is established by EZH2, part of the Polycomb repressive complex, and is erased by JMJD3 and UTX.

CHAPTER 2: METHODS

2.1 Solutions and Buffers

0.1M Phosphate buffer

0.2M Solution A: NaH_2PO_4 24.0g/L

0.2M Solution B: Na_2HPO_4 28.4g/L

To 1,000mL Solution B, add Solution A slowly to bring pH to 7.3 (about 220mL Solution A).

Dilute 1/2 with diH_2O when needed to make 0.1M

Tail prep buffer

10mL 1M Tris-Cl

20mL 5M NaCl

20mL 0.5M EDTA

50mL 10% SDS

900mL diH_2O

1X TBS

7.88g Tris-Cl

9.0g NaCl

1,000mL diH_2O

H_2O Brij

1,000mL of diH_2O

2.5mL of 30% Brij 35 solution (Sigma)

Tris Brij

100mL 1M Tris-Cl pH 7.5

100mL 1M NaCl

5mL 1M MgCl₂

2.5mL 30% Brij 35

797.5mL diH₂O

Tau secret formula

10mL 1M Tris-Cl pH 7.5

1.5mL 1M NaCl

0.5mL 1M MgCl₂

88mL diH₂O

2.2 Mouse work

2.2.1 Mouse lines

Lsd1^{fl/fl} mice (Wang et al., 2007) were crossed to *CAGG-CreERTM* (Hayashi and McMahon, 2002), a tamoxifen inducible Cre, to generate *CAGG-CreERTM, Lsd1^{fl/+}* mice, which were then intercrossed to produce *CAGG-CreERTM, Lsd1^{fl/fl}* mice. This cross also produced *CAGG-CreERTM* negative animals with *Lsd1^{fl/fl}*, which were used as littermate controls in all experiments. The line was maintained by crossing *CAGG-CreERTM* negative, *Lsd1^{fl/fl}* mice with *CAGG-CreERTM, Lsd1^{fl/fl}* mice.

2.2.2 Mouse genotyping by PCR

At weaning, a 5mm piece of mouse tail was removed with a razor blade and digested overnight in a 50°C water bath with 500µL tail prep buffer and 5µL of 20mg/mL protease K (Ambion). This digest was then phenol/chloroform extracted by adding 500µL phenol/chloroform and vigorously vortexing followed by separation of the aqueous and organic layers by centrifugation (5 minutes). The 250µL of the aqueous (top) layer was extracted, brought back up to 500µL with water, and then re-extracted with 500µL phenol/chloroform. The aqueous layer of the second extraction was recovered (400µL) and DNA was precipitated with ethanol by adding 40µL of 3M sodium acetate and 800µL of ice cold 100% ethanol, followed by inversion. The mixture was then centrifuged at 4°C for 10 minutes to produce a pellet and the supernatant was discarded. The pellet was washed with 150µL of 70% ethanol (room temperature) and centrifuged again for 5 minutes, followed by careful removal of the ethanol and allowed to dry at room temperature for 5 minutes and finally reconstituted with water. This DNA served as the template for genotyping PCR reactions.

For genotyping, each PCR reaction contained 3µL of template DNA diluted either 1/100 (*Cre*) or 1/1000 (*Lsd1*) and 22µL of PCR reaction mix. Each PCR reaction mix contained 2.5 µL 10X AmpliTaq Gold 360 buffer, 0.5 µL 10mM dNTPs, 1.0 µL each primer (50 µM stock, Table 2-1), 35.0 µL 25mM MgCl₂, 0.2 µL AmpliTaq Gold 360 Polymerase and water. The *Lsd1* genotyping reaction yields three possible products: 483bp for wildtype, 751bp for floxed, and 289bp for deleted. The *Cre* genotyping reaction yields a positive control product (250bp) and 320bp product when the *Cre* transgene is present.

2.2.3 Tamoxifen injections

Each mouse was weighed to determine appropriate dosage for 75.0 mg tamoxifen per kilogram of body mass. Tamoxifen for injections was prepared from a 10mg/mL in 100% ethanol stock by vigorously vortexing with 300µL corn oil for 30 seconds followed by 1 minute of centrifugation to separate corn oil and ethanol. The ethanol was evaporated off by vacuum centrifugation at

room temperature for 15 minutes (Pallas lab vacuum centrifuge). Mice were intraperitoneally injected once a day on days 1, 2, 4, 5, and 7 of a seven day period using a one milliliter syringe with a 25 gauge needle.

2.2.4 Quantification of *Lsd1* deletion

Hippocampus, cortex and cerebellum tissues from tamoxifen injected *Lsd1*^{CAGG} mice were collected at 24 hours after the last injection (hippocampus) and the terminal neurodegeneration phenotype (cortex and cerebellum) and genomic DNA was extracted as described in 2.2.2. Intact *Lsd1* alleles were quantified with qPCR on the Bio-Rad CFX96 Real-Time System using the following primers: *Lsd1* forward: 5'-CCAACACTAAAGAGTATCCCAAGAATA-3'; *Lsd1* reverse: 5'-GGTGATTATTATAGGTTTCAGGTGTTTC-3'; *Actb* forward: 5'-AGCCAACCTTTACGCCTAGCGT-3'; *Actb* reverse: 5'-TCTCAAGATGGACCTAATACGGC-3'. The *Lsd1* reverse primer anneals to exon 6 of *Lsd1*, which is deleted in *Lsd1*^{CAGG}. Each reaction contained 7.5μL Bio-Rad iQ Sybr Green Supermix, 1.5μL of 1/100 diluted forward primer, 1.5μL of 1/100 diluted reverse primer, 1μL of 1/20 diluted sample, and water. Starting quantities of intact *Lsd1* alleles were normalized to the amount of *ActB* for each sample to determine the amount of deletion.

2.2.5 Morris Water Maze

A cohort of 15 control and 23 *Lsd1*^{CAGG} mice were tamoxifen injected, and then trained on the Morris water maze 28 days later. Training was carried out in a round, water-filled tub (52 inch diameter). Mice were trained with 4 trials per day for 5 days with a maximum trial length of 60 seconds and a 15 minute intertrial interval. Subjects that did not reach the platform in the allotted time were manually guided to it. Mice were allowed 5 seconds on the platform to survey spatial cues. Following the 5 day training period, probe trials were performed by removing the escape platform and measuring the amount of time spent in the quadrant that originally contained the escape platform over a 60 second trial. All trials were videotaped and performance analysed by

determining the mean values of latency to mount the platform and tracking mice with MazeScan (Clever Sys, Inc.).

2.2.6 Fear Conditioning

Three days after completion of the Morris water maze, the same cohort was subjected to fear conditioning. On Day 1, mice were placed in a fear conditioning apparatus (Colbourn) and allowed to explore for 3 minutes. Following this habituation period, three conditioned stimulus-unconditioned stimulus pairings were presented with a 1 minute intertrial interval. The conditioned stimulus consisted of a 20 second 85db tone and the unconditioned stimulus consisted of a 2 second foot shock that co-terminated with each conditioned stimulus. On Day 2, mice were presented with a context test by placement in Day 1 conditioning apparatus and amount of freezing behavior was recorded by camera and quantified by Colbourn software. On Day 3, subjects were presented with a tone test by exposure to conditioned stimulus in a novel context. Mice were allowed to explore novel context for 2 minutes then presented with the 85db tone for 6 minutes with freezing behavior recorded.

2.2.7 Mouse Tissue Fixation

Mice were given a lethal dose of isoflurane via inhalation (1mL in an isoflurane chamber), then transcardially perfused with ice cold 4.0% paraformaldehyde in 0.1M phosphate buffer. Brain, spinal cord and muscle tissues were dissected and post fixed in cold paraformaldehyde solution for 2 hours. Tissues were then either cryoprotected by sinking in 30% sucrose 0.1M phosphate buffer and frozen embedded in O.C.T. Compound (Tissue Tek), or embedded in paraffin by the Neuropathology and Histopathology core facility at Emory University. For frozen embedding in O.C.T. Compound, tissues were soaked in O.C.T. Compound for 10 minutes, then place in a mold cup with new O.C.T. Compound and placed on a metal heating block surrounded by dry ice inside a covered ice bucket. Once frozen, the tissues were stored at -80°C.

2.3 Staining

2.3.1 Immunofluorescence - Mouse

Frozen mouse brain tissue was sectioned on a cryostat at 12 μ m thickness and washed twice with 1X TBS for 5 minutes, then treated with freshly made 0.8% sodium borohydride for 10 minutes to reduce background. Antigen retrieval was then performed by microwaving at 10% power three times for 5 minutes in 0.01M sodium citrate. Slides were then cooled for 30 minutes and washed once with 1X TBS for 5 minutes, then permeabilized in 0.5% Triton X-100, 1X TBS for 20 minutes, followed by blocking in 10% goat serum, 0.1% Triton X-100, 1X TBS for one hour. Slides were then incubated with primary antibodies (Table 2-2) overnight at 4°C in 2% goat serum, 0.1% Triton X-100, 1X TBS in a humidity chamber. To remove primary antibody, the slides were washed three times for 10 minutes with 1X TBS. Slides were then incubated with fluorescent secondary antibodies (Invitrogen A11001 and Invitrogen A11012) for one hour at room temperature in a humidity chamber then washed three times with 1X TBS, the second wash containing 20 μ L DAPI, then dried by dabbing on a paper towel and coverslipped with Prolong.

2.3.2 Immunohistochemistry – Mouse

Paraffin embedded tissue was sectioned by the Emory Neuropathology and Histopathology core facility. Slides were dewaxed by washing with xylenes for 10 minutes, then 100% ethanol for 30 seconds, then 95% ethanol for 30 seconds twice. For antigen retrieval, slides were microwaved in 0.001M Citrate in a coplin jar within a large plastic container filled with 0.5 inches of diH₂O at 100% power for 5 minutes. The evaporated citrate solution was refilled with water from the plastic container, then microwaved again for 5 minutes at 100% power and allowed to cool on benchtop for 30 minutes. Slides were then paired with a blank slide and inserted into the capillary action slide handle and treated with 3% hydrogen peroxide in H₂O Brij at 40°C for 5 minutes inside a sealed beaker with wet paper towels (humidity beaker) to quench endogenous peroxidase activity, then rinsed three times with H₂O Brij. To block nonspecific staining, slides were

incubated with 2% goat serum in Tris Brij at 40°C for 15 minutes, then drained but not rinsed and applied with primary antibody (Table 2-2) diluted in either “Tau secret formula” (monoclonals) or in 1.0% BSA (polyclonals) and incubated overnight at 4°C in the humidity beaker. Slides were washed three times with Tris Brij and then incubated with biotinylated secondary antibody (Vector Labs BA-1000 and BA-9200) diluted 5µL/mL in 2% goat serum in Tris Brij at 37°C for 30 minutes in the humidity beaker, then rinsed three times with Tris Brij. During this incubation, 50µL of Reagent A and 50µL of Reagent B from Vector Labs Elite ABC reagent (PK-6200) were mixed together with 1.25mL of Tris Brij and incubated on ice for 30 minutes, then brought up to 2.5mL with Tris Brij. Slides were then washed three times with Tris Brij, and then incubated with final ABC reagent solution for 60 minutes at 37°C in the humidity beaker. Slides were then developed with Vector Labs SK-4110 3,3'-diaminobenzidine (DAB) reagent (one drop DAB, one drop H₂O₂, one drop buffer, and 2.5mL H₂O) for 2-5 minutes until medium brown in color, washed once with H₂O Brij, then counterstained with hematoxylin (one part hematoxylin, two parts H₂O Brij) for 1 minute. Finally, slides were washed once with H₂O Brij, twice with Tris Brij, then once with H₂O Brij, dried in the hood overnight and coverslipped with Permount.

2.3.3 Immunohistochemistry - Human

All washes and incubations were done on an orbital rotator in mesh tissue culture cups unless noted otherwise. Frozen free floating sections of 20-50µm thickness, cut by the Emory Neuropathology and Histopathology core facility, were washed five times for 3 minutes with 0.1M phosphate buffer to remove cryoprotectant. Then, sections were treated with 3.0% H₂O₂ for 15 minutes to quench endogenous peroxidase activity, and then washed five times for 3 minutes with 0.1M phosphate buffer, then once with 1X TBS for 3 minutes. Sections were then permeabilized and blocked by incubating in 10µg/mL avidin, 0.1% Triton X-100, and 8% goat serum in 1X TBS for 45 minutes at 4°C, then washed with 1X TBS three times for 3 minutes. Primary antibodies (Table 2-2) were diluted in 50µg/mL, 2% goat serum in 1X TBS and

incubated with tissues overnight at 4°C followed by four washes with 1X TBS for 3 minutes. Sections were then incubated with biotinylated goat secondary antibody (Vector Labs BA-1000 and BA-9200) in 2% goat serum in 1X TBS for one hour at 4°C followed by four 1X TBS washes for 3 minutes. Signal amplification was performed with Vector Labs Elite ABC reagent, which was prepared by mixing two drops of reagent A and two drops of reagent B with 2.5mL 1X TBS then incubated on ice for 30 minutes, then brought up to 5.0mL with 1X TBS prior to treatment of tissue. Sections were incubated with fully prepared ABC reagent for 1 hour at 4°C, then washed four times with 1X TBS. To detect immunoreactivity, sections were then treated with DAB (Sigma prepared by manufacturer's instructions) for 3-4.5 minutes (until medium brown in color) then moved to four 3 minute 1X TBS washes to stop the reaction. Sections were then mounted on slides by floating them in 0.1M sodium nitrate then placing them on slides. Slides were then dried overnight and serially dehydrated by incubating (not rotating) in H₂O for 3 minutes, 70% ethanol for 3 minutes, twice in 95% ethanol for 3 minutes, twice in 100% ethanol for 3 minutes, then three times in xylenes for 3 minutes, and coverslipped with Permount.

For the peptide block control experiment, the LSD1 primary antibody (Table 2-2) was preincubated for 24 hours at 4°C with 74 fold molar excess of target peptide (Abcam 17763).

2.3.4 Immunofluorescence – Human

For immunofluorescence, sections were prepared as with IHC, except that tissue was incubated with two primary antibodies (Table 2-2), and with two secondary antibodies, fluorescent goat anti-mouse (Invitrogen A11001) and biotinylated goat anti-rabbit (Vector Labs BA-1000). Fluorescent signal amplification of the biotinylated secondary was carried out with Vector Labs Elite ABC reagent as with immunohistochemistry, but developed by incubating with PerkinElmer TSA Plus Cyanine 3 System diluted 1:100 in 0.0015% H₂O₂, 1X TBS for 10 minutes at room temperature, then washed twice for 3 minutes in 1X TBS. Sections were then mounted as with immunohistochemistry, then air dried for one hour. Slides were incubated with 1X TBS and 20μL

DAPI for 5 minutes, and then rinsed twice with 1X TBS for 5 minutes, then once with 70% ethanol for 5 minutes. Finally, sections were treated with autofluorescence inhibitor (Millipore 2160) for 5 minutes, then rinsed three times with 70% ethanol for 1 minute and once with 1X TBS for 3 minutes, dabbed on a paper towel to dry, then coverslipped with Prolong.

2.3.5 Quantification of LSD1 Colocalization with pTau and pTDP-43

Three random fields per section that contained NFTs marked by pTau at 20X and pTDP-43 inclusions at 40X were manually examined. Beginning with the pTau/pTDP-43 fluorescence channel, each aggregate structure was visually inspected, and then the microscope was switched to the LSD1 fluorescence channel and inspected for LSD1 signal. Structures were scored as positive for LSD1 colocalization if the LSD1 staining pattern was localized to a majority of the aggregate structure. 535 NFTs and 103 pTDP inclusions were scored.

2.3.6 TUNEL Assay

Frozen embedded brain tissue was sectioned at 12 μ m thickness on a cryostat, and then washed for 30 minutes in PBS. Slides were permeabilized in 0.1% Triton X-100, 0.1% sodium citrate for 2 minutes followed by two 2 minute washes in PBS. For antigen retrieval, slides were microwaved in a coplin jar for 1 minute at 10% power in preboiled 0.1M sodium citrate then rapidly cooled by adding deionized water then pouring off the buffer, repeating this twice. Slides were then washed in PBS for 2 minutes and blocked for 30 minutes at room temperature in 0.1M Tris, 3.0% BSA, 10% goat serum. Slides were washed twice with PBS for 2 minutes then incubated with 50 μ L (5 μ L enzyme and 45 μ L labeling reagent) of TUNEL labelling solution (Roche *In situ* Cell Death Detection Kit, Fluorescein) for 1 hour at 37°C in a humidity chamber. Slides were then washed three times with PBS, the second containing 20 μ L DAPI, then dabbed dry with a paper towel and coverslipped.

2.4 RNA Sequencing

2.4.1 RNA isolation

Mice were anesthetized with a lethal dose of isoflurane, followed by decapitation and hippocampus dissection. Hippocampi were snap frozen with liquid nitrogen in 1mL Trizol and stored at -80°C. For RNA isolation, samples were thawed at 37°C then kept on ice prior to homogenization with a Polytron homogenizer with a 5 second pulse. After a five minute incubation at room temperature, one tenth the sample volume of 1-bromo-3chloropropane was added, mixed by inversion and incubated for 3 minutes at room temperature. Samples were then centrifuged at 13,000 X g for 15 minutes at 4°C to separate the aqueous and organic layers. As much of the aqueous layer was recovered as possible, then RNA was precipitated with isopropanol. Pellets were then washed with 75% ethanol and resuspended in 50µL deionized water.

2.4.2 Sequencing library preparation

RNA library preparation and sequencing were performed by HudsonAlpha Genomic Services Lab. RNA was Poly(A) selected and 300bp size selected. Libraries were sequenced for 25 million 50bp paired end reads. All RNA-seq FastQ files will be uploaded to Gene Expression Omnibus (GEO).

2.4.3 RNA sequencing Analysis

Short read FASTQ files were quality trimmed using FASTX toolkit (v. 0.0.14) to trim three bases from the 5' end of the reads. Paired-end reads were then mapped to the mm9 genome using tophat2 (Kim et al., 2013) and the UCSC knownGene gtf file. The following parameters were used in the tophat2 call “-N 1 -g 1 -read-gap-length 1 -mate-inner-dis 170”. Reads that had the same starting location and strand with mate-pairs that also had the same location and strand were considered to be PCR duplicates and removed from subsequent analyses using Picard tools (v.

1.103). Differentially expressed transcripts were determined using Cufflinks and Cuffdiff (v2.1.1) (Trapnell et al., 2010). Downstream analyses were performed in R/Bioconductor (Gentleman et al., 2004) and used gene summarized expression levels normalized using Fragments Per Kilobase per Million (FPKM) from Cufflinks. Hierarchical clustering was performed using the pvclust R package where significance was determined using bootstrapping (Suzuki and Shimodaira, 2006). Principle Components Analysis (PCA) was conducted using the “prcomp” function of the stats package in R/ Bioconductor. Enriched gene ontologies were determined using the package “GOstats” (v. 3.1.1) (Falcon and Gentleman, 2007). Gene Set Enrichment Analysis (GSEA) was performed using a pre-ranked gene list determined by cuffdiff test statistic and GSEA (v. 2.1.0) (Subramanian et al., 2005). Hierarchical clustering of gene expression data was performed using average clustering in the heatmap.2 package. UCSC-style display of gene expression data were plotted using the “rtracklayer” package (Lawrence et al., 2009) and custom R scripts as previously described (Scharer et al., 2013).

2.4.4 Comparison to Human Gene Expression Data

Normalized gene expression data from late onset Alzheimer’s disease (LOAD) (Zhang et al., 2013), frontal temporal dementia (FTD) (Chen-Plotkin et al., 2008) and Parkinson’s disease (PD) (Zhang et al., 2005) patients were downloaded from Gene Expression Omnibus gene sets GSE44772, GSE13162 and GSE20295, respectively. Comparison to *Lsd1^{CAGG}* gene expression data was performed by mapping mouse and human genes using the NCBI homologue database (Wheeler et al., 2001). Correlation of *Lsd1^{CAGG}* gene expression changes and those found in LOAD, FTD and PD patients were assessed using Spearman’s rank correlation (ρ). *P*-values were determined by analysis of variance (ANOVA).

<i>Lsd1</i>	Forward	5'-GCACCAACACTAAAGAGTATCC-3'
	Reverse	5'-CCACAGAACTTCAAATFACTAAT-3'
<i>Cre</i>	Forward	5'-GAACCTGATGGACATGTTTCAGG-3'
	Reverse	5'-AGTGCGTTTCGAACGCTAGAGCCTGT-3'
<i>Cre</i> Control	Forward	5'-TTACGTCCATCGTGGACAGC-3'
	Reverse	5'-TGGGCTGGGTGTTAGCCTTA-3'

Table 2-1 Genotyping Primers

Mouse genotyping for the *Cre* transgene and floxed allele of *Lsd1* were performed with the listed primers. Lyophilized stocks were reconstituted to 50 μ M. The *Lsd1* Forward and Reverse were mixed together in equal parts and the *Cre* Forward, *Cre* Reverse, *Cre* Control Forward and *Cre* Control Reverse were mixed together in equal parts prior to use in the PCR reaction.

Target	Manufacturer	Experiment	Dilution
NeuN	Millipore MAB377	Mouse IF – Figure 3-4	1:100
LSD1	Abcam 17721	Mouse IF – Figures 3-4, 3-5, 3-6	1:200
		Human IHC – Figure 3-14, and Figure 3-15	1:500
		Human IF – Figure 3-14	1:500
		Mouse IHC – Figure 3-1, and Figure 3-5	1:500
pTau (AT8 epitope)	ThermoFisher MN 1020	Human IHC – Figure 3-14 and Figure 3-15	1:1,000
		Human IF – Figure 3-14	1:1,000
		Mouse IHC – Figure 3-16	1:1,000
pTDP-43	Cosmo Bio TIP-PTD-P02	Human IHC – Figure 3-14	1:1,000
		Mouse IHC – Figure 3-16	1:4,000
pTDP-43	Cosmo Bio TIP-PTD-M01	Human IF – Figure 3-14	1:1,000
α -Synuclein	J. Trojanowski and V. Lee Labs	Human IHC – Figure 3-15	1:10,000
Map2	Chemicon AB5622	Mouse IHC – Figure 3-1	1:500
Tau	Accurate BYA10741	Mouse IHC – Figure 3-1	1:200
GFAP	Dako Z0334	Mouse IHC – Figure 3-1	1:100
SV2	DSHB SV2	Mouse IF – Figure 3-2	1:50
A β	Signet 9220-02	Mouse IHC – Figure 3-16	1:1,000
KLF4	R&D Systems AF3158	Mouse IHC – Figure 3-10	1:100
c-MYC	Santa Cruz SC-40	Mouse IHC – Figure 3-10	1:100
OCT-4	BD Transduction Labs 611202	Mouse IHC – Figure 3-10	1:300
FOXO-1	Santa Cruz SC-11350	Mouse IHC – Figure 3-10	1:100
PCNA	Santa Cruz SC-56	Mouse IHC – Figure 3-12	1:250
H3S10p	Active Motif 39254	Mouse IHC – Figure 3-12	1:1000
NESTIN	Abcam ab11306	Mouse IHC – Figure 3-11	1:1000
VIMENTIN	Dako M072529-2	Mouse IHC – Figure 3-11	1:50
MBP	Millipore MAB386	Mouse IHC – Figure 3-2	1:100

Table 2-2 Primary Antibodies

Primary antibodies for immunohistochemistry and immunofluorescence staining experiments are given. Also listed are the manufacturer and catalog number, experiment and dilution used.

**CHAPTER 3: LSD1 PROTECTS AGAINST HIPPOCAMPAL AND CORTICAL
NEURODEGENERATION**

This manuscript is under review at *Nature Communications*: Michael A. Christopher*, Dexter A. Myrick*, Benjamin G. Barwick, Allan I. Levey and David J. Katz (2016). LSD1 Protects Against Hippocampal and Cortical Neurodegeneration.

*These authors contributed equally.

3.1 Abstract

To investigate the mechanisms that maintain differentiated cells, we inducibly deleted the histone demethylase LSD1/KDM1A throughout adult mice. Loss of LSD1 leads to paralysis, along with widespread hippocampus and cortex neurodegeneration, and learning and memory defects. Here, we focus on the hippocampus neuronal cell death, as well as the potential link between LSD1 and human neurodegenerative disease. We find that loss of LSD1 induces transcription changes in common neurodegeneration pathways, along with the reactivation of stem cell genes, in the degenerating hippocampus. These data implicate LSD1 in the prevention of neurodegeneration via the inhibition of inappropriate transcription. Surprisingly, we also find that transcriptional changes in the hippocampus are similar to Alzheimer's Disease (AD) and Frontotemporal Dementia (FTD) cases, and LSD1 is specifically mislocalized to pathological protein aggregates in these cases. These data raise the possibility that pathological aggregation could compromise the function of LSD1 in AD and FTD.

3.2 Introduction

LSD1/KDM1a (hereafter referred to as LSD1) is an amine oxidase histone demethylase. In conjunction with the CoREST complex, it specifically demethylates mono- and di-methylation of lysine 4 on histone H3 (H3K4me1/2), but not H3K4me3 (Shi et al., 2004; You et al., 2001). Alternatively, when associated with the Androgen Receptor complex, LSD1 has been shown to demethylate H3K9me2 (Metzger et al., 2005). LSD1 homozygous mutant mice arrest at embryonic day 5.5 and fail to properly elongate the egg cylinder, before being resorbed by embryonic day 7.5 (Wang et al., 2009; Wang et al., 2007). In addition, loss of LSD1 results in olfactory receptor choice (Lyons et al., 2013) and circadian rhythm defects (Nam et al., 2014) when conditionally deleted in mice, along with defects in plasma cell (Su et al., 2009) and hematopoietic differentiation (Saleque et al., 2007) *in vitro*, and pituitary (Wang et al., 2007), hematopoietic stem cell (Kerenyi et al., 2013) and trophoblast stem cell (Zhu et al., 2014)

differentiation defects *in vivo*. These defects, along with developmental phenotypes in yeast (Su et al., 2009), *Arabidopsis* (Jiang et al., 2007), *Drosophila* (Di Stefano et al., 2007; Rudolph et al., 2007) and *C. elegans* (Katz et al., 2009), indicate that LSD1 may function during changes in cell fate. For example, in mouse embryonic stem cells (ES cells), LSD1 binds to the promoter and enhancers of critical stem cell genes, *Oct4*, *Sox2*, *Klf4* and *Myc* (Whyte et al., 2012). Upon differentiation, LSD1 is required to remove H3K4me1 to repress the transcription of these stem cell genes and enable proper ES cell differentiation. Similarly, LSD1 has also been implicated in regulating stem cell gene transcription during the differentiation of hematopoietic stem cells (Whyte et al., 2012).

Although LSD1 has many roles throughout development, little is known about its function in differentiated cells. However, one hint comes from studies of the LSD1-containing CoREST complex, which has been suggested to function in the maintenance of cell fate by repressing the transcription of neuronal genes in non-neuronal cell types (Ballas et al., 2001; Chong et al., 1995). Based on this finding, we hypothesized that LSD1 may function similarly in the maintenance of other differentiated cell types. To address this possibility, we conditionally deleted *Lsd1* throughout adult mice. Loss of LSD1 leads to paralysis, along with widespread neuronal cell death in the hippocampus and cortex, and associated learning and memory deficits. Here we have chosen to focus on the function of LSD1 in preventing hippocampus neurodegeneration, and the potential link to human neurodegenerative disease. In the degenerating hippocampus, we detect transcriptional changes in pathways implicated in human neurodegeneration. This suggests that LSD1 may prevent neuronal cell death by repressing common neurodegenerative pathways. In the degenerating neurons, we also detect the inappropriate expression of stem cell genes. This indicates that LSD1 may be part of an epigenetic maintenance program that continuously prevents inappropriate transcription. Surprisingly, we also find that LSD1 mislocalizes with pathological aggregates specifically in Alzheimer's Disease (AD) and Frontotemporal dementia (FTD) cases, and the genome-wide

transcriptional changes in the degenerating *Lsd1* hippocampus specifically correlate with those found in AD and FTD cases. These data raise the possibility that LSD1 function could be affected in these dementias.

3.3 Results

3.3.1 LSD1 is continuously required to prevent neurodegeneration

To determine if LSD1 is required in terminally differentiated cells, we inducibly deleted *Lsd1* in all cells of completely developed adult mice by crossing floxed *Lsd1* mice (Lambrot et al., 2015; Lyons et al., 2013; Macfarlan et al., 2011; Wang et al., 2007; Wasson et al., 2016) to the *Cagg-Cre* tamoxifen inducible *Cre* transgene (Guy et al., 2007; Hayashi and McMahon, 2002; Sangiorgi and Capecchi, 2008; Schulz et al., 2012; Yauch et al., 2008) (hereafter referred to as *Lsd1^{CAGG}*). We do not observe any defects in non-tamoxifen-injected *Cre* positive *Lsd1^{CAGG}* mice, nor in tamoxifen-injected *Cre* minus *Lsd1^{CAGG}* littermate controls (hereafter used as controls in all subsequent experiments). However, all ($n = 45$) tamoxifen-injected *Lsd1^{CAGG}* mice developed a severe motor deficit approximately eight weeks after deletion, characterized initially by weakness in the hindlimbs followed by weakness in the forelimbs. These deficits are associated with hindlimb claspings, failure to maintain body posture, docile behavior, an inability to keep eyes open and ultimately, death (Figure 3-1a-c). Development of this motor defect occurred rapidly, with generally one week elapsing between initial onset and full defect. Importantly, the full motor defect occurred within approximately eight weeks after tamoxifen injection regardless of age at *Lsd1* deletion (Figure 3-1c). This suggests that LSD1 is required throughout adulthood to protect against the development of these deficits. Though both male and females ultimately exhibit the motor defect, the number of days after tamoxifen injection to reach the terminal motor phenotype was longer in males compared to females (Figure 3-1c inset). It is unclear at the moment why there is a small sex specific difference in the timing of this defect.

To investigate this phenotype further, we examined the spinal cords, neuromuscular junctions, muscles, and brains of *Lsd1*^{CAGG} mice. Mutant spinal cords appeared morphologically normal and the number of motor neurons in the spinal cord did not significantly differ from control littermates (Figure 3-2a,b). We also did not detect any defects in the morphology of neuromuscular junctions, or in myelination of the spinal cord (Figure 3-2c-f). Upon examination of limb muscles, we observed severe atrophy in the soleus muscle, as indicated by the much smaller diameter of the muscle cells, and moderate atrophy of the tibialis anterior muscle (Figure 3-2g-j). However, we did not find any evidence of muscle degeneration, suggesting the motor defect is not due to complications in muscles.

Although we do not detect degeneration in the spinal cord or hind limb muscle, we find widespread severe neurodegeneration in the hippocampus and cerebral cortex of *Lsd1*^{CAGG} mice (Figure 3-1d,e). As a result, we have initially focused here on the function of LSD1 in preventing this neurodegeneration. In the future, we plan to further elucidate the role of LSD1 in preventing paralysis. Within the hippocampus, many neuronal nuclei of the CA1, CA3, dentate gyrus, and cerebral cortex were pyknotic, and displayed a corresponding loss of the dendrite marker MAP2, as well as the axon marker Tau (Figure 3-1f-o). Of these hippocampal regions, the CA1 was the most affected with 77.3±5.2% pyknotic nuclei (average with s.e.m.), while the CA2 and CA3 were moderately affected (Figure 3-3a,b). Within individuals, the percent of condensed nuclei in all regions of the hippocampus was higher in the posterior of the brain and less affected anteriorly (Figure 3-3c-f). Between individuals, the dentate gyrus was more variably affected, with the nuclei sometimes being completely pyknotic, completely unaffected, or intermediately affected (Figure 3-1j,k and Figure 3-3g-j). In addition, we consistently observed pyknotic neuronal nuclei in the cerebral cortex, amygdala, thalamus and motor cortex, though the effect in the amygdala and thalamus was less severe than the hippocampus or cortex. (Figure 3-1d,e,l,m and Figure 3-3k-r). Within the cerebral cortex, most of the pyknotic nuclei were typically found in layers II/III, IV and VI (Figure 3-3k,l). Finally, in the cortex of *Lsd1*^{CAGG} mice, and to a lesser extent in the

hippocampus, we observed a strong reactive gliosis response (Figure 3-1p-s), an effect previously associated with neuronal distress (Pekny and Nilsson, 2005). Importantly, it is possible that the neurodegeneration in the motor cortex contributes to the observed paralysis phenotype. However, at the moment it is not possible to determine definitively if this is the case.

To confirm that the pyknotic nuclei in the hippocampus and cortex of *Lsd1*^{CAGG} mice have undergone cell death, we performed TUNEL. Nearly every pyknotic nucleus exhibited positive TUNEL staining, indicating that they were undergoing or had undergone cell death (Figure 3-1t-w). Also, the neuronal cell death was observed at the terminal phenotype regardless of the age of the mice when *Lsd1* was inducibly deleted. Importantly, because we have focused on temporal control of LSD1, rather than cell specificity, we do not yet know whether this requirement for LSD1 is cell autonomous. Nevertheless, these data indicate that LSD1 is continuously required for the survival of hippocampal and cortex neurons.

Since LSD1 is required for the survival of hippocampal and cortex neurons, we verified LSD1 expression in these affected brain regions. Immunofluorescence detected LSD1 protein in the nuclei of NeuN positive neurons throughout the brain, including the hippocampus and cerebral cortex where we observe neurodegeneration (Figure 3-4a-1). In addition, immunohistochemistry verified that LSD1 protein is lost in the degenerating nuclei of *Lsd1*^{CAGG} mice. Specifically, LSD1 was undetectable in most cortical nuclei and nearly all hippocampal nuclei, including all of the pyknotic nuclei in both regions (Figure 3-1x-aa). In contrast, LSD1 was present in many of the remaining normal uncondensed nuclei (Figure 3-1y,aa).

Despite the severe neurodegeneration of the hippocampus and cortex, the cerebellum appeared normal. This can be seen, for example, by the absence of pyknotic nuclei and the normal distribution of the dendrite marker MAP2 (Figure 3-5a-d). To determine whether the lack of neuronal cell death in this region could be due to the failure of *Lsd1* deletion there, we performed quantitative PCR to assess the extent of remaining, undeleted, *Lsd1* in different brain regions. This analysis demonstrated high levels of deletion in the hippocampus and to a lesser

extent in the cerebral cortex. However, there was very little *Lsd1* deletion in the cerebellum (Figure 3-5g). Overall, the extent of deletion matches the level of remaining LSD1 protein in each brain region at the terminal stage, with very little LSD1 in the hippocampus, low levels of LSD1 in the cortex, and higher levels of LSD1 in the cerebellum (Figure 3-1x-aa and Figure 3-5e,f). This distribution suggests that the specificity of the neurodegeneration in *Lsd1*^{CAGG} mice may be due to the specificity of *Lsd1* deletion. Notably, though *Lsd1* deletion in the hippocampus occurred within the first 24 hours after tamoxifen injection (Figure 3-5g), the loss of LSD1 protein in the hippocampus occurred much later. For example, in the hippocampi of mice just beginning to display hindlimb weakness (approximately one week before the terminal phenotype) we observed some remaining LSD1 immunoreactivity and far fewer pyknotic nuclei (Figure 3-5h,i). This indicates that there is slow RNA or protein turnover in hippocampal neurons, a finding that is consistent with the continuous requirement for LSD1 in these cells.

Previous mouse models of neurodegeneration display moderate levels of neuronal loss over an extended period of time (many months) (Oakley et al., 2006; Yoshiyama et al., 2007), so the extent of neuronal cell death that we observed in *Lsd1*^{CAGG} mice within eight weeks was striking. Therefore, we considered the possibility that LSD1 is generally required for cell viability. If this were the case, deletion of *Lsd1* throughout the mouse would be expected to result in a similar disruption in other organs and cell types. To address this possibility, we examined the liver and kidneys of terminal *Lsd1*^{CAGG} mice using dual IF. Hepatocytes and nephron epithelial cells lacking LSD1 appeared morphologically normal (Figure 3-6a-l). Additionally, Purkinje neurons lacking LSD1 in the cerebellum did not display any morphological signs of cell death despite the absence of LSD1 (Figure 3-5e,f). Taken together, these data suggest that LSD1 is not required for general cell viability. This conclusion is consistent with what has been reported in the literature elsewhere (Duteil et al., 2014; Kerenyi et al., 2013; Lyons et al., 2013; Saleque et al., 2007; Wang et al., 2007; Whyte et al., 2012; Zhu et al., 2014). Thus, the continuous requirement

for LSD1 to prevent neuronal cell death in the hippocampus and cortex appears to be specific to these neurons.

3.3.2 Loss of LSD1 results in learning and memory defects

To determine, whether LSD1-dependent neurodegeneration leads to learning and memory deficits, we assessed female *Lsd1*^{CAGG} mice in the Morris water maze and fear conditioning assays, 28 days after tamoxifen injection (prior to the onset of motor defects). Compared to littermate controls, *Lsd1*^{CAGG} mice had significant defects in the latency to mount the platform in the water maze assay on Day 5 (Figure 3-7a). This is despite the fact that *Lsd1*^{CAGG} mice swam at speeds not significantly different than their littermate controls (Figure 3-8a). Also, on Day 5, there is an increase in overall distance traveled as *Lsd1*^{CAGG} mice swim randomly rather than locating the platform (Figure 3-8b). Together these results suggest that the impaired performance of *Lsd1*^{CAGG} mice in the water maze is not due to motor deficits. On Day 6, when the platform was removed, controls spent nearly half of their time swimming in the platform quadrant, while *Lsd1*^{CAGG} mice spent approximately equal time swimming in each of the four quadrants (Figure 3-7b). Thus, these data suggest that *Lsd1*^{CAGG} mice have reduced spatial learning capacity. *Lsd1*^{CAGG} mice were also impaired in contextual fear conditioning, spending less time freezing (30.0±8.3% average with s.e.m.) compared to controls (47.9±4.5% average with s.e.m.) (Figure 3-7c). The contextual fear conditioning was reduced in *Lsd1*^{CAGG} mice at all points, and this reduction was statistically significant at 120,180 and 360 seconds (Figure 3-7c). However, *Lsd1*^{CAGG} mice froze normally in response to a conditioned tone during cued fear conditioning (Figure 3-7d). These data suggest that *Lsd1*^{CAGG} mice have defects in contextual, but not cued, learning and memory. This specificity is consistent with the observed pattern of neuronal cell death in these mice. Importantly, though we do not detect any evidence of visual impairment, it is possible that a slight defect in visual impairment also contributes to the deficit observed in the water maze and contextual fear conditioning assays.

3.3.3 LSD1 inhibits reactivation of stem cell transcription

Previous work has implicated the LSD1 containing CoREST complex in repressing neuronal genes in non-neuronal cell types (Ballas et al., 2001; Chong et al., 1995). This raised the possibility that LSD1 may be functioning similarly in terminally differentiated hippocampal neurons to block the expression of genes associated with alternative cell fates. To test this possibility, we examined hippocampal gene expression changes in terminal *Lsd1*^{CAGG} mice by RNA-seq. At this terminal stage, there was no difference in the number of pyknotic nuclei in *Lsd1*^{CAGG} mutants versus the number of normal nuclei in unaffected controls, indicating that neurons in *Lsd1*^{CAGG} were actively undergoing neuronal cell death, but not yet cleared (Figure 3-9a). Comparison of global gene expression by unsupervised hierarchical clustering and principle components analysis in two *Lsd1*^{CAGG} mutants and two tamoxifen-injected *Cre* minus littermate controls, showed that the expression states were similar between biological replicates, but different between *Lsd1*^{CAGG} mutants and controls (Figure 3-9b,c and Supplementary Data 1). Also, analysis of differentially expressed genes between *Lsd1*^{CAGG} mutant and control hippocampi revealed more significantly upregulated (281) than significantly downregulated (124) genes (Figure 3-9d,e, Supplementary Data 1, FDR < 0.05).

LSD1 has previously been shown to repress the expression of several critical stem cell genes during differentiation in multiple stem cell populations (Saleque et al., 2007; Whyte et al., 2012; Zhu et al., 2014). Therefore, we hypothesized that LSD1 may also be continuously required in terminally differentiated neurons to repress the transcription of stem cell genes to block the re-initiation of a stem cell fate. To address this possibility, we examined the expression of stem cell genes in our *Lsd1*^{CAGG} hippocampus RNA-seq dataset (Supplementary Data 1). Remarkably, three pluripotency genes (*Klf4*, *Myc*, and *Foxo1*), two of which are iPSC factors (Takahashi and Yamanaka, 2006), were amongst the most significantly upregulated genes in *Lsd1*^{CAGG} mice (Figure 3-10a-c and Supplementary Data 1). IHC analysis confirmed that KLF4, c-MYC, and FOXO1 proteins were reactivated specifically in the hippocampal neurons of *Lsd1*^{CAGG} mice, but

not in controls (Figure 3-10e-j). KLF4 and FOXO1 reactivation occurred in the degenerating pyknotic nuclei, as well as in some of the remaining non-condensed nuclei (Figure 3-10e,f,i,j), while c-MYC was reactivated only in the remaining uncondensed nuclei (Figure 3-10g,h). Interestingly, although we did not observe increased *Oct4* expression in our RNA-seq dataset (Figure 3-10d), one out of four mice analyzed displayed reactivation of OCT4 protein specifically in pyknotic hippocampal nuclei (Figure 3-10k,l). This expression pattern appeared to be specific, as it was not observed in any of the controls or in other brain regions of the affected animal. These results suggest that LSD1 is continuously required to repress the inappropriate expression of stem cell genes in hippocampal neurons.

Amongst the most highly activated genes in our RNA-seq dataset we also noticed the upregulation of the neuronal stem cell genes *Vimentin* and *Nestin* (Figure 3-11a,b). To determine whether VIMENTIN and NESTIN may also be reactivated in the dying neurons of *Lsd1^{CAGG}* mice, we performed IHC to detect the expression of these proteins. IHC detected VIMENTIN protein in a subset of hippocampal neurons, though at a higher frequency in *Lsd1^{CAGG}* mice than controls, while NESTIN protein is found in the reactive glia of the *Lsd1^{CAGG}* hippocampus and cortex (Figure 3-11c-h).

3.3.4 Loss of LSD1 induces common neurodegeneration pathways

To identify additional pathways associated with the hippocampal neuronal cell death, we also performed gene ontology (GO) and Gene Set Enrichment Analysis (GSEA) on our RNA-seq datasets. Amongst the pathways that are affected by the loss of LSD1, we observed the upregulation of inflammatory response genes and complement cascade genes, along with the downregulation of oxidative phosphorylation genes and genes involved in neurotransmission (ion transport) (Figure 3-9f,g). All four of these pathways have been previously linked to neurodegeneration. For example, several studies have implicated the inflammatory response pathway in neurodegeneration. Activation of the inflammatory response pathway could contribute

to neurodegeneration via macrophage-mediated phagocytosis (Cameron and Landreth, 2010). There is also evidence linking the complement cascade pathway to neurodegeneration. Activation of the complement cascade pathway could lead to neuronal cell death through axonal pruning (Stephan et al., 2012). In addition, impaired neurotransmission could contribute to neuronal cell death through the loss of electrical potential (Selkoe, 2002). Finally, a defect in oxidative phosphorylation, with the accompanying mitochondrial dysfunction, could lead to neurodegeneration via the generation of reactive oxygen species (Lin and Beal, 2006). To determine the extent that these four neurodegeneration-associated pathways are misregulated in our *Lsd1*^{CAGG} hippocampus RNA-seq, we plotted the enrichment of these gene sets in our dataset for each of these four pathways. This analysis demonstrated that all four of these common neurodegeneration pathways are highly affected (Figure 3-12a-d). Importantly, while each of these pathways has been implicated in neurodegeneration, it is difficult to determine whether these pathways contribute to neuronal cell death, or whether they may simply be a consequence of the neurodegeneration.

3.3.5 *Lsd1*^{CAGG} gene expression changes correlate with expression changes in AD and FTD cases

The common neurodegeneration pathways affected by loss of LSD1 are also affected in human neurodegeneration patients. For example, systems biology approaches in human late onset Alzheimer's Disease (LOAD) brains have identified a critical microglia and immune transcription network upregulated in AD cases (Zhang et al., 2013). Interestingly, we noticed that many genes in the LOAD microglia and immune gene signature, including the critical receptor *Tyrobp*, are highly enriched in the *Lsd1*^{CAGG} hippocampus (Supplementary Data 1). Also, many of these microglia and immune genes are amongst the 281 most significantly upregulated genes in our RNA-seq dataset (Supplementary Data 1). Therefore, to determine if the LOAD microglia and immune response module is similarly misregulated in our mice, we compared the expression

changes in the *Lsd1^{CAGG}* hippocampus to previously published expression changes at orthologous loci in LOAD cases (Zhang et al., 2013). This analysis demonstrated that loss of LSD1 in the mouse hippocampus leads to microglia and immune response gene expression changes that are highly similar to those that occur in the prefrontal cortex of LOAD cases. The microglia and immune expression changes in the *Lsd1^{CAGG}* hippocampus also highly overlap with those that occur in the frontal cortex of FTD cases with progranulin mutations (FTD-progranulin) (Chen-Plotkin et al., 2008) (Figure 3-12e,f).

Surprisingly, a similar correlation with AD and FTD cases is also found with the other neurodegeneration pathways that are misregulated in our RNA-seq dataset. For example, in the Kyoto Encyclopedia of Genes and Genomes (KEGG) complement cascade genes, expression changes in the *Lsd1^{CAGG}* hippocampus highly overlap with the upregulation that occurs in the prefrontal cortex of AD and FTD cases (Figure 3-12g,h). A correlation is observed in pathways that are downregulated in the *Lsd1^{CAGG}* hippocampus as well. For example, we find a large overlap with expression changes in the neurotransmission genes (Synaptic Transmission Module) that were also identified using systems biology approaches in LOAD cases (Figure 3-12k,l) (Zhang et al., 2013). Similarly, we observe a high correlation with the transcriptional changes in oxidative phosphorylation genes (Figure 3-12i,j). Finally, amongst the top upregulated genes in the *Lsd1^{CAGG}* hippocampus we noticed the cell cycle gene *PCNA* (Figure 3-12m, and Supplementary Data 1). Evidence for the potential re-initiation of the cell cycle has been found in AD cases (Busser et al., 1998). Therefore, to determine if *PCNA*, and other cell cycle markers, are being reactivated in degenerating *Lsd1^{CAGG}* neurons, we performed IHC analysis. This analysis confirmed the reactivation of *PCNA* protein, along with that of another cell cycle marker, H3S10p, specifically in the remaining non-pyknotic hippocampal nuclei (Figure 3-12n-q). Intriguingly, the observation that c-MYC, *PCNA* and H3S10p were only reactivated in the remaining uncondensed nuclei of the *Lsd1^{CAGG}* hippocampus raises the possibility that these neurons may be attempting to re-initiate the cell cycle prior to neuronal cell death.

The high degree of overlap within multiple neurodegeneration pathways between *Lsd1*^{CAGG} mice and human dementia cases was unexpected. Thus, we considered the possibility that the expression changes in our mice might overlap more broadly with AD and FTD cases. To address this possibility, we next compared the expression changes in the *Lsd1*^{CAGG} hippocampus with the expression changes in AD and FTD cases genome-wide. Remarkably, we found that the genome-wide expression changes in the prefrontal cortex of LOAD cases highly correlate with the expression changes in the hippocampus of *Lsd1*^{CAGG} mice (Figure 3-13a). Likewise, the correlation was highly significant when compared to the frontal cortex of FTD-progranulin (Figure 3-13b).

The genome-wide correlation in expression changes with AD and FTD cases could indicate the possible involvement of LSD1 in these diseases. However, it is also possible that the overlap is being primarily driven by the consequences of neuronal cell death. To address this second possibility we compared the expression changes in the *Lsd1*^{CAGG} hippocampus with other neurodegenerative diseases that have similar levels of neuronal cell death. If the genome-wide correlation is being driven by a common underlying mechanism, rather than neuronal cell death, we would expect the correlation to be less significant in these comparisons. Importantly, we observe relatively little overlap with the expression changes in the substantia nigra of Parkinson's disease (PD), a region with extensive neuronal cell death (Figure 3-13c) (Zhang et al., 2005). Furthermore, compared to the high degree of correlation that we observe in FTD-progranulin cases, we find a dramatic reduction in the correlation when compared to sporadic FTD cases, despite the fact that these sporadic FTD cases have levels of neuronal cell death that are the same as FTD-progranulin cases (Figure 3-13d). The large decrease in gene expression overlap, that we observe in Parkinson's and sporadic FTD cases, suggests that the genome-wide overlap in expression with AD and FTD cases, is not simply due to neuronal cell death. Finally, we also compared *Lsd1*^{CAGG} hippocampus expression changes to changes in the cerebellum of AD and FTD cases. Compared to the prefrontal cortex, the cerebellum is relatively unaffected in AD and

FTD cases. In both AD and FTD, we find that expression changes in the cerebellum overlap much less than the prefrontal cortex (Figure 3-13e,f). This discrepancy indicates that within AD and FTD cases, the overlap in expression may be driven by the extent of neurodegeneration, rather than brain region.

3.3.7 LSD1 is mislocalized in human dementias

The RNA-seq data suggest that deletion of *Lsd1* alone is sufficient to recapitulate transcriptional changes observed in the affected brain regions of AD and FTD-progranulin cases, including many of the individual gene categories that have previously been implicated in the etiology of these dementias. These data potentially implicate the loss of LSD1 function in these human dementias. As a result, we wondered whether LSD1 might be affected in AD and FTD patients. AD is characterized by protein aggregates of amyloid β ($A\beta$) and Tau, while FTD is associated with aggregates of either Tau or Tar DNA binding protein 43 (TDP-43) (Glennner and Wong, 1984; Masters et al., 1985; Neumann et al., 2006). These pathological aggregates are thought to lead to downstream pathways of neurodegeneration, but it remains unclear mechanistically how these aggregates are linked to neuronal cell death.

To determine if LSD1 may be affected in AD and FTD patients, we examined the localization of LSD1 in post-mortem AD, FTD with TDP-43 inclusions (FTD-TDP43), and age-matched control cases. We also examined the localization of LSD1 in Parkinson's disease (PD) cases, as a disease control with pathological protein aggregates. Similar to the expression in mice, LSD1 immunoreactivity was found in neuronal nuclei throughout the frontal cortex and hippocampus of age-matched control cases (Figure 3-14a,b). In contrast, in all 14 AD cases analyzed, LSD1 was found both in neuronal nuclei as well as inappropriately associated with cytoplasmic tangle-like aggregates and neurites, (Figure 3-14c,d). This pattern is highly reminiscent of the neurofibrillary tangles and neuropil threads marked by pTau in the same AD cases (Figure 3-14c-f). In addition, in all 14 FTD-TDP43 cases analyzed, LSD1 was abnormally

associated with neurites in the frontal cortex, and cytoplasmic inclusions in the hippocampus (Figure 3-14j,k). This pattern is highly similar to the pTDP-43 aggregation observed in FTD-TDP43 cases (Figure 3-14j-m). To confirm the co-localization of LSD1 with pTau and pTDP-43 we performed dual IF. This analysis demonstrated that LSD1 co-localizes with pTau in 56.3% of neurofibrillary tangles in AD ($n = 14$ patients), and with pTDP-43 in 52.4% of neurites in FTD-TDP43 ($n = 5$ patients) (Figure 3-14g-i,n-q). Within AD cases the extent of co-localization ranges from 19%-76%, while in FTD-TDP43 cases, the co-localization ranges from 43%-71%. The finding that LSD1 is localized to pathological aggregates raises the possibility that it could be increasingly sequestered in the cytoplasm. This could result in less LSD1 being available to function in the nucleus of affected neurons in AD and FTD cases.

To confirm the specificity of the LSD1 localization, we performed several controls. Preincubation of the LSD1 Antibody (Ab) with its target LSD1 peptide completely abrogated the immunoreactivity (Figure 3-15a,b). We also did not observe the localization of LSD1 to the amyloid β core of senile plaques in the same AD cases where we observed co-localization with pTau (Figure 3-15c,d). Nor did not observe LSD1 localized to any Lewy body-like structures (aggregates of α -synuclein), or any other abnormal localization of LSD1, in the substantia nigra of PD cases (Figure 3-15e-h). These results suggest the mislocalization of LSD1 to neurofibrillary tangles in AD, and pTDP-43 inclusions in FTD cases, is specific. Notably, the co-localization of proteins with these pathological aggregates is exceedingly rare. For example, though many proteins have been recently described as enriched in the insoluble fraction of AD brains, only one was confirmed to be co-localized with neurofibrillary tangles (Bai et al., 2013).

3.3.8 *Lsd1*^{CAGG} mice do not have protein aggregates

Since LSD1 associates with pathological aggregates in AD and FTD-TDP43 cases, we considered the possibility that the neuronal cell death that we observe in the *Lsd1*^{CAGG} mice could be due to the induction of pathological aggregates in the mice. To test this possibility, we

performed IHC on the brains of terminal *Lsd1*^{CAGG} mice using antibodies to A β , pTau, and pTDP-43, along with Gallyas (silver, nonspecific aggregates) staining (Figure 3-16a-h). We find no evidence of any pathological protein aggregates or tangles associated with the degenerating neurons or otherwise. This suggests that if loss of LSD1 is involved in AD and/or FTD, it is likely downstream of pathological aggregation. This finding is consistent with the mislocalization of LSD1 to pathological aggregates in the human cases (Figure 3-14).

3.3.9 Increased stem cell gene expression in AD and FTD patients

The loss of LSD1 in mice is associated with the surprising reactivation of stem cell transcription in hippocampal neurons. If LSD1 is affected in AD and/or FTD, these diseases could be associated with a similar increase in stem cell gene expression. To test this possibility, we re-examined the expression of stem cell genes in previously published microarray experiments from LOAD and FTD-progranulin post-mortem cases (Chen-Plotkin et al., 2008; Zhang et al., 2013). This analysis revealed a significant increase in the expression of *Klf4*, *Myc*, *Oct4*, *Foxo1*, and *Vimentin* in LOAD cases compared to controls (Figure 3-17a,c,e,g,k), while *PCNA* expression was unchanged (Figure 3-17i). In FTD-progranulin cases there was also a significant increase in the expression of *Klf4* and *Foxo1*, as well as a trend toward the increased expression of *Myc*, *Oct4*, *PCNA* and *Vimentin* (Figure 3-17b,d,f,h,j,l). These data are consistent with the possibility that LSD1 function could be compromised in AD and FTD patients.

3.4 Discussion

Despite its well-known role throughout development, LSD1 protein can also be found in terminally differentiated cells. To determine if there is an ongoing role for LSD1 in terminally differentiated cells, we conditionally deleted *Lsd1* throughout the adult mouse. Loss of LSD1 results in paralysis, along with widespread neuronal cell death in the hippocampus and cortex. In this manuscript, we have focused on this neuronal cell death and the potential connection to AD and FTD.

Loss of LSD1 in mice is sufficient to cause widespread hippocampus and cortex neuronal cell death. However, the absence of LSD1 protein does not appear to affect hepatocytes in the liver, nephron epithelial cells in the kidney, or Purkinje neurons in the cerebellum. These results demonstrate that LSD1 prevents cell death specifically in the hippocampus and cortex of the mouse. To further investigate the neuronal cell death in hippocampus neurons, we examined gene expression changes genome-wide. Previous analyses of human neurodegeneration cases and experimental models have implicated common pathways leading to neuronal cell death. These include; activation of genes in the microglia and immune pathways, a defect in oxidative phosphorylation, loss of synaptic transmission, and failure to maintain cell cycle arrest. Remarkably, the loss of LSD1 affects all of these common neurodegenerative pathways. Therefore, it is possible that the loss of LSD1 creates a perfect storm where multiple neurodegenerative pathways are affected simultaneously, with one or more of these pathways leading to the observed neuronal cell death.

The prevailing view in developmental biology is that cells are irreversibly committed to their differentiated cell fate. Indeed, the very word “fate” promotes the idea that a differentiated cell has reached its final destiny. However, there may be a requirement for differentiated cells to actively maintain their differentiated status. The LSD1-containing CoREST complex has been previously implicated in repressing neuronal genes in non-neuronal cells (Ballas et al., 2001; Chong et al., 1995). Based on this, we considered the possibility that LSD1 could be similarly required to maintain terminally differentiated hippocampus and cortex neurons by repressing gene transcription associated with alternative cell fates. In the degenerating neurons of *Lsd1*^{CAGG} mice, we detect the re-activation of stem cell transcription factors, such as KLF4, OCT4, c-MYC and FOXO1. This demonstrates that LSD1 is continuously required in terminally differentiated neurons to block the re-activation of these factors. Also, we also detect a widespread decrease in the expression of neuronal pathways. This suggests that LSD1 is also required, directly or indirectly, to maintain the expression of these genes. Therefore, we propose that LSD1 is a key

component of an epigenetic maintenance program that reinforces the differentiated state of hippocampal neurons by continuously restraining the re-activation of factors associated with alternative cell fates.

At this moment, it is unclear why the loss of LSD1 results in a severe motor defect. Nevertheless, *Lsd1*^{CAGG} mice develop a motor defect that is similar to AD and FTD mouse models (Jawhar et al., 2012; Yoshiyama et al., 2007). For example the P301S mice, which overexpress an aggregation prone form of human Tau, have a motor defect that is reminiscent of *Lsd1*^{CAGG} mice (Yoshiyama et al., 2007). The concordance of phenotypes between P301S mice and *Lsd1*^{CAGG} mice is consistent with Tau and LSD1 acting in a common pathway. Also consistent with this possibility, we find that that LSD1 inappropriately mislocalizes to cytoplasmic aggregates of pTau in AD, and global gene expression changes in the degenerating *Lsd1*^{CAGG} hippocampus correlate with changes in AD and FTD-progranulin cases. Finally, the re-examination of stem cell genes that are specifically affected by the loss of LSD1 in the mouse hippocampus demonstrates that these genes are also increased in AD and FTD cases. Together these data indicate a potential link between the loss of LSD1 and these human dementia cases. This could occur through the following potential model: as neurons age, the accumulation of protein aggregates sequesters LSD1 in the cytoplasm, and interferes with the continuous requirement for LSD1. Normally, LSD1 maintains terminally differentiated neurons, and prevents the activation of common neurodegenerative pathways, by continuously repressing the transcription of inappropriate genes. As a result, the inhibition of LSD1 by the pathological aggregates in the aging neurons of AD and FTD brains creates a situation where neurons are subject to an onslaught of detrimental processes. This results in neuronal cell death and dementia.

3.5 Figures

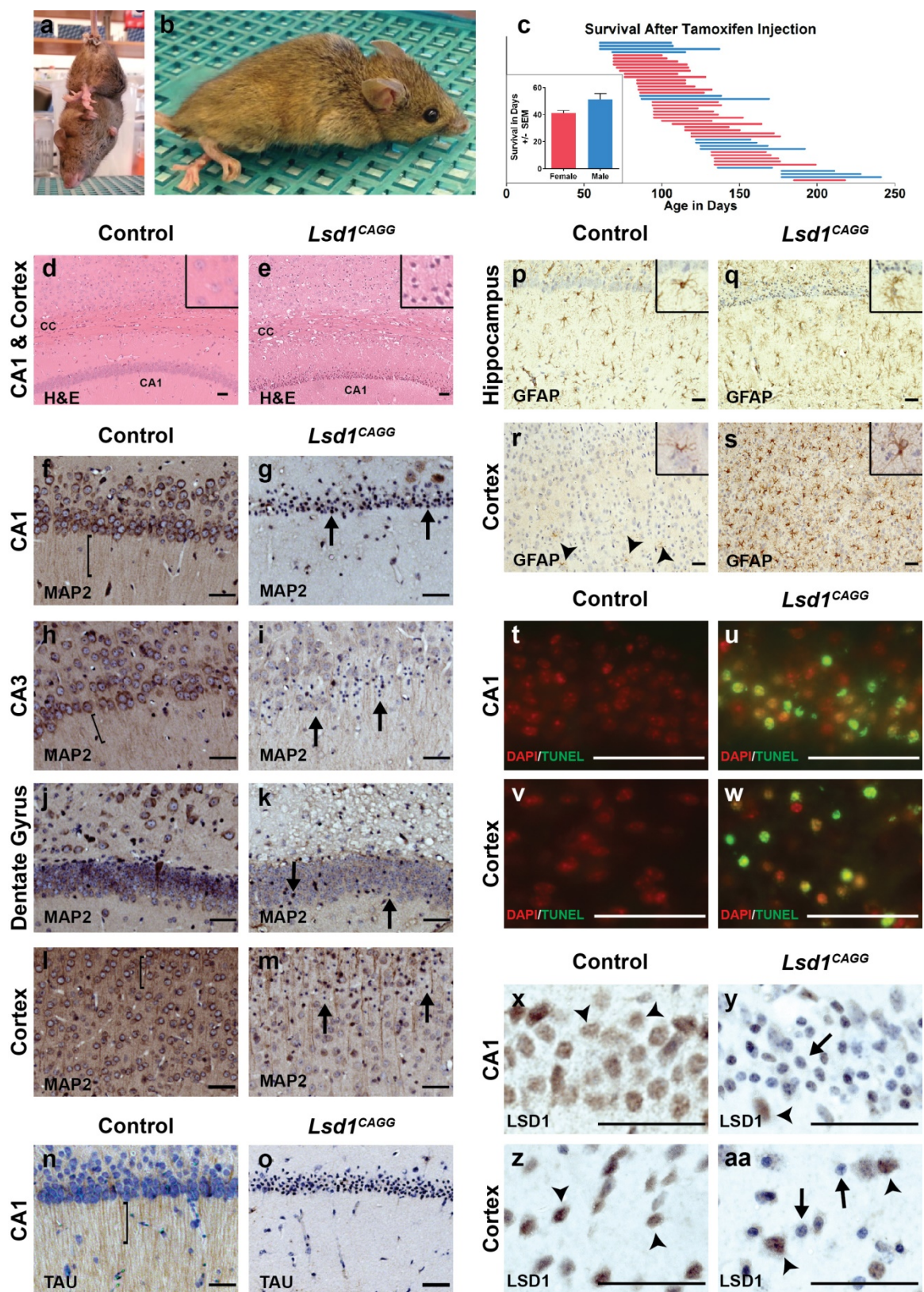


Figure 3-1 | Neurodegeneration in *Lsd1*^{CAGG} mice.

(a,b) Representative images of *Lsd1*^{CAGG} mice with the terminal motor defect including hindlimb clasping (a) and failure to maintain posture (b). (c) The age of each individual male (blue) or female (red) mouse at the final tamoxifen injection (start of the each line) to inducibly delete *Lsd1*, and the number of days (length of the line) until the terminal motor defect is reached. Inset shows survival in days for each sex. Data are shown as mean survival in days \pm s.e.m. (d,e) H&E staining of tamoxifen injected *Cre* minus control (control) (d) and *Lsd1*^{CAGG} (e) CA1 and cortex. Insets are magnified views of non-pyknotic (d) and pyknotic (e) nuclei. CC denotes corpus callosum. (f-m) MAP2 immunohistochemistry (IHC) of control (f, h, j, l) and *Lsd1*^{CAGG} (g, i, k, m) CA1 (f,g), CA3 (h,i), dentate gyrus (j,k) and cortex (l,m). Brackets highlight dendrites and arrows highlight pyknotic nuclei. (n,o) Tau IHC of control (n) and *Lsd1*^{CAGG} (o) CA1. Bracket highlights axons. (p-s) GFAP IHC of control (p,r) and *Lsd1*^{CAGG} (q,s) hippocampus (p,q) and cortex (r,s). Arrowheads highlight sparse astrocytes in control cortex. Insets show magnified view of representative astrocytes. (t-w) Merge of DAPI (red) and TUNEL (green) in control (t,v) and *Lsd1*^{CAGG} (u,w) CA1 (t,u) and cortex (v,w). (x-aa) LSD1 IHC of control (x,z) and *Lsd1*^{CAGG} (y,aa) CA1 (x,y) and cortex (z,aa). Arrowheads highlight non-pyknotic LSD1 immunoreactive nuclei. Arrows highlight pyknotic LSD1 negative nuclei. All IHC (f-o,p-s,x-aa) is counterstained with hematoxylin. All *Lsd1*^{CAGG} images are taken at the terminal phenotype. Scale bars= 50 μ m.

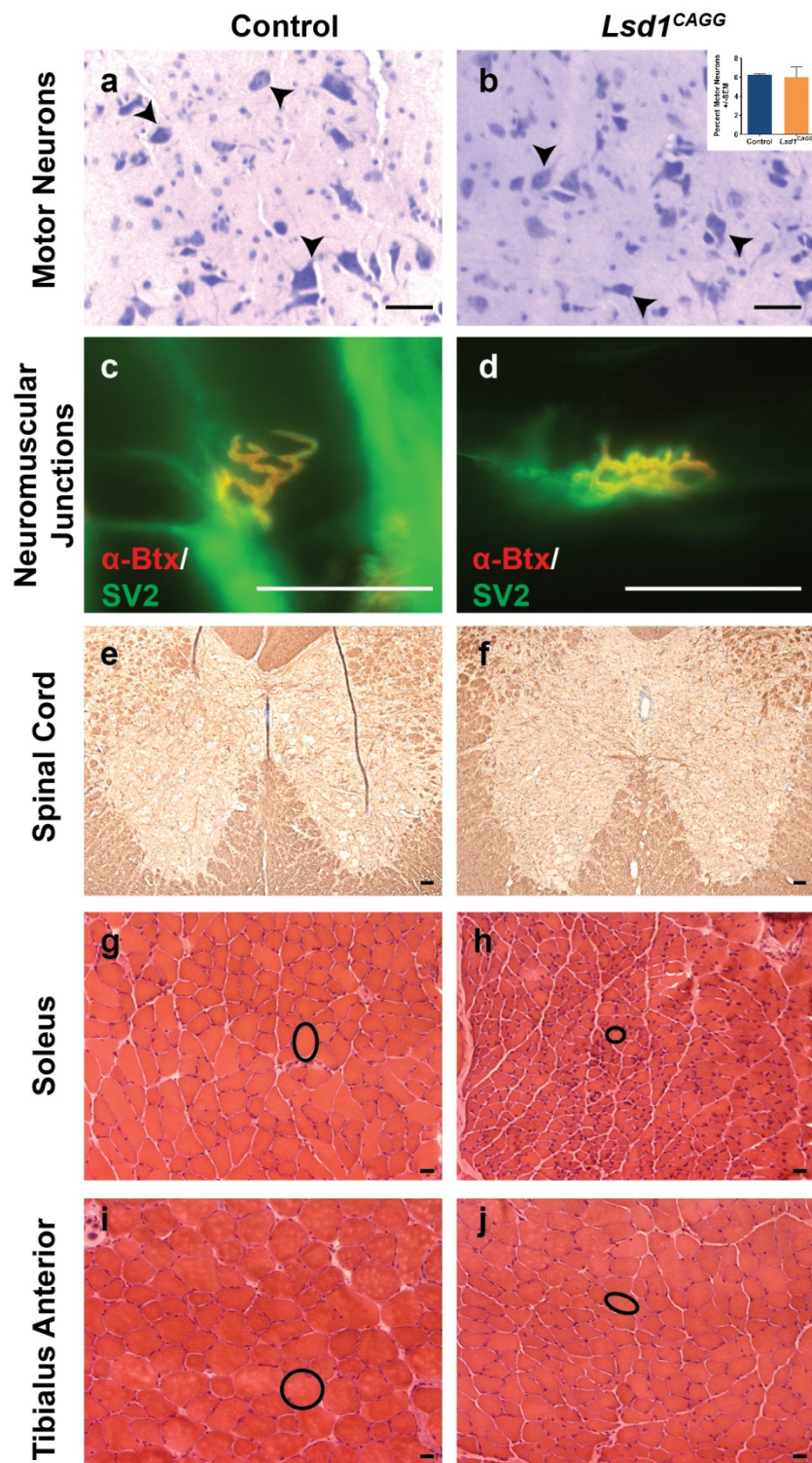


Figure 3-2 | Absence of spinal cord motor neuron and muscle defects in *Lsd1^{CAGG}* Mice.

(a,b) Thionin staining of control **(a)** and *Lsd1^{CAGG}* **(b)** ventral horn spinal cord motor neurons (arrowheads). Inset shows histogram of percentage motor neurons (per total ventral horn nuclei) for control ($n = 3$) and *Lsd1^{CAGG}* ($n = 4$). Values represent mean \pm s.e.m. **(c,d)**

Immunofluorescence of neuromuscular junctions showing SV2 (presynaptic motor neurons, green) and fluorescent α -bungarotoxin (muscle acetylcholine receptors, red) in control **(c)** and *Lsd1^{CAGG}* **(d)**. Co-localization SV2 and α -btx demonstrate an intact junction. **(e,f)**

Immunohistochemistry (IHC) of myelin basic protein (MBP) in lower cervical spinal cord showing no difference in myelin amount or distribution between control **(e)** and *Lsd1^{CAGG}* **(f)**.

IHC is counterstained with hematoxylin. **(g-j)** H&E staining of soleus **(g,h)** and tibialis anterior muscles **(i,j)** showing muscle fiber size (circles) in controls **(g,i)** compared to reduced cell size in *Lsd1^{CAGG}* **(h,j)**. Absence of gaps in the tissue and absence of centrally located nuclei indicate a lack of muscle degeneration. Scale bars= 50 μ m.

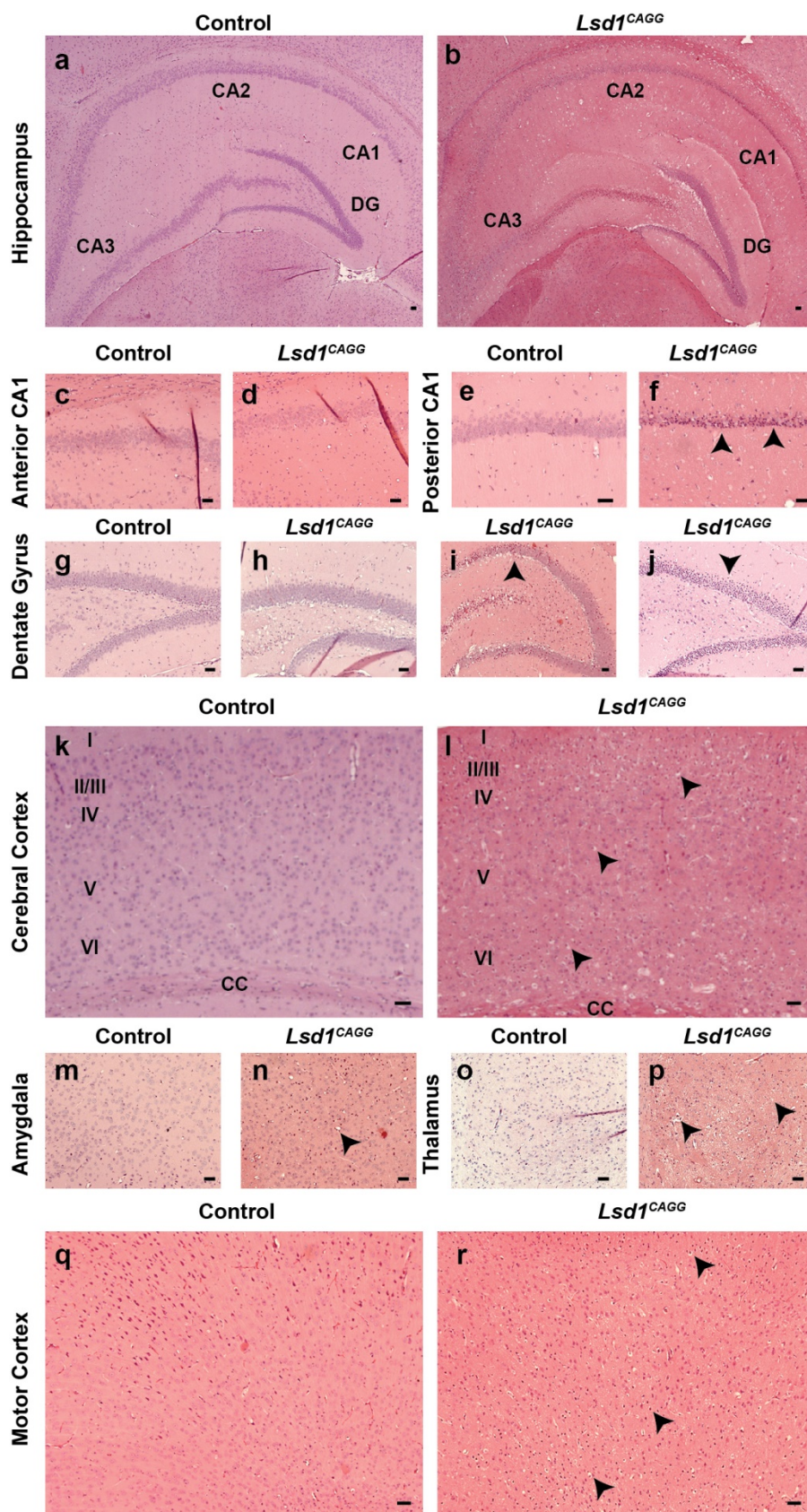


Figure 3-3 | Neurodegeneration in *Lsd1^{CAGG}* mice.

(a-r) H&E staining of control and *Lsd1^{CAGG}* hippocampus (a,b), anterior and posterior CA1 (c-f), dentate gyrus (g-j), cerebral cortex (k,l), amygdala (m,n), thalamus (o,p), and motor cortex (q,r). (a,b) Distribution of pyknosis in *Lsd1^{CAGG}* hippocampus with CA1 being most affected, and CA2 and CA3 moderately affected (b), compared to control with no pyknosis (a). (c-f) Increasing severity of pyknosis from anterior (d) to posterior (f) from the same *Lsd1^{CAGG}* hippocampus compared to control with no pyknosis (c,e). (g-j) Varying severity of pyknosis from three *Lsd1^{CAGG}* dentate gyruses; unaffected (h), moderately affected (i) completely affected (j) compared to control with no pyknosis (g). (k,l) Distribution of pyknosis in cerebral cortex of *Lsd1^{CAGG}* (l) in layers II/III, IV and VI, compared to control with no pyknosis (k), CC designates corpus callosum. (m-r) Distribution of pyknosis in the amygdala (n), thalamus (p) and motor cortex (r) of *Lsd1^{CAGG}* compared to control of same brain regions with no pyknosis (m,o,q). Arrowheads denote pyknotic nuclei. Scale bars= 50µm.

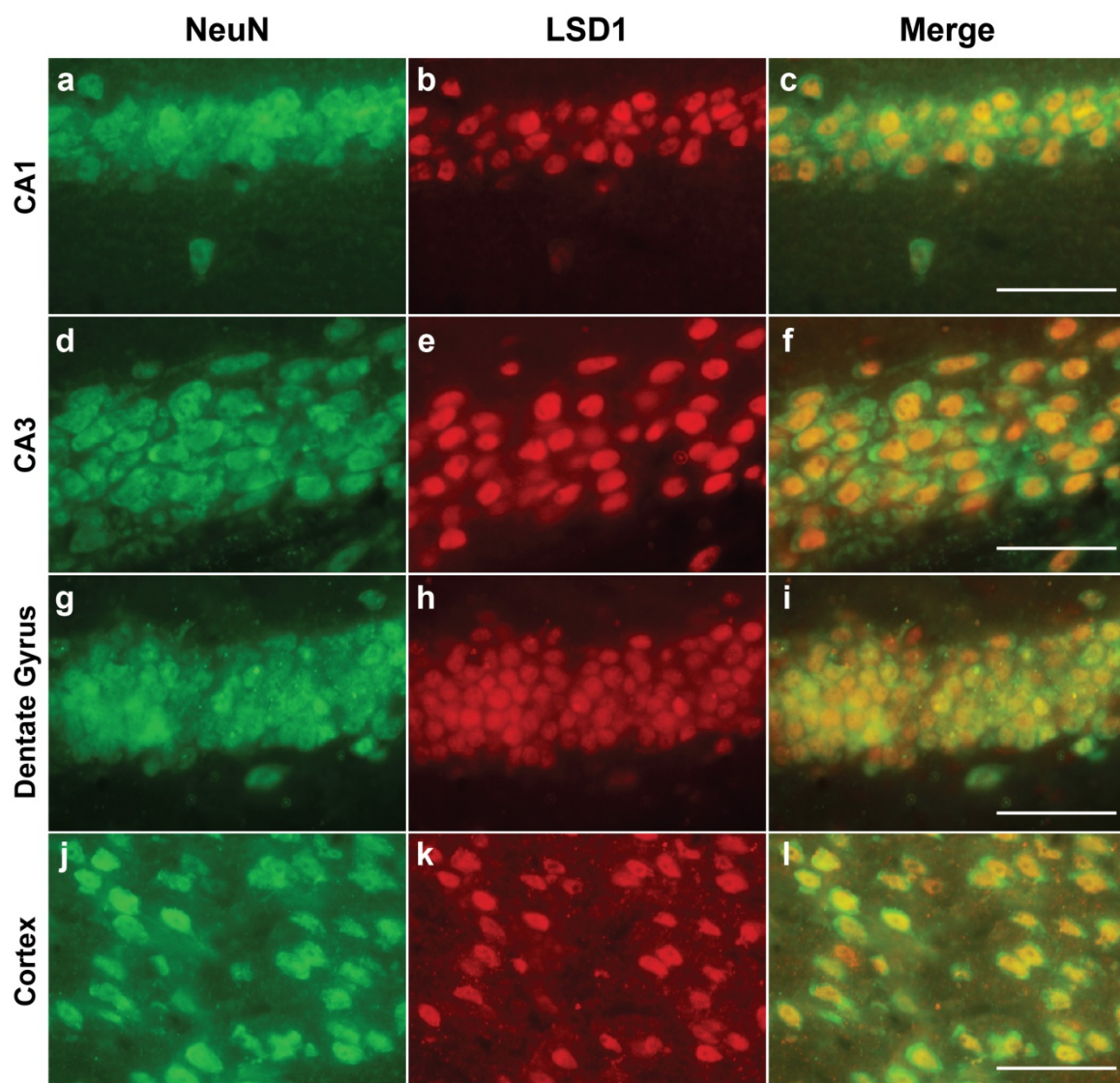


Figure 3-4 | LSD1 expression in adult murine hippocampal and cortical neurons.

(**a-l**) Immunofluorescence labelling with the neuronal nucleus marker NeuN (**a,d,g,j**, green), LSD1 (**b,e,h,k**, red) and merged (**c,f,i,l**) showing LSD1 protein in neurons of the CA1 (**a-c**) and CA3 (**d-f**) of the hippocampus, dentate gyrus (**g-i**) and cortex (**j-l**) of wild-type mice. Scale bars= 50µm.

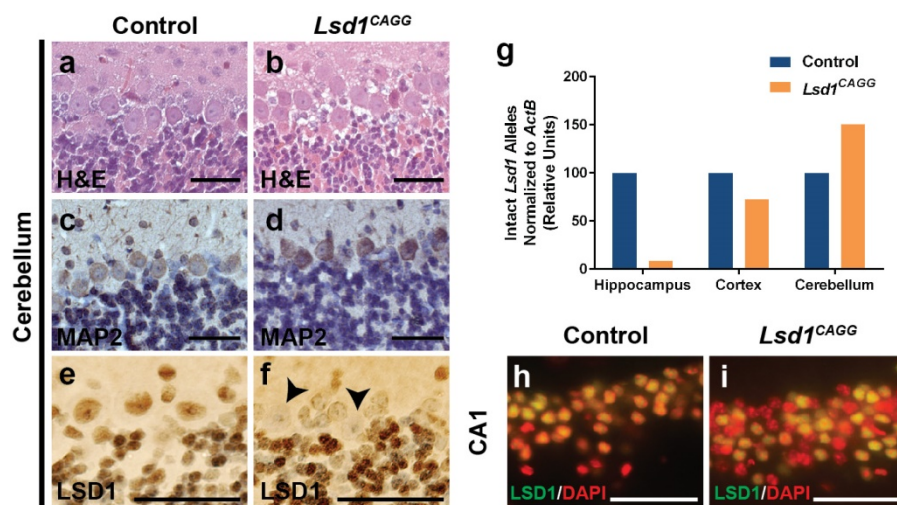


Figure 3-5 | Absence of neurodegeneration in the *Lsd1*^{CAGG} cerebellum.

(a,b) H&E staining of control (a) and *Lsd1*^{CAGG} (b) cerebellum showing similar cellular morphology and lack of pyknotic nuclei in *Lsd1*^{CAGG}. (c,d) MAP2 immunohistochemistry (IHC) in control (c) and *Lsd1*^{CAGG} (d) showing similar distribution in cerebellar neurons. (e,f) LSD1 IHC in control (e) and *Lsd1*^{CAGG} (f) cerebellum showing lack of LSD1 in some (arrowheads), but not all *Lsd1*^{CAGG} purkinje neurons. (g) Quantification of intact *Lsd1* alleles (revealing the extent of *Lsd1* deletion) in control (blue) and *Lsd1*^{CAGG} (orange) hippocampus 24 hours after tamoxifen injection, and in cortex and cerebellum at terminal phenotype. Data are shown as relative units normalized to *ActB*, where the control value is set to 100. (h,i) Merge of LSD1 (green) immunofluorescence and DAPI (red) in control (h) and *Lsd1*^{CAGG} (i) CA1 nuclei showing LSD1 protein remaining in non-pyknotic nuclei approximately one week before the *Lsd1*^{CAGG} terminal motor phenotype. All IHC (c-f) is counterstained with hematoxylin. Scale bars= 50µm.

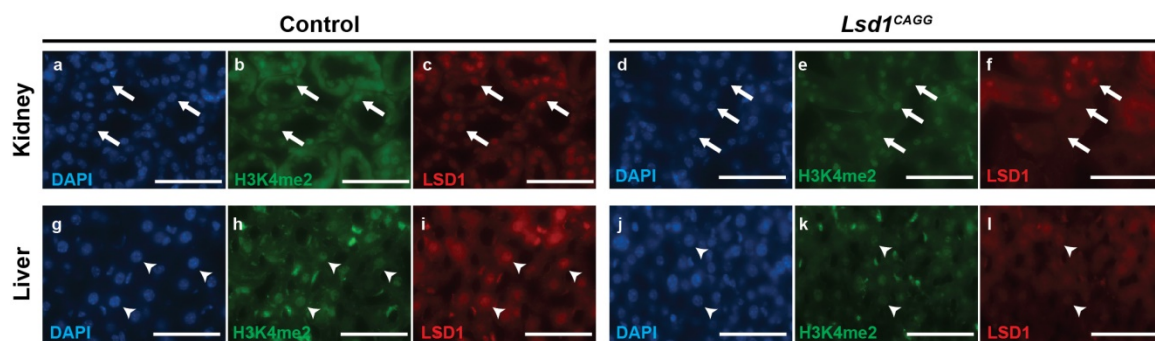


Figure 3-6 | LSD1 is not required for kidney and liver cell viability.

(a-l) Representative immunofluorescence images showing LSD1 (red), staining control H3K4me2 (green) and DAPI (blue) in mouse epithelial cells of the kidney nephron (**a-f**, arrows) and hepatocytes of the liver (**g-l**, arrowheads). LSD1 is normally ubiquitously expressed in controls (**c,i**). In *Lsd1*^{CAGG} mice, LSD1 is absent (**f,l**), but kidney and liver morphology remains normal compared to controls (**a,d,g,j**). Absence of LSD1 immunoreactivity is not due to lack of antibody penetrance (**b,e,h,k**). Scale bars= 50µm.

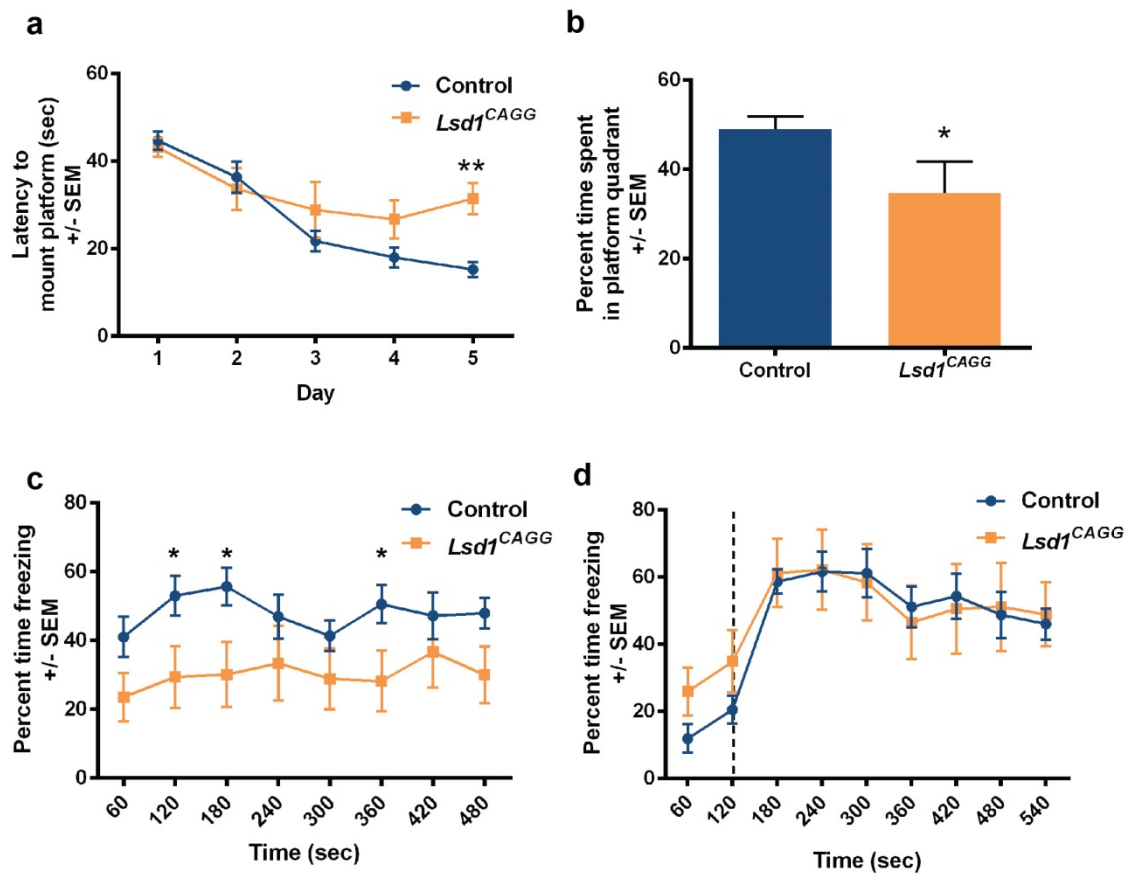


Figure 3-7 | Loss of LSD1 results in learning and memory deficits.

(a) Latency to mount platform (in seconds) in the Morris water maze across the 5 day training period of control (blue, $n = 15$) and $Lsd1^{CAGG}$ (orange, $n = 12$) mice. Data are shown as mean \pm s.e.m. $**P < 0.01$ on Day 5 compared by repeated measures two-way ANOVA with *post hoc* Sidak's multiple comparisons test. (b) Percent time spent swimming in platform quadrant during probe (day 6) after 5 days of water maze training for control (blue $n = 15$) and $Lsd1^{CAGG}$ mice (orange, $n = 11$) mice. Data are shown as mean \pm s.e.m. $*P < 0.05$ by unpaired t-test. (c) Percent time spent freezing during contextual fear response after fear conditioning of control (blue, $n = 12$) and $Lsd1^{CAGG}$ (orange, $n = 8$) mice. Data are shown as mean \pm s.e.m. $*P < 0.05$ by unpaired t-test at individual timepoints. $P = 0.052$ for difference between genotypes by repeated measures two-way ANOVA. (d) Percent time spent freezing during cued fear response after fear conditioning of control (blue, $n = 12$) and $Lsd1^{CAGG}$ (orange, $n = 8$) mice. Data are shown as mean \pm s.e.m. Dashed line represents sound of tone.

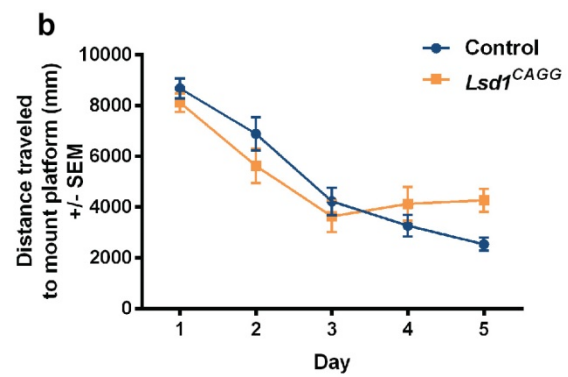
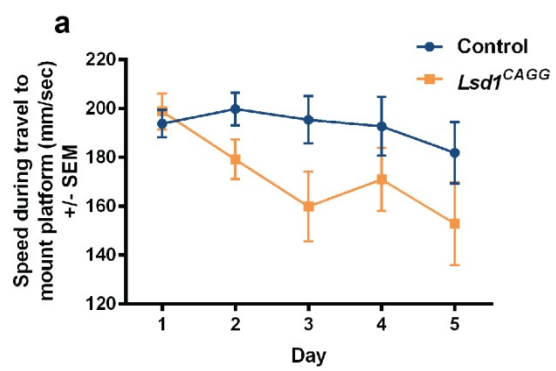


Figure 3-8 | *Lsd1^{CAGG}* mice have learning and memory deficits.

(a) Speed during travel to mount platform in Morris water maze across 5 day training period of control (blue, $n = 15$) and *Lsd1^{CAGG}* (orange, $n = 12$) mice. Data are shown as mean \pm s.e.m. No significant difference between genotypes by repeated measures two-way ANOVA. (b) Distance traveled to mount platform in Morris water maze across 5 day training period of control (blue, $n = 15$) and *Lsd1^{CAGG}* (orange, $n = 12$) mice. Consistent with the increased latency to mount platform (Fig. 2a), *Lsd1^{CAGG}* mice travel longer distance on Day 5. Data are shown as mean \pm s.e.m.

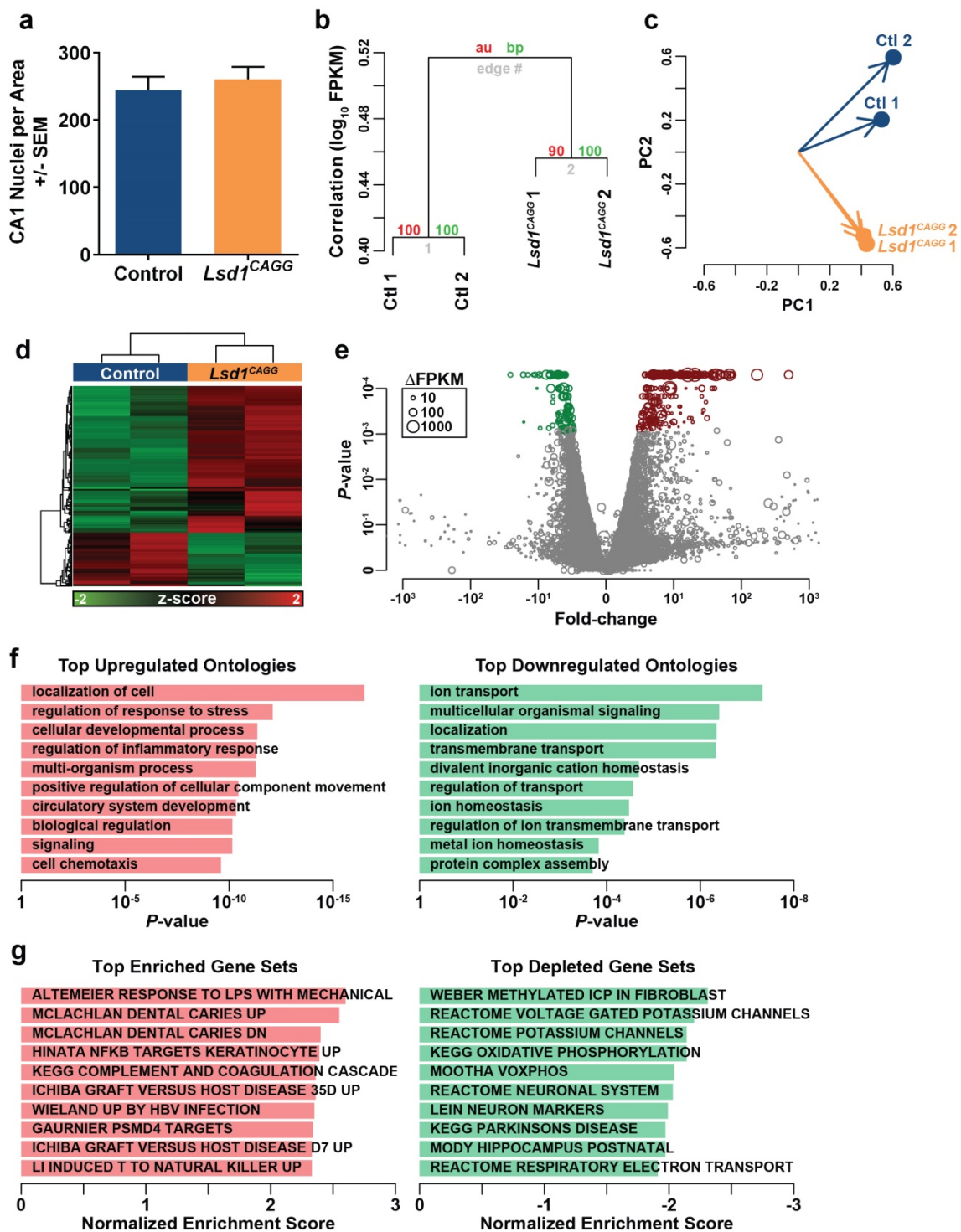


Figure 3-9 | Differential expression of genes in *Lsd1^{CAGG}* hippocampus.

(a) Total number of nuclei per area counted in control ($n = 4$) and terminal *Lsd1^{CAGG}* ($n = 10$) CA1. Data are shown as mean \pm s.e.m. (b) Hierarchical clustering of gene expression across 24,412 transcripts (FPKM > 0.5) shows that control and *Lsd1^{CAGG}* replicates significantly segregate by gene expression. The y-axis represents the \log_{10} FPKM correlation. Approximate Unbiased *P*-values (AU, red) and Bootstrap Probabilities (BP, green) for each cluster are shown. (c) Principle component analysis (PCA) of 24,412 transcripts (FPKM > 0.5) shows consistent separation of control and *Lsd1^{CAGG}* samples in the first two principle components. (d) Heatmap of most significantly differentially expressed (281 upregulated, 124 downregulated) RNA-seq transcripts between *Lsd1^{CAGG}* and control hippocampi. Samples are hierarchically clustered by relative expression of differentially expressed transcripts. Relative higher (red) or lower (green) expression is indicated. (e) Volcano plot of fold-changes in gene expression (x-axis) by statistical significance (*P*-value; y-axis). Each circle represents a transcript and the normalized change in expression is represented by the size of the circle (legend). Those transcripts that are significantly (FDR < 0.05) differentially expressed are represented in red (281 upregulated) and green (124 downregulated). (f) Histogram of Gene Ontology analysis shows ontologies that are associated with those genes that are upregulated (red) and those genes that are downregulated (green) in the *Lsd1^{CAGG}* RNA-seq dataset. The top 10 ontologies are shown with *P*-values. (g) Histogram of Gene Set Enrichment Analysis shows the most enriched (red) and depleted (green) gene sets in the *Lsd1^{CAGG}* RNA-seq dataset. The top 10 gene sets are shown with normalized enrichment scores.

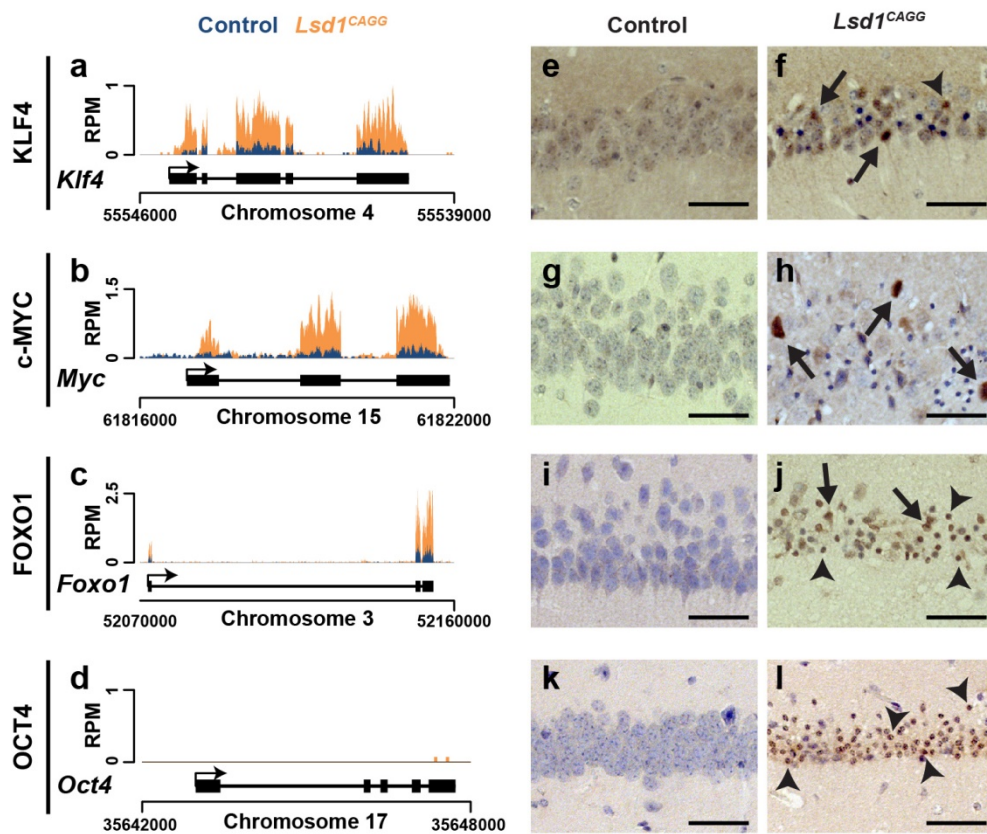


Figure 3-10 | Ectopic activation of stem cell genes in *Lsd1^{CAGG}* mice.

(a-d) Genome browser style plot of RNA-seq reads per million (RPM) from control (blue) and overlaid *Lsd1^{CAGG}* (orange) hippocampi showing expression of the genes *Klf4* (a), *Myc* (b), *Foxo1* (c), *Oct4* (d). (e-l) Immunohistochemistry (IHC) with antibodies to KLF4 (e,f), c-MYC (g,h), FOXO1 (i,j), and OCT4 (k,l) in control (e,g,i,k) and *Lsd1^{CAGG}* (f,h,j,l) CA1 neuronal nuclei. Arrows denote non-pyknotic nuclei and arrowheads denote pyknotic nuclei. All IHC is counterstained with hematoxylin. All *Lsd1^{CAGG}* images are taken at the terminal phenotype. Scale bars= 50µm.

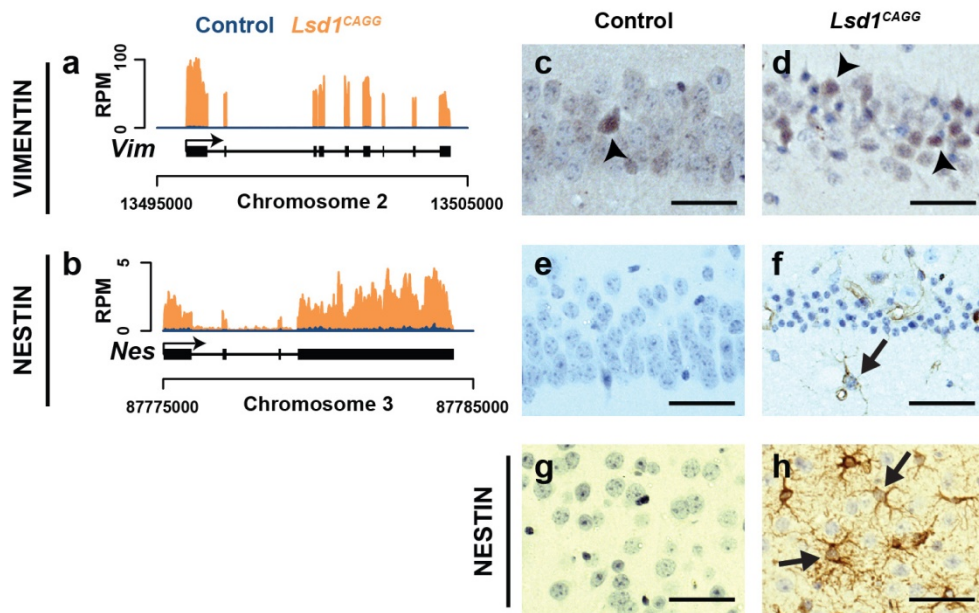


Figure 3-11 | Neural stem cell gene expression in *Lsd1*^{CAGG} mice.

(a,b) Genome browser style plot of RNA-seq reads per million (RPM) from control (blue) and overlaid *Lsd1*^{CAGG} (orange) hippocampus showing expression of the genes *Vimentin* (a) and *Nestin* (b). (c-h) Immunohistochemistry (IHC) with antibodies to VIMENTIN (c,d) and NESTIN (e-h) in control CA1 (c,e) and cortex (g), and *Lsd1*^{CAGG} CA1 (d,f) and cortex (h). VIMENTIN immunoreactivity was present in CA1 neurons in both control (c, arrowheads) and *Lsd1*^{CAGG} (d, arrowheads), with more immunoreactive neurons in *Lsd1*^{CAGG}. NESTIN immunoreactivity was found in glial-shaped cells in *Lsd1*^{CAGG} hippocampus (f) and cortex (h, arrows) and absent in control (e,g). All IHC is counterstained with hematoxylin. All *Lsd1*^{CAGG} images were taken at the terminal phenotype. Scale bars= 50µm.

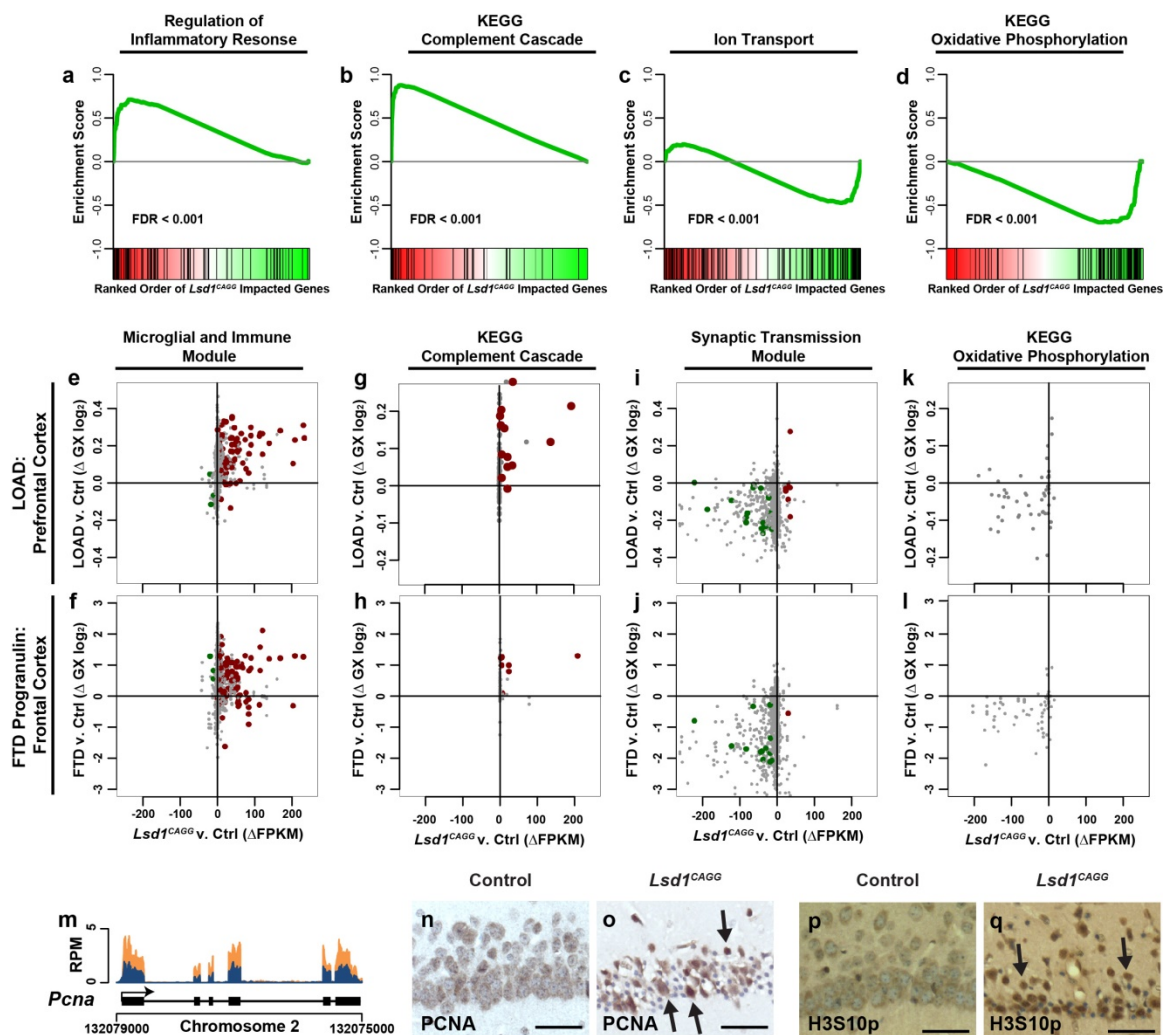


Figure 3-12 | Loss of LSD1 induces common neurodegeneration pathways.

(**a-d**) Gene set enrichment plots of neurodegeneration pathways where *Lsd1*^{CAGG} impacted transcripts (x-axis) are sorted by magnitude of upregulation (red) to downregulation (green). The position of each gene from the gene set is represented as a black tick mark (x-axis). Enrichment score (y-axis) shows where enrichment of genes from the set occurs in the *Lsd1*^{CAGG} transcriptome. Gene sets shown are regulation of inflammatory response (**a**), Kyoto Encyclopedia of Genes and Genomes (KEGG) complement cascade (**b**), ion transport (**c**), and KEGG oxidative phosphorylation (**d**). FDR is shown for each plot. (**e-l**) Scatter plots showing correlated changes in gene expression of genes from the Microglial and Immune Module (Zhang et al., 2013) (**e,f**), KEGG complement cascade (**g,h**), Synaptic Transmission Module (Zhang et al., 2013) (**i,j**) and KEGG oxidative phosphorylation (**k,l**) gene sets between the *Lsd1*^{CAGG} and control hippocampus (FPKM, x-axes) compared to changes in log₂ gene expression between late onset AD (LOAD) and control prefrontal cortex (Zhang et al., 2013) (**e,g,i,k**; y-axis), or compared to changes between FTD-progranulin and control frontal cortex (Chen-Plotkin et al., 2008) (**f,h,j,l**; y-axis). The most significantly changed genes in the *Lsd1*^{CAGG} hippocampus (Figure 3-9d,e) are shown in red (upregulated) and green (downregulated). All other genes with a direct mouse/human orthologue are shown in grey. Genes with correlated expression changes are found in the top right and bottom left quadrants, while genes that do not correlate are found in the other quadrants. (**m**) Genome browser style plot (as described in Figure 3-10a-d) showing *Pcna* expression in *Lsd1*^{CAGG} hippocampus (orange) compared to control (blue). (**n-q**) Immunohistochemistry with antibodies to PCNA (**n,o**), and H3S10p (**p,q**) in control (**n,p**) and *Lsd1*^{CAGG} (**o,q**) CA1 neuronal nuclei. Arrows denote non-pyknotic nuclei. All IHC is counterstained with hematoxylin. All *Lsd1*^{CAGG} images are taken at the terminal phenotype. Scale bars= 50µm.

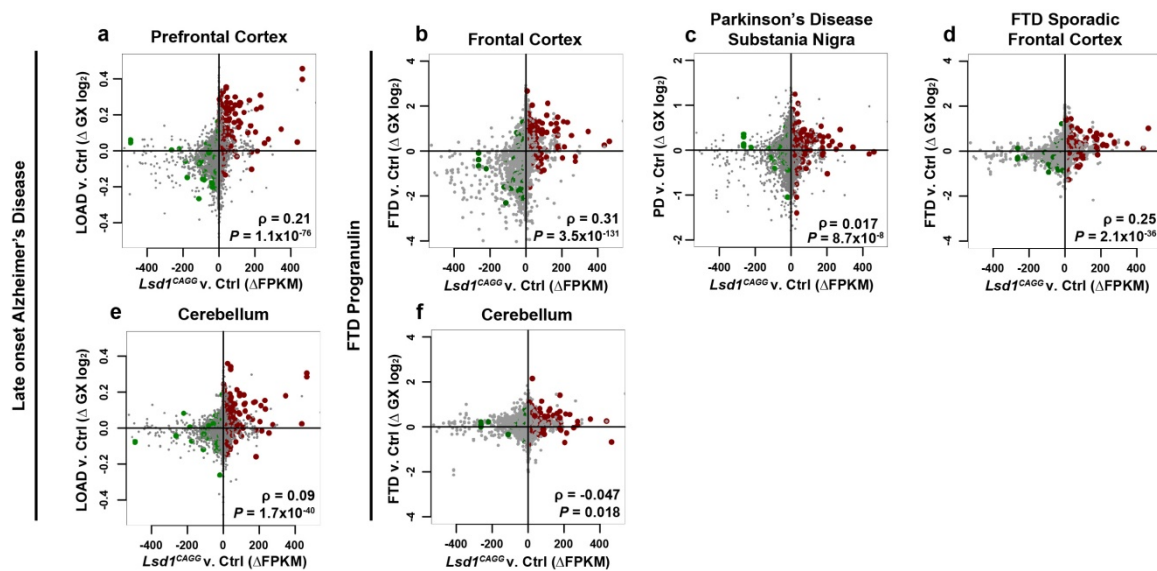


Figure 3-13 | Expression changes in *Lsd1^{CAGG}* mice correlate with those in AD and FTD.

(a-f) Scatter plots (as described in Figure 3-12e-l) showing genome-wide correlated changes in gene expression between the *Lsd1^{CAGG}* and control hippocampus (FPKM, x-axes) compared to \log_2 gene expression changes in late onset AD (LOAD) prefrontal cortex (Zhang et al., 2013) (a; y-axis), FTD-progranulin frontal cortex (Chen-Plotkin et al., 2008) (b; y-axis), PD substantia nigra (Zhang et al., 2005) (c; y-axis), sporadic FTD frontal cortex (Chen-Plotkin et al., 2008) (d; y-axis), LOAD cerebellum (Zhang et al., 2013) (e; y-axis), FTD-progranulin cerebellum (Chen-Plotkin et al., 2008) (f; y-axis). *P*-values and ρ Pearson correlation coefficient are given.

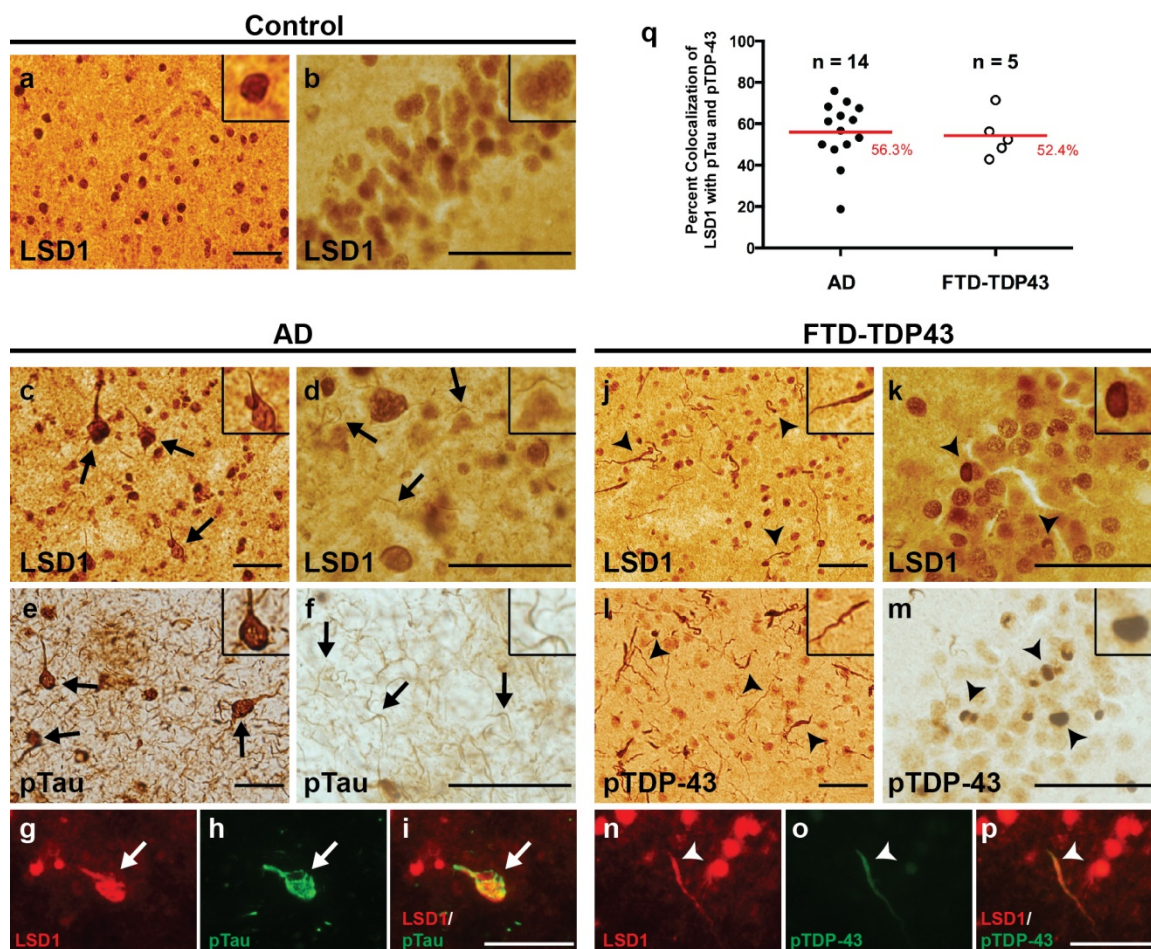


Figure 3-14 | LSD1 co-localization with pTau and pTDP-43 aggregates in AD and FTD.

(a,b) LSD1 immunohistochemistry (IHC) showing expression of LSD1 in age-matched control frontal cortex (a) and hippocampus (b). (c,d) Representative IHC images showing LSD1 immunoreactivity localized to cytoplasmic tangle-like aggregates (c, arrows) and neurites (d, arrows) in AD frontal cortex. (e,f) IHC images showing pTau (AT8 epitope) neurofibrillary tangles (e, arrows) and neuropil threads (f, arrows) from the same AD frontal cortex as (c,d). (g-i) Representative image of LSD1 (g, red), pTau (h, green), and merged (i) immunofluorescence (IF) showing co-localization of LSD1 with a pTau neurofibrillary tangle in AD (arrow). (j,k) Representative IHC image showing LSD1 immunoreactivity localized to abnormal deposits in neurites (j, arrowheads) and cytoplasmic inclusions (k, arrowheads) in FTD-TDP43 frontal cortex (j) and hippocampus (k). (l,m) IHC images showing pTDP-43 in neurites and cytoplasmic inclusions (l,m, arrowheads) from the same FTD-TDP43 frontal cortex (l) and hippocampus (m) as (j) and (k), respectively. (n-p) Representative image of LSD1 (n, red), pTDP-43 (o, green) and merged (p) IF showing co-localization of LSD1 with pTDP-43 in a neurite in FTD-TDP43 (arrowhead). Insets are magnified views of LSD1 nuclear localization (a,b) and representative pathologies (c-f, j-m). Scale bars= 50 μ m. (q) The percentage of neurofibrillary tangles (pTau) with LSD1 colocalization in AD ($n = 14$ cases assayed, closed circles), and neurites (pTDP-43) with LSD1 colocalization in FTD-TDP43 ($n = 5$ cases assayed, open circles), with the average percentage shown (red bar).

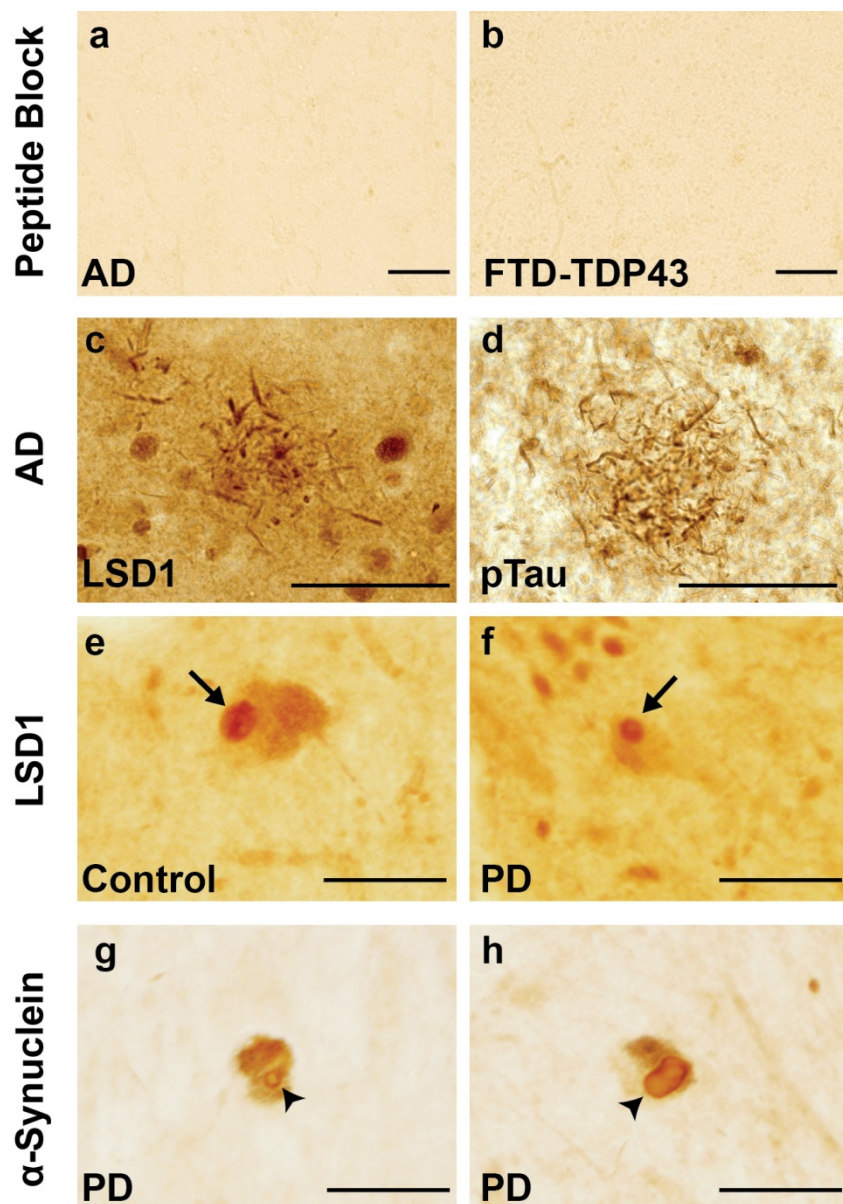


Figure 3-15 | LSD1 mislocalization is specific to AD and FTD.

(a,b) LSD1 IHC with primary antibody preincubated with the target peptide shows an absence of signal in AD (a) and FTD-TDP43 (b). (c,d) LSD1 (c) and pTau (AT8 epitope) (d) immunohistochemistry (IHC) showing immunoreactivity localized to neurites (c) and neuropil threads (d) around a senile plaque, but not to the amyloid core of the plaque. (e,f) LSD1 IHC in control (e) and PD (f) dopaminergic neurons of the substantia nigra shows LSD1 localized to the nucleus (arrows) and not Lewy bodies. (g,h) α -Synuclein IHC in PD shows formation of Lewy bodies in dopaminergic neurons of the substantia nigra (arrowheads). Scale bars= 50 μ m.

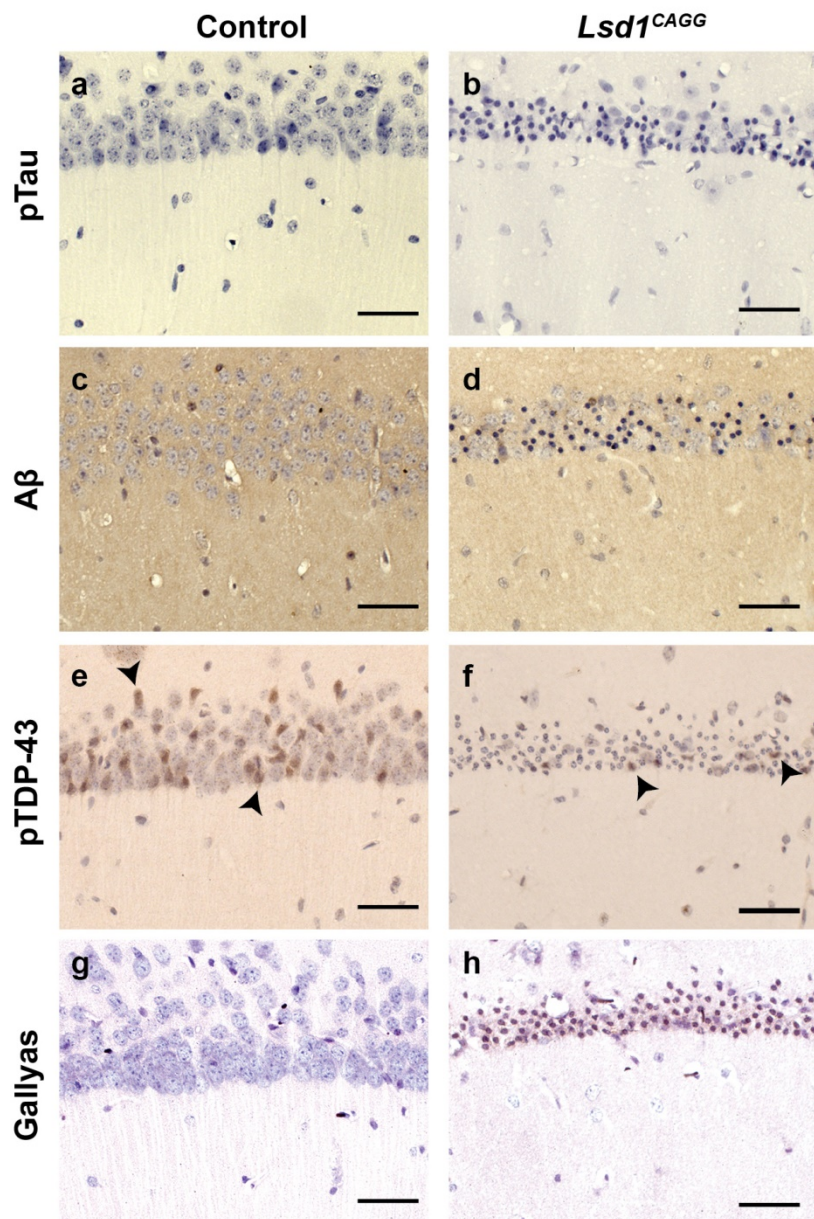


Figure 3-16 | Absence of pathological protein aggregates in *Lsd1^{CAGG}* mice.

(a-f) pTau (AT8 epitope) (a,b), A β (c,d), and pTDP-43 (e,f) immunohistochemistry in control (a,c,e) and *Lsd1^{CAGG}* (b,d,f) CA1 neurons showing absence of aggregate forms of the proteins. pTDP-43 is found sporadically in control nuclei (e, arrowheads) and shows a similar staining pattern in *Lsd1^{CAGG}* non-pyknotic nuclei (f, arrowheads), but there is no evidence of pTDP-43 aggregation. (g,h) Gallyas silver staining in control (g) and *Lsd1^{CAGG}* (h) CA1 neurons showing lack of any protein aggregation (positive stain is black). Scale bars= 50 μ m.

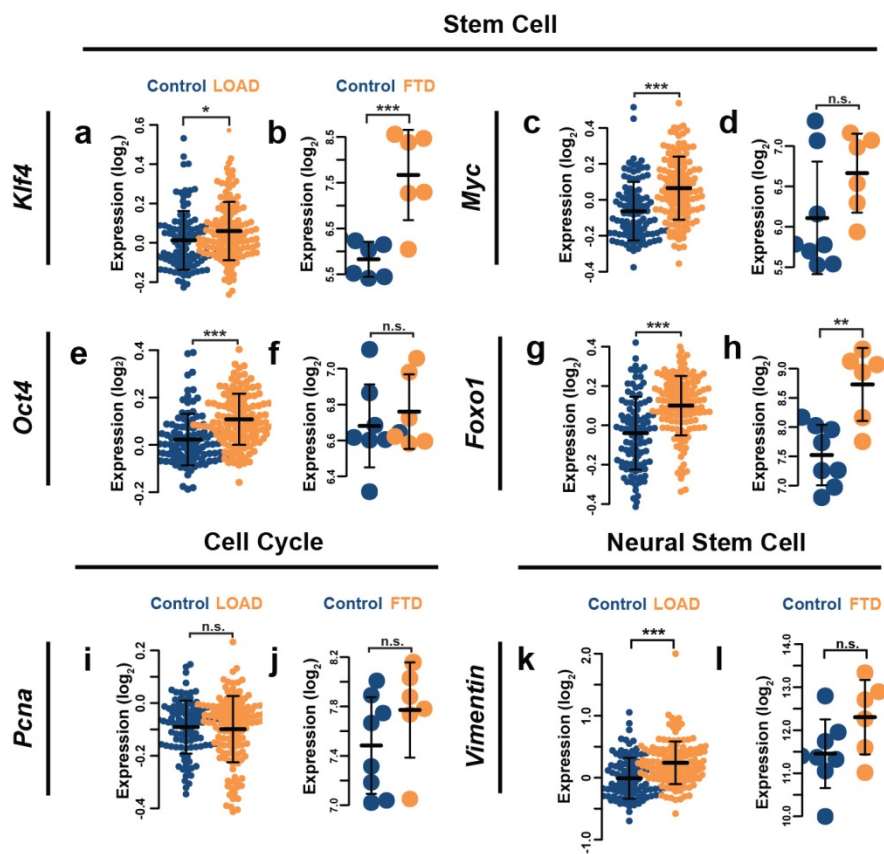


Figure 3-17 | Stem cell gene expression in human dementia.

(a-n) Beeswarm plots showing expression of *Klf4* (a,b), *Myc* (c,d), *Oct4* (e,f), *Foxo1* (g,h), *PCNA* (i,j) and *Vimentin* (k,l) in control (blue) versus LOAD prefrontal cortex (Zhang et al., 2013) (a,c,e,g,i,k, orange), or control (blue) versus FTD-progranulin frontal cortex (Chen-Plotkin et al., 2008) (b,d,f,h,j,l, orange). Values represent the \log_2 expression of each patient and bars represent mean \pm s.d., * $P < 0.05$, ** $P < 0.01$, *** $P < 0.001$, n.s.: not significant.

CHAPTER 4: DISCUSSION

4.1 LSD1 is Neuroprotective

LSD1 appears to be critical for the maintenance of the central nervous system. Inducible deletion of *Lsd1* throughout adult mice leads to widespread neurodegeneration throughout the cerebral cortex and hippocampus as well as a severe motor deficit that ultimately kills the mice. In addition, global gene expression changes occur that are highly reminiscent of those documented in human cases of late-onset Alzheimer's Disease (LOAD) (Zhang et al., 2013) and Frontotemporal Dementia with progranulin mutation (FTD-progranulin) (Chen-Plotkin et al., 2008). Neurodegenerative tissues are expected to share an expression signature of neuronal cell death. However, it is surprising that the expression changes of a complex human disease can be recapitulated by deletion of a single gene in a mouse. Furthermore, these changes appear to specifically mirror those of only LOAD and FTD-progranulin, as I did not observe a significant overlap in expression changes between *Lsd1*^{CAGG} mice and Parkinson's Disease, nor sporadic FTD. This lack of similarity with other neurodegenerative diseases suggests that the overlap observed with LOAD and FTD-progranulin is being driven by a shared mechanism, rather than a common neurodegeneration signature. Consistent with this idea, there are enrichments and depletions of gene ontologies in *Lsd1*^{CAGG} mice that have been implicated in these diseases. Specifically, there is a dramatic upregulation of genes involved in neuroinflammation and the inflammatory complement cascade, both of which have been implicated in neurodegenerative disease (Ahmed et al., 2007; Gjoneska et al., 2015; Zhang et al., 2013). The majority of genes in the neuroinflammatory pathway are involved in microglial activation. Since these cells are the resident macrophages of the central nervous system, many of these genes are involved in immunological function. The complement cascade pathway coats the synapses of neurons with complement proteins, which signals to microglia to target those synapses for pruning (Stevens et al., 2007). This process is also seen during neurodevelopment, when massive synaptic pruning takes place (Paolicelli et al., 2011). During the course of AD and FTD, this system is highly reactivated, to the detriment of the neurons. Together, the complement pathway and microglia

break down the synaptic network of the neurons during the course of the neurodegeneration. However, it remains unclear whether this effect is the primary driver of human neurodegeneration, or if it happens in response to the deposition of pathological protein and aggregates, and is a secondary contributor. In either case, deletion of *Lsd1* is sufficient to trigger this response in mice.

Several other pathways are affected in the same manner in both AD and FTD patients and in *Lsd1*^{CAGG} mice. Expression of genes in the oxidative phosphorylation pathway is reduced, an effect observed in AD. It is unclear what leads to this reduced expression in the disease. However, LSD1 has been shown to positively regulate the expression of these genes in adipose tissue, presumably by the removal of H3K9me (Duteil et al., 2014). It is possible that this mechanism is conserved in neurons and expression of these genes is lost in the absence of LSD1. Like the effects of neuroinflammation on neurodegeneration, it is unclear how loss of oxidative phosphorylation genes contributes to the disease. Several hypotheses have been proposed, including the generation of reactive oxygen species, that damage neurons (Lin and Beal, 2006). There also appears to be a greater requirement for mitochondria in neurons than in other cells (Lin and Beal, 2006). Therefore, when expression of these genes is lost, mitochondrial capacity is reduced, causing a depletion of the ATP pool, which could lead to neuronal cell death. Alternatively, this could be a signature of neuronal cell death and not specific to LSD1-mediated neurodegeneration.

Another pathway affected by loss of LSD1 is synaptic transmission (Zhang et al., 2013). Work by Rosenfeld and colleagues has shown that the neuronal specific isoform of LSD1 (LSD1n) binds to enhancers and promoters involved in neuronal activity in cortical neuron cultures (Wang et al., 2015). Both canonical LSD1 and LSD1n are expressed in the brain, while LSD1n appears to only have specificity for H4K20me2, suggesting they may have different roles. When LSD1n is absent, there is a reduction in the activation of these genes and their associated

enhancer RNAs during stimulation, which suggests LSD1n binds to and activates these by removing H4K20me2 to facilitate neuronal activity. In *Lsd1*^{CAGG} mice we see reduced expression of these genes, consistent with the Rosenfeld group. Therefore, it is possible the effect we see on neuronal genes is due to loss of LSD1n when total LSD1 is removed. Alternatively, reduced expression of these genes could be a secondary effect in *Lsd1*^{CAGG} mice, where the neuronal expression program is downregulated as a consequence of neuronal cell death. This effect is also observed in AD and FTD in a correlative manner, further suggesting loss of LSD1 in mice is sufficient to recapitulate human neurodegeneration associated with dementia.

At this time, I do not yet know whether LSD1-mediated neurodegeneration is cell autonomous, although some evidence points to this being likely. LSD1 protein remains in the nuclei of most hippocampal and cortical neurons for several weeks after deletion is induced, but is then lost from these nuclei approximately one week before the neuron cell death occurs. Furthermore, every pyknotic neuronal nucleus I have assayed for LSD1 protein is negative. Together, these data suggest LSD1 protein is lost from the nuclei of neurons just before neuronal cell death occurs in *Lsd1*^{CAGG} mice. Although this is the simplest explanation for LSD1-mediated neurodegeneration, it remains possible that loss of LSD1 in other cell types could be contributing to the phenotype. For example, I have observed a strong reactive gliosis response in the brains of *Lsd1*^{CAGG} mice in the form of astrocytes and to some extent, an increase in the number of microglia present in the hippocampus and cortex. It is possible that LSD1 is normally responsible for the proper regulation of the neuroinflammatory properties of these glial cells and that inducible deletion of *Lsd1* leads to aberrant neuroinflammation that ultimately causes the neurodegeneration. A third possibility is that LSD1 is required in oligodendrocytes and that loss of myelination causes the observed neurodegeneration. However, I believe this to not be the case, as the staining pattern and structure of myelin in the brain does not appear to change in the absence of LSD1. To truly tease apart this issue of cell autonomy, we intend to delete *Lsd1* with

an inducible neuronal and glial cell-type specific Cre. When LSD1 is lost from the critical cell type, the neurodegeneration will occur with that specific Cre.

In addition to molecular phenotypes, we observed learning and memory deficits in mice with *Lsd1* deletion. This can be seen by the impaired performance on the Morris water maze and contextual fear conditioning. Both of these assays rely on the mice having the visual capacity to recognize the context of an environment in order to correctly respond to an unpleasant stimulus. This is an important caveat with regard to *Lsd1*^{CAGG} mice. At this time, I cannot rule out the possibility of visual impairment, which would lead to false positives in the assay. However, the mice show no obvious signs of visual impairment, such as accidentally walking into the sides of their home cages. In contrast to tasks of contextual learning, *Lsd1*^{CAGG} mice display a normal response when conditioned to fear a cued tone. This specificity of learning impairment is consistent with the neurodegeneration observed in after *Lsd1* deletion. Contextual learning takes place in the hippocampus, where we observe the most neurodegeneration, while cued learning takes place in the amygdala, where we observe just a small amount of neurodegeneration. Although the most obvious explanation for the learning impairment is the neurodegeneration in the hippocampus, we did not thoroughly confirm that mice used for the assay had hippocampal degeneration at the time of the assay. Of two *Lsd1*^{CAGG} mice brains stained for histology, neither showed obvious signs of neurodegeneration. However, immunohistochemistry for LSD1 protein revealed a reduction in the amount of hippocampal nuclei with LSD1 compared to control. Therefore, an alternative explanation is that LSD1 protein is necessary for contextual learning in intact hippocampi. Further evidence of this has been reported by Rosenfeld and colleagues (Wang et al., 2015), who report a neuron specific isoform of LSD1, LSD1n. They find that deletion of exon 8a with *Nestin-Cre*, which specifically deletes in embryonic neuronal stem cells (Tronche et al., 1999), produces viable adult mice without neurodegeneration, or any other obvious phenotypes. However, the mice have deficits on the Barnes maze, which assays contextual

learning ability by training mice to find a hole that allows them to escape an open field (Barnes et al., 1980). This overlap in learning deficits with *Lsd1*^{CAGG} mice suggests LSD1 plays an active role in hippocampal learning. Consistent with this is the observation that cortical neuron preps with *Lsd1n* deletion have a repressed activation of genes observed with KCl treatment. This treatment mimics neuronal activity stimulation, which activates many of the genes bound by LSD1 in cortical neuron cultures (Wang et al., 2015). Rosenfeld and colleagues argue this activation is directed by LSD1n-mediated removal of H4K20me, a repressive histone modification. This is consistent with our mouse model, where presumably LSD1n is lost as well as canonical LSD1 (LSD1c). Interestingly, deletion of LSD1n alone leaves LSD1c intact in neurons and does not lead to neurodegeneration. This suggests that LSD1-mediated neurodegeneration occurs through loss of LSD1c and not LSD1n. Teasing apart these roles in neurological disease will be of particular interest.

The most obvious and initial phenotypes of *Lsd1*^{CAGG} mice is the onset of paralysis and lethargy approximately four weeks following deletion in adults. The phenotype starts with hindlimb weakness, displayed as a clasp when the animal is suspended by its tail. Ultimately, the mice progress to a stage where they require prepared wet food in the bedding of their home cage, instead of in the hopper which requires climbing to access. These symptoms are classically indicative of cerebellar ataxia. Mice with cerebellar ataxia typically display neurodegeneration in the cerebellum, where higher order movement is coordinated, such as walking with a normal gait (Guyenet et al., 2010). However, *Lsd1*^{CAGG} mice do not display any obvious degeneration in the cerebellum. In fact, we observe morphologically normal Purkinje neurons of the cerebellum lacking LSD1 protein even weeks after deletion. Therefore it is possible that LSD1 is only required in a subset of neurons and cerebellar neurons are exempt.

In order to provide an explanation for the paralysis observed in *Lsd1*^{CAGG} mice, we also examined other structures involved in motor coordination. In the brain, the motor cortex does

display a moderate amount of neurodegeneration in the form of pyknotic neuronal nuclei. However, whether degeneration of the motor cortex could contribute to the observed phenotype is unclear. Lesioning the motor cortex does not lead to behavior like that observed in *Lsd1*^{CAGG} mice (Farr and Wishaw, 2002), and is thought to take part in refining movement rather than general control (Kleim et al., 1998). However, I cannot rule out the possibility that achieving a threshold of neuronal death in the motor cortex could lead to motor deficits like that observed in *Lsd1*^{CAGG} mice. In the spinal cord, we have shown that *Lsd1*^{CAGG} mice have motor neurons present in normal amounts. This is in contrast to mice transgenically expressing a human mutation of superoxide dismutase 1 (*Sod1*), found in familial amyotrophic lateral sclerosis (ALS), which become paralyzed at 5-6 months of age and show marked loss of spinal cord motor neurons (Gurney et al., 1994). Therefore, I concluded that loss of spinal cord motor neurons is likely not the cause of paralysis in *Lsd1*^{CAGG} mice. However, other motor neuron dysfunction may be occurring. One possibility is that in the absence of LSD1, motor neurons develop issues with electrical conductivity, which would lead to difficulties with locomotion. Alternatively, there could be loss of synaptic connection at neuromuscular junctions. I assayed the amount of intact neuromuscular junctions in *Lsd1*^{CAGG} mice, and did not find any difference with controls. Furthermore, the morphology of leg muscles indicated muscular atrophy opposed to degeneration, suggesting muscles are not dying in the absence of LSD1, but are wasting due to lack of use. Altogether, no obvious aberrations occur in the locomotor circuitry of *Lsd1*^{CAGG} mice. Electrophysiological assessment of motor neurons will be needed to rule out defects in their conductivity, at which point degeneration in the brain will likely be the source of the observed paralysis.

4.2 Interaction of LSD1 and pTau

Most surprising from this study was the finding that LSD1 colocalizes with pTau in Alzheimer's Disease (AD). Mass spectrometry experiments to identify novel proteins interacting

with Tau tangles and A β plaques have yielded few hits (Bai et al., 2013). The strategy for these experiments is to analyze the detergent insoluble proteome of a pool of AD patient brains via mass spectrometry. The researchers proposed that proteins interacting with pTau and A β , which are detergent insoluble, will remain in the insoluble fraction due to a strong interaction and will thus be detected by mass spectrometry. However, of the 36 proteins identified as significantly enriched in the insoluble fraction of AD patient brains, only one was found to colocalize with protein aggregates. Thus, detection of novel proteins that colocalize with pathological protein aggregates associated with neurodegeneration is quite rare.

The observation that LSD1 colocalizes with pTau in AD suggests the proteins are physically interacting. Whether this interaction is direct or indirect remains to be determined. However, the observation that LSD1 colocalizes with pTau in the cytoplasm suggests the nuclear pool of LSD1 could be depleted in AD cases. Since ubiquitous deletion of *Lsd1* in adult mice leads to widespread neurodegeneration of the hippocampus and cortex, along with recapitulation of the molecular signatures of AD and learning and memory deficits, it is quite possible that loss of nuclear LSD1 is a major contributor to the neuronal cell death that causes the disease. Future experiments will aim to quantify the extent of LSD1 remaining in the nucleus as well as dissect the interaction between LSD1 and pTau. Furthermore, the interaction of LSD1 and pTau will be especially interesting for use as a target for drug development.

Two approaches for distinguishing the relationship between LSD1 and pTau come to mind. The first is a genetic approach that aims to synthetically exacerbate a mouse model of tauopathy (Yoshiyama et al., 2007) by removing one copy of the *Lsd1* gene. This tauopathy model (termed PS19) overexpresses a transgene of the human Tau gene that harbors a proline to serine missense mutation at residue 301. This mutation leads to hyperphosphorylation of Tau protein and formation of Tau tangles in mice, specifically in neurons. Around three months of age, PS19 mice develop a mild amount of Tau tangles in hippocampal neurons. Over the next six

months, the Tau burden worsens, leading to neuronal cell death, and expands to include spinal cord motor neurons, at which point the mice begin to display hindlimb weakness that ultimately progresses to paralysis. At around nine months of age, 80% of the mice die due to complications of the paralysis phenotype and also have a moderate amount of neurodegeneration in the hippocampus and cortex. This model of human neurodegeneration has many similarities to *Lsd1*^{CAGG} mice, with one major difference; *Lsd1*^{CAGG} mice develop neurodegeneration within eight weeks after deletion, rather than over the course of a mouse lifetime. It is with this difference in timing and the observation that LSD1 colocalizes with pTau in human AD that we hypothesized that the PS19 phenotype can be synergistically altered by removing one copy of *Lsd1*.

To test this hypothesis, we have crossed floxed *Lsd1* mice (Wang et al., 2007) to *Vasa-Cre* mice (Gallardo et al., 2007), which expresses *Cre* specifically in the germline, to delete one allele of *Lsd1*. These heterozygous *Lsd1* mice were then crossed to PS19 mice, which are heterozygous for *Lsd1* and hemizygous for the Tau transgene. Preliminarily, we have observed in three mice that in the presence of heterozygous *Lsd1*, the PS19 phenotype manifests at a faster rate and with more hippocampal degeneration than when two alleles of *Lsd1* are present. This suggests that LSD1 and pTau are interacting or in a pathway together that leads to neurodegeneration. Additionally, like what I have observed in AD patients, there appears to be colocalization of LSD1 with pTau in PS19 mice. However, this data is still preliminary at this time, as only three *Lsd1*^{Δfl};*PS19*⁺ mice have been created.

In addition to synthetically affecting the PS19 phenotype, we predict that neurodegeneration will have a molecular signature reminiscent of deletion of both copies of *Lsd1*. Transcriptional analysis of hippocampal tissue of these synthetic effect mice are expected to display upregulation of genes involved in neuroinflammation, as well as downregulation of genes involved in synaptic maintenance and oxidative phosphorylation. Since I have shown that these

genes show transcriptional changes in this manner in *Lsd1*^{CAGG} mice with full deletion of *Lsd1*, observing the same changes in these synthetic effect mice would suggest that the neurodegeneration occurs through a shared mechanism: the reduction of nuclear LSD1. The rationale of this synthetic effect experiment relies on the assumption that mice heterozygous for *Lsd1* have a reduced LSD1 nuclear pool that is sufficient to maintain neurons outside of perturbations, but is unable to compensate for the loss of LSD1 protein that occurs when LSD1 is sequestered by pTau. Therefore, future studies will need to determine the nuclear levels of LSD1 in heterozygous neurons, as well as during the course of neurodegeneration when the PS19 transgene is present. I predict that nuclear LSD1 levels will decrease as pTau builds up, and the occurrence of neurodegeneration will correlate with nuclear LSD1 levels falling below a critical threshold. Taken together, these experiments point to a functional relationship between LSD1 and pTau in mouse model of human tauopathy, where pTau accumulation leads to neurodegeneration through altering the LSD1 nuclear pool.

The second approach for understanding the relationship between LSD1 and pTau is to explore their colocalization biochemically. The observation that LSD1 and pTau colocalize in human AD suggests these proteins physically interact, though whether this interaction is direct or indirect is completely unknown. Notably, LSD1 was not identified as one of the proteins enriched in the insoluble fraction of AD patient brain lysates in a recent study (Bai et al., 2013). However, it is possible that an interaction between LSD1 and pTau is disrupted by detergent treatment and therefore prevents the detection of LSD1 in the insoluble fraction. Co-immunoprecipitation experiments from AD patient brain homogenates could provide insight on the nature of LSD1 and pTau colocalization. Additionally, *in vitro* techniques could be used to explore a possible interaction. But such experiments would be challenging, as Tau aggregation is difficult to achieve *in vitro*.

Together, our data support a model where LSD1 is continuously required throughout the life of neurons to appropriately regulate transcription. During the course of human dementia, pathological protein aggregates accumulate, which sequester LSD1 and prevent its normal function in the nucleus. The reduced nuclear pool of LSD1 leads to inappropriate transcription of pathways associated with neurodegeneration. This ultimately results in the neuronal cell death observed in these diseases. In this model, LSD1 inhibition becomes a pivotal moment in the course of the disease, suggesting it could be an important therapeutic target (Figure 4-1).

Many questions remain regarding the relationship of LSD1 and pTau. It is not immediately clear why a histone demethylase, whose primary role takes place in the nucleus, would be interacting with a cytoskeletal protein in the cytoplasm. LSD1 has been shown to demethylate non-histone targets, p53 (Huang et al., 2007) and the maintenance DNA methyltransferase DNMT1 (Wang et al., 2009), but both of these interactions presumably take place in the nucleus. This does not rule out the possibility that LSD1 could have a cytoplasmic role. Recent evidence suggests that Tau lysine residues are methylated while in the neurofibrillary form (Thomas et al., 2012) as well as normally in its non-aggregated form (Funk et al., 2014). However, the role of this lysine methylation is poorly understood. Given its ability to demethylate non-histone targets, LSD1 could possibly demethylate Tau as part of normal neuron biology, or as Tau aggregation proceeds. This would provide an opportunity for LSD1 to be mislocalized from the nucleus potentially sequestered by pTau. As more pTau aggregates, more LSD1 is pulled away from the nucleus into the cytoplasm, which reduces the nuclear levels of LSD1 and shifts the balance of epigenetic regulation by LSD1 into an unfavorable position.

One last piece of evidence that would suggest LSD1 is truly related to human dementia would involve examining healthy, elderly human brains with neurofibrillary tangles. Neurofibrillary tangles have a higher correlation with disease severity than A β plaques (Arriagada et al., 1992), suggesting they may play a more important role in the development of the disease.

However, many healthy elderly brains display neurofibrillary tangle formation without cognitive impairment (Price and Morris, 1999). If LSD1 mislocalization with pTau is part of the etiology of AD, I would predict that examination of healthy aged brains would show an absence or a dramatic reduction of LSD1 colocalization with pTau compared to late stage AD. Thus, LSD1 colocalization with pTau would be a predictor of cognitive impairment and impairment only occurs when LSD1 is colocalized with pTau.

4.3 LSD1 Continuously Maintains the Differentiated State of Neurons

In a seminal paper, Conrad Waddington described cells in a developing embryo as being like a ball rolling down a hill (Goldberg et al., 2007). Each starts at the top (undifferentiated), then descends due to gravity, making path choices in the form of valleys (cell fate choices), until it ultimately reaches the bottom of the hill (terminally differentiated), where it can never return to the top (undifferentiated state). We now know this process is directed by transcription factors and epigenetic enzymes through the expression of different transcriptional programs. This analogy is accurate for natural development. However, several experiments have challenged this idea terminal differentiation. Somatic cell nuclear transfer (Campbell et al., 1996; Gurdon et al., 1958) and inducible pluripotency reprogramming (Takahashi and Yamanaka, 2006) revert a differentiated cell or nucleus back into a completely undifferentiated state. In both of these experiments, the donor cells or nuclei contain all the genetic information necessary to produce an organism. The chromatin must be epigenetically reprogrammed to both silence the differentiated cell fate program and activate the undifferentiated program. These experiments present an enormous shift in the developmental paradigm, because they suggest that terminal differentiation can be overcome, albeit in artificial systems. Nevertheless, they demonstrated that the widely held view of differentiation was incomplete.

In Chapter 3 of this study we show that stem cell gene transcription is ectopically reactivated in the absence of LSD1. Although I observed that robust reactivation occurred in

neurons, it remains unclear whether this requirement for stem cell gene repression is neuron-specific or more general. Indeed, if the requirement is general, it would dramatically change our view of differentiation from those established by Waddington. Conversely, if this is a neuronal-specific phenomenon, it raises many questions as to why neurons maintain such a propensity to reactivate stem cell gene transcription. This is quite striking for a cell type that is terminally differentiated compared to others, given their post-mitotic status and complex structure and asymmetry. Future experiments will aim to determine if other cell types require continuous repression of stem cell genes with LSD1, as well as whether there is something unique about the chromatin environment of these genes in neurons.

One way to address this question is through inducible pluripotency reprogramming experiments. If LSD1 is required to repress expression of stem cell genes in differentiated cells, then it would potentially act as a blockade of reprogramming. Reprogramming experiments in cells with either LSD1 inhibition or deletion would perhaps show more robust propensity for reprogramming, or reprogram at a faster rate. Indeed, unpublished data from our lab has found that reprogramming using pargyline, an LSD1 inhibitor, results in faster development of induced pluripotent stem cells (iPSC), consistent with LSD1 acting as a barrier to reprogramming. Interestingly, the reprogrammed cells have a transcriptional profile that is more correlated with differentiated cells than cells after normal iPSC reprogramming, suggesting that LSD1 also participates in silencing of the differentiation program during the course of reprogramming. This is likely to occur similarly to what was described with LSD1 inhibited during mESC differentiation, where LSD1 represses transcription associated with the previous cell fate. Together, these data suggest that LSD1 generally acts to regulate transcription of genes associated with other cell fates, both during and after cell fate transitions (Figure 4-2).

An interesting developmental question is what happens when stem cell gene expression is allowed to occur in neurons without the activation of apoptotic pathways. To date, little is known

about the capacity of differentiated cells to cope with ectopic expression of stem cell genes. One hint comes from Yamanaka and colleagues, who developed a mouse model of inducible transient expression of iPSC factors. They find that incompletely dedifferentiated tumors arise from transient expression of the factors, and that these tumors more closely resemble pluripotent cells than differentiated. This suggests that the epigenetic mechanisms that underlie their reprogramming could also contribute to human tumorigenesis. Regrettably, their system did not induce expression of the factors in the brain. Therefore, to test this, inducing deletion of *Lsd1* in an apoptosis pathway mutant mouse could allow for the continued expression of stem cell genes in neurons. It seems likely the neurons would be susceptible to tumorigenesis, but alternatively a lack of tumor formation would suggest that neurons possess characteristics that privilege them from stem cell gene expression-derived tumorigenesis.

A notable question that remains from this study is whether the reactivation of stem cell gene transcription contributes to the observed neuronal cell death in the absence of LSD1. Some evidence supports this hypothesis. During the course of inducible pluripotency reprogramming, the four Yamanaka factors (OCT4, c-MYC, SOX2 and KLF4) each bind to the promoter of p53 (Soufi et al., 2012). It is thought that through this binding, tumor suppressor pathways are activated, leading to apoptosis. This mechanism is a potential explanation of the relatively low efficiency of inducible pluripotency reprogramming. Therefore, it is possible that stem cell gene reactivation in the absence of LSD1 triggers apoptotic pathways by activation of p53. To test this hypothesis, deletion of the factors or p53 along with LSD1 should rescue the LSD1-mediated neurodegeneration phenotype. Consistent with these ideas, we have shown that there is an upregulation of pluripotency factor expression in post-mortem AD and FTD brain samples relative to controls. This raises an exciting possibility, that human neurodegeneration occurs through the loss of neuronal cell fate, established decades earlier, and reversion to transcriptional programs associated with development.

The observation that neurons can revert to stem cell transcriptional programs by removing one enzyme, in many ways, contradicts many of the ideas posed in Waddington's model. The idea of terminal differentiation implies that the cell is "locked in" to that cell fate, which is now the default in its current state. In this light, the reprogramming experiments of Gurdon and Yamanaka are perceived as overcoming the differentiated state to reprogram. To use Waddington's analogy, the ball must be actively pushed up the hill by the factors carrying out the reprogramming. However, when LSD1 is lost from adult neurons, we observed that stem cell gene transcription is reactivated. This suggests that LSD1 acts as a blockade to stem cell transcription. This implies that stem fate could be the default program and that a defined set of factors are necessary to not only establish, but continuously maintain the differentiated state. In this respect, Waddington's original landscape analogy falters. I propose that the ball would no longer begin at the top of a hill, but rather in the middle of a plane balanced like a seesaw. To move the ball, forces have to be applied and relieved in concert to shift the plane. In our modified model, the cell's fate is at the mercy of epigenetic regulators—it can be changed when enough repression of the stem cell program and activation of the differentiation program (forces) are achieved.

4.4 Conclusions and Future Directions

I have shown here that loss LSD1 in adult neurons leads to cell death that is reminiscent of human neurodegeneration. I have also shown that LSD1 is mislocalized in human dementias. Together these data suggest that LSD1 inhibition could be part of the mechanism of neuronal cell death observed in human dementias. By sequestering LSD1 in the cytoplasm, the nuclear pool of LSD1 is reduced, which is sufficient to cause neuronal cell death in mice. My work also suggests that the cell fate of neurons is not terminally differentiated. Deletion of *Lsd1* leads to ectopic expression of stem cell genes in differentiated adult neurons. This observation suggests that the commonly held developmental view of differentiation that cells become terminally differentiated

is not completely true and there is some capacity for expression of genes associated with the undifferentiated state to occur.

Future studies will aim to further dissect the relationship between LSD1 and pTau. We are currently exploring this interaction functionally using mouse genetics by removing one wildtype allele of *Lsd1* from a tauopathy mouse model. If pTau-mediated neurodegeneration works through LSD1 sequestration, then limiting the LSD1 pool by removing half its genetic load should decrease the time it takes to reduce the nuclear LSD1 pool below a critical level that causes neuronal cell death. I predict that if these mice display this synergistic phenotype, the molecular signature of the neuronal cell death should match that documented here in *Lsd1*^{CAGG} mice. Furthermore, the biochemical interaction between LSD1 and pTau will need to be explored. It remains to be seen how they interact and what leads to this interaction. I have proposed here that lysine methylation on Tau could recruit LSD1 to Tau in the cytoplasm where it gets sequestered by aggregated forms of Tau. We are currently testing this model.

4.5 Figures

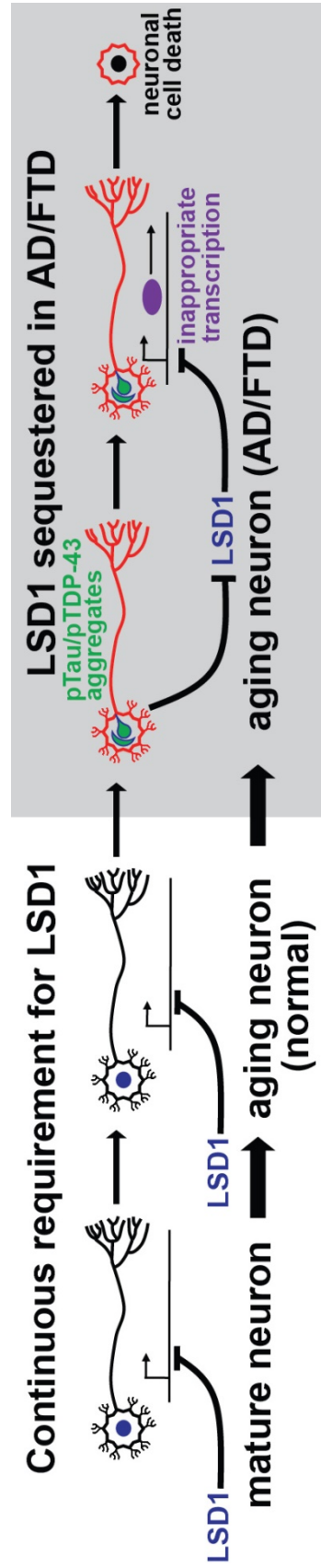


Figure 4-1| Model of LSD1-mediated human neurodegeneration

LSD1 (blue) is continuously required throughout the lifetime of healthy individuals to repress inappropriate transcription in terminally differentiated neurons. In AD and FTD, LSD1 is inhibited through sequestration in the cytoplasm by pTau and pTDP-43 aggregates (green). This results in the inappropriate transcription of genes that would normally be repressed by LSD1, leading to neuronal cell death.

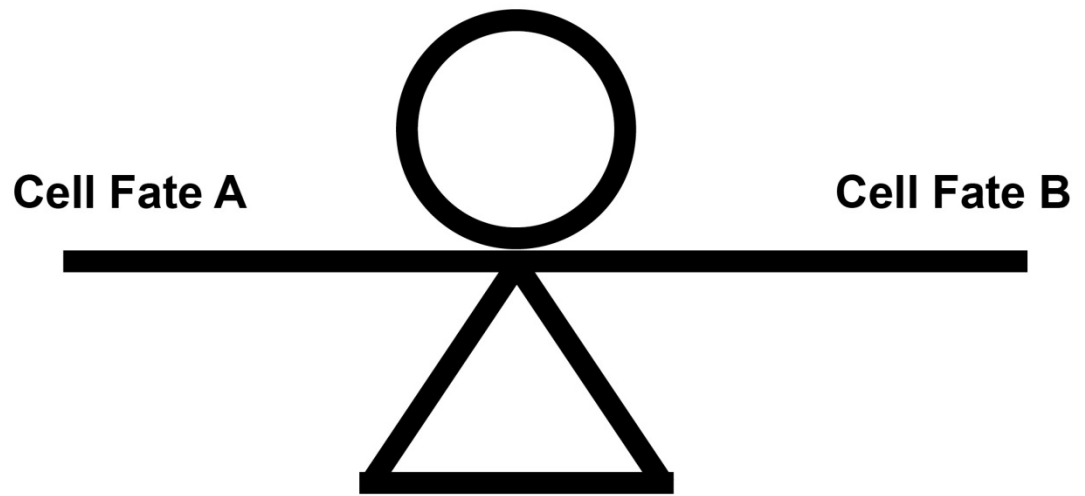
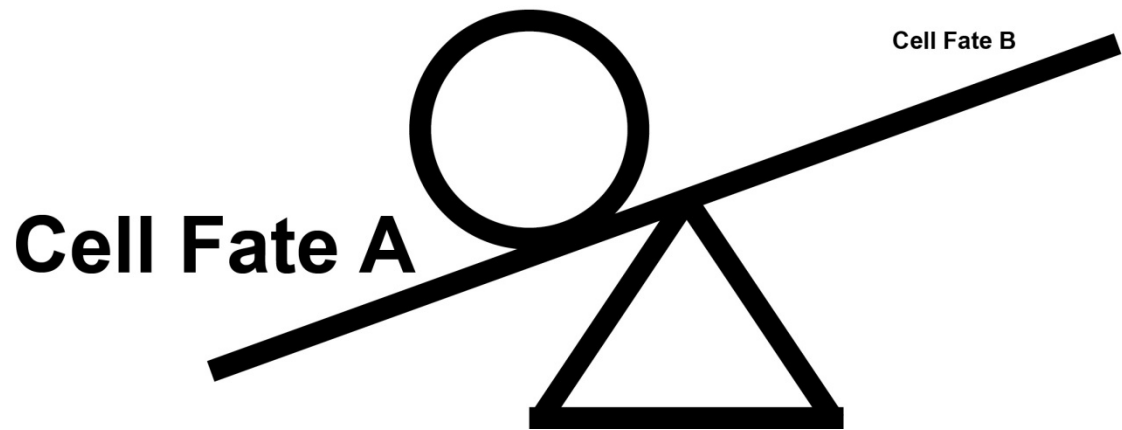
A**Undifferentiated****B****Differentiation**

Figure 4-2 | New model Waddington's epigenetic landscape

Waddington's model of the epigenetic landscape depicted a differentiating cell being analogous to a ball rolling down a hill. In this analogy, the hill is fixed and the differentiated state is what applies the force to the ball. In this new model of differentiation, the ball begins in the center of balanced plane (A) and has the potential to differentiate into one of two cell types, A or B, when forces are applied that shift the balance of the plane and allow the ball to roll to one side. In this example, the epigenetic landscape has shifted toward cell type A. This is achieved through the combination of upregulating factors that promote cell type A and repressing factors that promote cell type B through epigenetic regulation.

REFERENCES

- Adamo, A., Sese, B., Boue, S., Castano, J., Paramonov, I., Barrero, M.J., and Izpisua Belmonte, J.C. (2011). LSD1 regulates the balance between self-renewal and differentiation in human embryonic stem cells. *Nat Cell Biol* 13, 652-659.
- Ahmed, Z., Mackenzie, I.R., Hutton, M.L., and Dickson, D.W. (2007). Progranulin in frontotemporal lobar degeneration and neuroinflammation. *Journal of neuroinflammation* 4, 7.
- Amir, R.E., Van den Veyver, I.B., Wan, M., Tran, C.Q., Francke, U., and Zoghbi, H.Y. (1999). Rett syndrome is caused by mutations in X-linked MECP2, encoding methyl-CpG-binding protein 2. *Nature genetics* 23, 185-188.
- Arriagada, P.V., Growdon, J.H., Hedley-Whyte, E.T., and Hyman, B.T. (1992). Neurofibrillary tangles but not senile plaques parallel duration and severity of Alzheimer's disease. *Neurology* 42, 631-639.
- Ashley, C.T., Jr., Wilkinson, K.D., Reines, D., and Warren, S.T. (1993a). FMR1 protein: conserved RNP family domains and selective RNA binding. *Science* 262, 563-566.
- Ashley, C.T., Sutcliffe, J.S., Kunst, C.B., Leiner, H.A., Eichler, E.E., Nelson, D.L., and Warren, S.T. (1993b). Human and murine FMR-1: alternative splicing and translational initiation downstream of the CGG-repeat. *Nature genetics* 4, 244-251.
- Ausio, J., Dong, F., and van Holde, K.E. (1989). Use of selectively trypsinized nucleosome core particles to analyze the role of the histone "tails" in the stabilization of the nucleosome. *Journal of molecular biology* 206, 451-463.
- Bai, B., Hales, C.M., Chen, P.C., Gozal, Y., Dammer, E.B., Fritz, J.J., Wang, X., Xia, Q., Duong, D.M., Street, C., *et al.* (2013). U1 small nuclear ribonucleoprotein complex and RNA splicing

alterations in Alzheimer's disease. Proceedings of the National Academy of Sciences of the United States of America *110*, 16562-16567.

Baker, M., Mackenzie, I.R., Pickering-Brown, S.M., Gass, J., Rademakers, R., Lindholm, C., Snowden, J., Adamson, J., Sadovnick, A.D., Rollinson, S., *et al.* (2006). Mutations in progranulin cause tau-negative frontotemporal dementia linked to chromosome 17. *Nature* *442*, 916-919.

Ballas, N., Battaglioli, E., Atouf, F., Andres, M.E., Chenoweth, J., Anderson, M.E., Burger, C., Moniwa, M., Davie, J.R., Bowers, W.J., *et al.* (2001). Regulation of neuronal traits by a novel transcriptional complex. *Neuron* *31*, 353-365.

Ballas, N., Grunseich, C., Lu, D.D., Speh, J.C., and Mandel, G. (2005). REST and its corepressors mediate plasticity of neuronal gene chromatin throughout neurogenesis. *Cell* *121*, 645-657.

Barnes, C.A., Nadel, L., and Honig, W.K. (1980). Spatial memory deficit in senescent rats. *Canadian journal of psychology* *34*, 29-39.

Bertram, L., Lill, C.M., and Tanzi, R.E. (2010). The genetics of Alzheimer disease: back to the future. *Neuron* *68*, 270-281.

Bramblett, G.T., Goedert, M., Jakes, R., Merrick, S.E., Trojanowski, J.Q., and Lee, V.M. (1993). Abnormal tau phosphorylation at Ser396 in Alzheimer's disease recapitulates development and contributes to reduced microtubule binding. *Neuron* *10*, 1089-1099.

Brockdorff, N., Ashworth, A., Kay, G.F., McCabe, V.M., Norris, D.P., Cooper, P.J., Swift, S., and Rastan, S. (1992). The product of the mouse Xist gene is a 15 kb inactive X-specific transcript containing no conserved ORF and located in the nucleus. *Cell* *71*, 515-526.

Brown, C.J., Hendrich, B.D., Rupert, J.L., Lafreniere, R.G., Xing, Y., Lawrence, J., and Willard, H.F. (1992). The human XIST gene: analysis of a 17 kb inactive X-specific RNA that contains conserved repeats and is highly localized within the nucleus. *Cell* 71, 527-542.

Busser, J., Geldmacher, D.S., and Herrup, K. (1998). Ectopic cell cycle proteins predict the sites of neuronal cell death in Alzheimer's disease brain. *J Neurosci* 18, 2801-2807.

Cameron, B., and Landreth, G.E. (2010). Inflammation, microglia, and Alzheimer's disease. *Neurobiol Dis* 37, 503-509.

Campbell, K.H., McWhir, J., Ritchie, W.A., and Wilmut, I. (1996). Sheep cloned by nuclear transfer from a cultured cell line. *Nature* 380, 64-66.

Chen-Plotkin, A.S., Geser, F., Plotkin, J.B., Clark, C.M., Kwong, L.K., Yuan, W., Grossman, M., Van Deerlin, V.M., Trojanowski, J.Q., and Lee, V.M. (2008). Variations in the progranulin gene affect global gene expression in frontotemporal lobar degeneration. *Human molecular genetics* 17, 1349-1362.

Chong, J.A., Tapia-Ramirez, J., Kim, S., Toledo-Aral, J.J., Zheng, Y., Boutros, M.C., Altshuler, Y.M., Frohman, M.A., Kraner, S.D., and Mandel, G. (1995). REST: a mammalian silencer protein that restricts sodium channel gene expression to neurons. *Cell* 80, 949-957.

Clemson, C.M., McNeil, J.A., Willard, H.F., and Lawrence, J.B. (1996). XIST RNA paints the inactive X chromosome at interphase: evidence for a novel RNA involved in nuclear/chromosome structure. *J Cell Biol* 132, 259-275.

Coffee, B., Zhang, F., Ceman, S., Warren, S.T., and Reines, D. (2002). Histone modifications depict an aberrantly heterochromatinized FMR1 gene in fragile x syndrome. *American journal of human genetics* 71, 923-932.

- Coffee, B., Zhang, F., Warren, S.T., and Reines, D. (1999). Acetylated histones are associated with FMR1 in normal but not fragile X-syndrome cells. *Nature genetics* 22, 98-101.
- Cohen, T.J., Guo, J.L., Hurtado, D.E., Kwong, L.K., Mills, I.P., Trojanowski, J.Q., and Lee, V.M. (2011). The acetylation of tau inhibits its function and promotes pathological tau aggregation. *Nat Commun* 2, 252.
- Colak, D., Zaninovic, N., Cohen, M.S., Rosenwaks, Z., Yang, W.Y., Gerhardt, J., Disney, M.D., and Jaffrey, S.R. (2014). Promoter-bound trinucleotide repeat mRNA drives epigenetic silencing in fragile X syndrome. *Science* 343, 1002-1005.
- Corder, E.H., Saunders, A.M., Strittmatter, W.J., Schmechel, D.E., Gaskell, P.C., Small, G.W., Roses, A.D., Haines, J.L., and Pericak-Vance, M.A. (1993). Gene dose of apolipoprotein E type 4 allele and the risk of Alzheimer's disease in late onset families. *Science* 261, 921-923.
- Coulondre, C., Miller, J.H., Farabaugh, P.J., and Gilbert, W. (1978). Molecular basis of base substitution hotspots in *Escherichia coli*. *Nature* 274, 775-780.
- Cruts, M., Gijssels, I., van der Zee, J., Engelborghs, S., Wils, H., Pirici, D., Rademakers, R., Vandenberghe, R., Dermaut, B., Martin, J.J., *et al.* (2006). Null mutations in progranulin cause ubiquitin-positive frontotemporal dementia linked to chromosome 17q21. *Nature* 442, 920-924.
- Dai, C., Liang, D., Li, H., Sasaki, M., Dawson, T.M., and Dawson, V.L. (2010). Functional identification of neuroprotective molecules. *PloS one* 5, e15008.
- Deal, R.B., and Henikoff, S. (2010). A simple method for gene expression and chromatin profiling of individual cell types within a tissue. *Developmental cell* 18, 1030-1040.

Di Stefano, L., Ji, J.Y., Moon, N.S., Herr, A., and Dyson, N. (2007). Mutation of *Drosophila* Lsd1 disrupts H3-K4 methylation, resulting in tissue-specific defects during development. *Curr Biol* 17, 808-812.

Dou, Y., Milne, T.A., Tackett, A.J., Smith, E.R., Fukuda, A., Wysocka, J., Allis, C.D., Chait, B.T., Hess, J.L., and Roeder, R.G. (2005). Physical association and coordinate function of the H3 K4 methyltransferase MLL1 and the H4 K16 acetyltransferase MOF. *Cell* 121, 873-885.

Drechsel, D.N., Hyman, A.A., Cobb, M.H., and Kirschner, M.W. (1992). Modulation of the dynamic instability of tubulin assembly by the microtubule-associated protein tau. *Molecular biology of the cell* 3, 1141-1154.

Duteil, D., Metzger, E., Willmann, D., Karagianni, P., Friedrichs, N., Greschik, H., Gunther, T., Buettner, R., Talianidis, I., Metzger, D., *et al.* (2014). LSD1 promotes oxidative metabolism of white adipose tissue. *Nat Commun* 5, 4093.

Eiges, R., Urbach, A., Malcov, M., Frumkin, T., Schwartz, T., Amit, A., Yaron, Y., Eden, A., Yanuka, O., Benvenisty, N., *et al.* (2007). Developmental study of fragile X syndrome using human embryonic stem cells derived from preimplantation genetically diagnosed embryos. *Cell stem cell* 1, 568-577.

Esch, F.S., Keim, P.S., Beattie, E.C., Blacher, R.W., Culwell, A.R., Oltersdorf, T., McClure, D., and Ward, P.J. (1990). Cleavage of amyloid beta peptide during constitutive processing of its precursor. *Science* 248, 1122-1124.

Falcon, S., and Gentleman, R. (2007). Using GOstats to test gene lists for GO term association. *Bioinformatics* 23, 257-258.

- Farr, T.D., and Whishaw, I.Q. (2002). Quantitative and qualitative impairments in skilled reaching in the mouse (*Mus musculus*) after a focal motor cortex stroke. *Stroke; a journal of cerebral circulation* 33, 1869-1875.
- Feng, J., Zhou, Y., Campbell, S.L., Le, T., Li, E., Sweatt, J.D., Silva, A.J., and Fan, G. (2010). Dnmt1 and Dnmt3a maintain DNA methylation and regulate synaptic function in adult forebrain neurons. *Nat Neurosci* 13, 423-430.
- Fisch, G.S., Simensen, R.J., and Schroer, R.J. (2002). Longitudinal changes in cognitive and adaptive behavior scores in children and adolescents with the fragile X mutation or autism. *Journal of autism and developmental disorders* 32, 107-114.
- Frost, B., Hemberg, M., Lewis, J., and Feany, M.B. (2014). Tau promotes neurodegeneration through global chromatin relaxation. *Nat Neurosci* 17, 357-366.
- Fu, Y.H., Kuhl, D.P., Pizzuti, A., Pieretti, M., Sutcliffe, J.S., Richards, S., Verkerk, A.J., Holden, J.J., Fenwick, R.G., Jr., Warren, S.T., *et al.* (1991). Variation of the CGG repeat at the fragile X site results in genetic instability: resolution of the Sherman paradox. *Cell* 67, 1047-1058.
- Funk, K.E., Thomas, S.N., Schafer, K.N., Cooper, G.L., Liao, Z., Clark, D.J., Yang, A.J., and Kuret, J. (2014). Lysine methylation is an endogenous post-translational modification of tau protein in human brain and a modulator of aggregation propensity. *The Biochemical journal* 462, 77-88.
- Gabel, H.W., Kinde, B., Stroud, H., Gilbert, C.S., Harmin, D.A., Kastan, N.R., Hemberg, M., Ebert, D.H., and Greenberg, M.E. (2015). Disruption of DNA-methylation-dependent long gene repression in Rett syndrome. *Nature* 522, 89-93.

- Gallardo, T., Shirley, L., John, G.B., and Castrillon, D.H. (2007). Generation of a germ cell-specific mouse transgenic Cre line, Vasa-Cre. *Genesis* 45, 413-417.
- Gentleman, R.C., Carey, V.J., Bates, D.M., Bolstad, B., Dettling, M., Dudoit, S., Ellis, B., Gautier, L., Ge, Y., Gentry, J., *et al.* (2004). Bioconductor: open software development for computational biology and bioinformatics. *Genome biology* 5, R80.
- Gjoneska, E., Pfenning, A.R., Mathys, H., Quon, G., Kundaje, A., Tsai, L.H., and Kellis, M. (2015). Conserved epigenomic signals in mice and humans reveal immune basis of Alzheimer's disease. *Nature* 518, 365-369.
- Glenner, G.G., and Wong, C.W. (1984). Alzheimer's disease and Down's syndrome: sharing of a unique cerebrovascular amyloid fibril protein. *Biochem Biophys Res Commun* 122, 1131-1135.
- Goldberg, A.D., Allis, C.D., and Bernstein, E. (2007). Epigenetics: a landscape takes shape. *Cell* 128, 635-638.
- Greer, E.L., and Shi, Y. (2012). Histone methylation: a dynamic mark in health, disease and inheritance. *Nature reviews Genetics* 13, 343-357.
- Gurdon, J.B., Elsdale, T.R., and Fischberg, M. (1958). Sexually mature individuals of *Xenopus laevis* from the transplantation of single somatic nuclei. *Nature* 182, 64-65.
- Gurney, M.E., Pu, H., Chiu, A.Y., Dal Canto, M.C., Polchow, C.Y., Alexander, D.D., Caliendo, J., Hentati, A., Kwon, Y.W., Deng, H.X., *et al.* (1994). Motor neuron degeneration in mice that express a human Cu,Zn superoxide dismutase mutation. *Science* 264, 1772-1775.
- Guy, J., Gan, J., Selfridge, J., Cobb, S., and Bird, A. (2007). Reversal of neurological defects in a mouse model of Rett syndrome. *Science* 315, 1143-1147.

Guyenet, S.J., Furrer, S.A., Damian, V.M., Baughan, T.D., La Spada, A.R., and Garden, G.A. (2010). A simple composite phenotype scoring system for evaluating mouse models of cerebellar ataxia. *Journal of visualized experiments : JoVE*.

Hagberg, B., Aicardi, J., Dias, K., and Ramos, O. (1983). A progressive syndrome of autism, dementia, ataxia, and loss of purposeful hand use in girls: Rett's syndrome: report of 35 cases. *Ann Neurol* 14, 471-479.

Hanahan, D., and Weinberg, R.A. (2011). Hallmarks of cancer: the next generation. *Cell* 144, 646-674.

Hanson, J.E., and Madison, D.V. (2007). Presynaptic FMR1 genotype influences the degree of synaptic connectivity in a mosaic mouse model of fragile X syndrome. *J Neurosci* 27, 4014-4018.

Hassig, C.A., Fleischer, T.C., Billin, A.N., Schreiber, S.L., and Ayer, D.E. (1997). Histone deacetylase activity is required for full transcriptional repression by mSin3A. *Cell* 89, 341-347.

Hayashi, S., and McMahon, A.P. (2002). Efficient recombination in diverse tissues by a tamoxifen-inducible form of Cre: a tool for temporally regulated gene activation/inactivation in the mouse. *Developmental biology* 244, 305-318.

He, Y.F., Li, B.Z., Li, Z., Liu, P., Wang, Y., Tang, Q., Ding, J., Jia, Y., Chen, Z., Li, L., *et al.* (2011). Tet-mediated formation of 5-carboxylcytosine and its excision by TDG in mammalian DNA. *Science* 333, 1303-1307.

Hon, G.C., Rajagopal, N., Shen, Y., McCleary, D.F., Yue, F., Dang, M.D., and Ren, B. (2013). Epigenetic memory at embryonic enhancers identified in DNA methylation maps from adult mouse tissues. *Nature genetics* 45, 1198-1206.

Huang, J., Sengupta, R., Espejo, A.B., Lee, M.G., Dorsey, J.A., Richter, M., Opravil, S., Shiekhatar, R., Bedford, M.T., Jenuwein, T., *et al.* (2007). p53 is regulated by the lysine demethylase LSD1. *Nature* 449, 105-108.

Huang, Y. (2006). Molecular and cellular mechanisms of apolipoprotein E4 neurotoxicity and potential therapeutic strategies. *Current opinion in drug discovery & development* 9, 627-641.

Hughes, C.M., Rozenblatt-Rosen, O., Milne, T.A., Copeland, T.D., Levine, S.S., Lee, J.C., Hayes, D.N., Shanmugam, K.S., Bhattacharjee, A., Biondi, C.A., *et al.* (2004). Menin associates with a trithorax family histone methyltransferase complex and with the *hoxc8* locus. *Mol Cell* 13, 587-597.

Ito, S., Shen, L., Dai, Q., Wu, S.C., Collins, L.B., Swenberg, J.A., He, C., and Zhang, Y. (2011). Tet proteins can convert 5-methylcytosine to 5-formylcytosine and 5-carboxylcytosine. *Science* 333, 1300-1303.

Jawhar, S., Trawicka, A., Jenneckens, C., Bayer, T.A., and Wirths, O. (2012). Motor deficits, neuron loss, and reduced anxiety coinciding with axonal degeneration and intraneuronal A β aggregation in the 5XFAD mouse model of Alzheimer's disease. *Neurobiol Aging* 33, 196 e129-140.

Jenuwein, T., and Allis, C.D. (2001). Translating the histone code. *Science* 293, 1074-1080.

Jeon, Y., and Lee, J.T. (2011). YY1 tethers Xist RNA to the inactive X nucleation center. *Cell* 146, 119-133.

Jiang, D., Yang, W., He, Y., and Amasino, R.M. (2007). Arabidopsis relatives of the human lysine-specific Demethylase1 repress the expression of FWA and FLOWERING LOCUS C and thus promote the floral transition. *Plant Cell* 19, 2975-2987.

- Kang, J., Lemaire, H.G., Unterbeck, A., Salbaum, J.M., Masters, C.L., Grzeschik, K.H., Multhaup, G., Beyreuther, K., and Muller-Hill, B. (1987). The precursor of Alzheimer's disease amyloid A4 protein resembles a cell-surface receptor. *Nature* *325*, 733-736.
- Katz, D.J., Edwards, T.M., Reinke, V., and Kelly, W.G. (2009). A *C. elegans* LSD1 demethylase contributes to germline immortality by reprogramming epigenetic memory. *Cell* *137*, 308-320.
- Kerenyi, M.A., Shao, Z., Hsu, Y.J., Guo, G., Luc, S., O'Brien, K., Fujiwara, Y., Peng, C., Nguyen, M., and Orkin, S.H. (2013). Histone demethylase Lsd1 represses hematopoietic stem and progenitor cell signatures during blood cell maturation. *Elife* *2*, e00633.
- Kim, D., Pertea, G., Trapnell, C., Pimentel, H., Kelley, R., and Salzberg, S.L. (2013). TopHat2: accurate alignment of transcriptomes in the presence of insertions, deletions and gene fusions. *Genome biology* *14*, R36.
- Kishi, N., and Macklis, J.D. (2004). MECP2 is progressively expressed in post-migratory neurons and is involved in neuronal maturation rather than cell fate decisions. *Molecular and cellular neurosciences* *27*, 306-321.
- Kleim, J.A., Barbay, S., and Nudo, R.J. (1998). Functional reorganization of the rat motor cortex following motor skill learning. *Journal of neurophysiology* *80*, 3321-3325.
- Laherty, C.D., Yang, W.M., Sun, J.M., Davie, J.R., Seto, E., and Eisenman, R.N. (1997). Histone deacetylases associated with the mSin3 corepressor mediate mad transcriptional repression. *Cell* *89*, 349-356.
- Laible, P.D., Greenfield, S.R., Wasielewski, M.R., Hansen, D.K., and Pearlstein, R.M. (1997). Antenna excited state decay kinetics establish primary electron transfer in reaction centers as heterogeneous. *Biochemistry* *36*, 8677-8685.

Lambert, J.C., and Amouyel, P. (2007). Genetic heterogeneity of Alzheimer's disease: complexity and advances. *Psychoneuroendocrinology* 32 *Suppl 1*, S62-70.

Lambrot, R., Lafleur, C., and Kimmins, S. (2015). The histone demethylase KDM1A is essential for the maintenance and differentiation of spermatogonial stem cells and progenitors. *FASEB journal : official publication of the Federation of American Societies for Experimental Biology* 29, 4402-4416.

Lawrence, M., Gentleman, R., and Carey, V. (2009). rtracklayer: an R package for interfacing with genome browsers. *Bioinformatics* 25, 1841-1842.

Lee, J.H., and Skalnik, D.G. (2005). CpG-binding protein (CXXC finger protein 1) is a component of the mammalian Set1 histone H3-Lys4 methyltransferase complex, the analogue of the yeast Set1/COMPASS complex. *The Journal of biological chemistry* 280, 41725-41731.

Lee, M.G., Villa, R., Trojer, P., Norman, J., Yan, K.P., Reinberg, D., Di Croce, L., and Shiekhatar, R. (2007). Demethylation of H3K27 regulates polycomb recruitment and H2A ubiquitination. *Science* 318, 447-450.

Lee, M.G., Wynder, C., Cooch, N., and Shiekhatar, R. (2005). An essential role for CoREST in nucleosomal histone 3 lysine 4 demethylation. *Nature* 437, 432-435.

Leonhardt, H., Page, A.W., Weier, H.U., and Bestor, T.H. (1992). A targeting sequence directs DNA methyltransferase to sites of DNA replication in mammalian nuclei. *Cell* 71, 865-873.

Lewis, J.D., Meehan, R.R., Henzel, W.J., Maurer-Fogy, I., Jeppesen, P., Klein, F., and Bird, A. (1992). Purification, sequence, and cellular localization of a novel chromosomal protein that binds to methylated DNA. *Cell* 69, 905-914.

- Lin, M.T., and Beal, M.F. (2006). Mitochondrial dysfunction and oxidative stress in neurodegenerative diseases. *Nature* 443, 787-795.
- Lister, R., Mukamel, E.A., Nery, J.R., Urich, M., Puddifoot, C.A., Johnson, N.D., Lucero, J., Huang, Y., Dwork, A.J., Schultz, M.D., *et al.* (2013). Global epigenomic reconfiguration during mammalian brain development. *Science* 341, 1237905.
- Lister, R., Pelizzola, M., Dowen, R.H., Hawkins, R.D., Hon, G., Tonti-Filippini, J., Nery, J.R., Lee, L., Ye, Z., Ngo, Q.M., *et al.* (2009). Human DNA methylomes at base resolution show widespread epigenomic differences. *Nature* 462, 315-322.
- Lu, T., Aron, L., Zullo, J., Pan, Y., Kim, H., Chen, Y., Yang, T.H., Kim, H.M., Drake, D., Liu, X.S., *et al.* (2014). REST and stress resistance in ageing and Alzheimer's disease. *Nature* 507, 448-454.
- Lyons, D.B., Allen, W.E., Goh, T., Tsai, L., Barnea, G., and Lomvardas, S. (2013). An epigenetic trap stabilizes singular olfactory receptor expression. *Cell* 154, 325-336.
- Macfarlan, T.S., Gifford, W.D., Agarwal, S., Driscoll, S., Lettieri, K., Wang, J., Andrews, S.E., Franco, L., Rosenfeld, M.G., Ren, B., *et al.* (2011). Endogenous retroviruses and neighboring genes are coordinately repressed by LSD1/KDM1A. *Genes & development* 25, 594-607.
- Mahadevan, L.C., Willis, A.C., and Barratt, M.J. (1991). Rapid histone H3 phosphorylation in response to growth factors, phorbol esters, okadaic acid, and protein synthesis inhibitors. *Cell* 65, 775-783.
- Masters, C.L., Multhaup, G., Simms, G., Pottgiesser, J., Martins, R.N., and Beyreuther, K. (1985). Neuronal origin of a cerebral amyloid: neurofibrillary tangles of Alzheimer's disease contain the same protein as the amyloid of plaque cores and blood vessels. *Embo J* 4, 2757-2763.

- Metzger, E., Wissmann, M., Yin, N., Muller, J.M., Schneider, R., Peters, A.H., Gunther, T., Buettner, R., and Schule, R. (2005). LSD1 demethylates repressive histone marks to promote androgen-receptor-dependent transcription. *Nature* 437, 436-439.
- Mo, A., Mukamel, E.A., Davis, F.P., Luo, C., Henry, G.L., Picard, S., Urich, M.A., Nery, J.R., Sejnowski, T.J., Lister, R., *et al.* (2015). Epigenomic Signatures of Neuronal Diversity in the Mammalian Brain. *Neuron* 86, 1369-1384.
- Morris, M., Maeda, S., Vossel, K., and Mucke, L. (2011). The many faces of tau. *Neuron* 70, 410-426.
- Nady, N., Lemak, A., Walker, J.R., Avvakumov, G.V., Karetka, M.S., Achour, M., Xue, S., Duan, S., Allali-Hassani, A., Zuo, X., *et al.* (2011). Recognition of multivalent histone states associated with heterochromatin by UHRF1 protein. *The Journal of biological chemistry* 286, 24300-24311.
- Nagy, L., Kao, H.Y., Chakravarti, D., Lin, R.J., Hassig, C.A., Ayer, D.E., Schreiber, S.L., and Evans, R.M. (1997). Nuclear receptor repression mediated by a complex containing SMRT, mSin3A, and histone deacetylase. *Cell* 89, 373-380.
- Nakamura, T., Mori, T., Tada, S., Krajewski, W., Rozovskaia, T., Wassell, R., Dubois, G., Mazo, A., Croce, C.M., and Canaani, E. (2002). ALL-1 is a histone methyltransferase that assembles a supercomplex of proteins involved in transcriptional regulation. *Mol Cell* 10, 1119-1128.
- Nam, H.J., Boo, K., Kim, D., Han, D.H., Choe, H.K., Kim, C.R., Sun, W., Kim, H., Kim, K., Lee, H., *et al.* (2014). Phosphorylation of LSD1 by PKCalpha is crucial for circadian rhythmicity and phase resetting. *Mol Cell* 53, 791-805.

Nan, X., Ng, H.H., Johnson, C.A., Laherty, C.D., Turner, B.M., Eisenman, R.N., and Bird, A. (1998). Transcriptional repression by the methyl-CpG-binding protein MeCP2 involves a histone deacetylase complex. *Nature* 393, 386-389.

Neumann, M., Sampathu, D.M., Kwong, L.K., Truax, A.C., Micsenyi, M.C., Chou, T.T., Bruce, J., Schuck, T., Grossman, M., Clark, C.M., *et al.* (2006). Ubiquitinated TDP-43 in frontotemporal lobar degeneration and amyotrophic lateral sclerosis. *Science* 314, 130-133.

Oakley, H., Cole, S.L., Logan, S., Maus, E., Shao, P., Craft, J., Guillozet-Bongaarts, A., Ohno, M., Disterhoft, J., Van Eldik, L., *et al.* (2006). Intraneuronal beta-amyloid aggregates, neurodegeneration, and neuron loss in transgenic mice with five familial Alzheimer's disease mutations: potential factors in amyloid plaque formation. *J Neurosci* 26, 10129-10140.

Okano, M., Bell, D.W., Haber, D.A., and Li, E. (1999). DNA methyltransferases Dnmt3a and Dnmt3b are essential for de novo methylation and mammalian development. *Cell* 99, 247-257.

Ooi, L., and Wood, I.C. (2007). Chromatin crosstalk in development and disease: lessons from REST. *Nature reviews Genetics* 8, 544-554.

Palop, J.J., Chin, J., and Mucke, L. (2006). A network dysfunction perspective on neurodegenerative diseases. *Nature* 443, 768-773.

Paolicelli, R.C., Bolasco, G., Pagani, F., Maggi, L., Scianni, M., Panzanelli, P., Giustetto, M., Ferreira, T.A., Guiducci, E., Dumas, L., *et al.* (2011). Synaptic pruning by microglia is necessary for normal brain development. *Science* 333, 1456-1458.

Pastor, W.A., Pape, U.J., Huang, Y., Henderson, H.R., Lister, R., Ko, M., McLoughlin, E.M., Brudno, Y., Mahapatra, S., Kapranov, P., *et al.* (2011). Genome-wide mapping of 5-hydroxymethylcytosine in embryonic stem cells. *Nature* 473, 394-397.

- Pekny, M., and Nilsson, M. (2005). Astrocyte activation and reactive gliosis. *Glia* 50, 427-434.
- Pieretti, M., Zhang, F.P., Fu, Y.H., Warren, S.T., Oostra, B.A., Caskey, C.T., and Nelson, D.L. (1991). Absence of expression of the FMR-1 gene in fragile X syndrome. *Cell* 66, 817-822.
- Price, J.L., and Morris, J.C. (1999). Tangles and plaques in nondemented aging and "preclinical" Alzheimer's disease. *Ann Neurol* 45, 358-368.
- Putchá, D., Brickhouse, M., O'Keefe, K., Sullivan, C., Rentz, D., Marshall, G., Dickerson, B., and Sperling, R. (2011). Hippocampal hyperactivation associated with cortical thinning in Alzheimer's disease signature regions in non-demented elderly adults. *J Neurosci* 31, 17680-17688.
- Rademakers, R., and Rovelet-Lecrux, A. (2009). Recent insights into the molecular genetics of dementia. *Trends in neurosciences* 32, 451-461.
- Roopra, A., Qazi, R., Schoenike, B., Daley, T.J., and Morrison, J.F. (2004). Localized domains of G9a-mediated histone methylation are required for silencing of neuronal genes. *Mol Cell* 14, 727-738.
- Rose, N.R., and Klose, R.J. (2014). Understanding the relationship between DNA methylation and histone lysine methylation. *Biochimica et biophysica acta* 1839, 1362-1372.
- Rothbart, S.B., Dickson, B.M., Ong, M.S., Krajewski, K., Houliston, S., Kireev, D.B., Arrowsmith, C.H., and Strahl, B.D. (2013). Multivalent histone engagement by the linked tandem Tudor and PHD domains of UHRF1 is required for the epigenetic inheritance of DNA methylation. *Genes & development* 27, 1288-1298.
- Rudolph, T., Yonezawa, M., Lein, S., Heidrich, K., Kubicek, S., Schafer, C., Phalke, S., Walther, M., Schmidt, A., Jenuwein, T., *et al.* (2007). Heterochromatin formation in *Drosophila* is initiated

through active removal of H3K4 methylation by the LSD1 homolog SU(VAR)3-3. *Mol Cell* 26, 103-115.

Saleque, S., Kim, J., Rooke, H.M., and Orkin, S.H. (2007). Epigenetic regulation of hematopoietic differentiation by Gfi-1 and Gfi-1b is mediated by the cofactors CoREST and LSD1. *Mol Cell* 27, 562-572.

Sangiorgi, E., and Capecchi, M.R. (2008). Bmi1 is expressed in vivo in intestinal stem cells. *Nature genetics* 40, 915-920.

Scharer, C.D., Barwick, B.G., Youngblood, B.A., Ahmed, R., and Boss, J.M. (2013). Global DNA methylation remodeling accompanies CD8 T cell effector function. *Journal of immunology* 191, 3419-3429.

Schoenherr, C.J., and Anderson, D.J. (1995). The neuron-restrictive silencer factor (NRSF): a coordinate repressor of multiple neuron-specific genes. *Science* 267, 1360-1363.

Schule, B., Armstrong, D.D., Vogel, H., Oviedo, A., and Francke, U. (2008). Severe congenital encephalopathy caused by MECP2 null mutations in males: central hypoxia and reduced neuronal dendritic structure. *Clinical genetics* 74, 116-126.

Schultz, D.C., Ayyanathan, K., Negorev, D., Maul, G.G., and Rauscher, F.J., 3rd (2002). SETDB1: a novel KAP-1-associated histone H3, lysine 9-specific methyltransferase that contributes to HP1-mediated silencing of euchromatic genes by KRAB zinc-finger proteins. *Genes & development* 16, 919-932.

Schultz, M.D., He, Y., Whitaker, J.W., Hariharan, M., Mukamel, E.A., Leung, D., Rajagopal, N., Nery, J.R., Urich, M.A., Chen, H., *et al.* (2015). Human body epigenome maps reveal noncanonical DNA methylation variation. *Nature* 523, 212-216.

- Schulz, C., Gomez Perdiguero, E., Chorro, L., Szabo-Rogers, H., Cagnard, N., Kierdorf, K., Prinz, M., Wu, B., Jacobsen, S.E., Pollard, J.W., *et al.* (2012). A lineage of myeloid cells independent of Myb and hematopoietic stem cells. *Science* 336, 86-90.
- Selkoe, D.J. (2002). Alzheimer's disease is a synaptic failure. *Science* 298, 789-791.
- Seward, D.J., Cubberley, G., Kim, S., Schonewald, M., Zhang, L., Tripet, B., and Bentley, D.L. (2007). Demethylation of trimethylated histone H3 Lys4 in vivo by JARID1 JmjC proteins. *Nature structural & molecular biology* 14, 240-242.
- Shen, L., Wu, H., Diep, D., Yamaguchi, S., D'Alessio, A.C., Fung, H.L., Zhang, K., and Zhang, Y. (2013). Genome-wide analysis reveals TET- and TDG-dependent 5-methylcytosine oxidation dynamics. *Cell* 153, 692-706.
- Shi, Y., Lan, F., Matson, C., Mulligan, P., Whetstine, J.R., Cole, P.A., and Casero, R.A. (2004). Histone demethylation mediated by the nuclear amine oxidase homolog LSD1. *Cell* 119, 941-953.
- Skene, P.J., Illingworth, R.S., Webb, S., Kerr, A.R., James, K.D., Turner, D.J., Andrews, R., and Bird, A.P. (2010). Neuronal MeCP2 is expressed at near histone-octamer levels and globally alters the chromatin state. *Mol Cell* 37, 457-468.
- Soufi, A., Donahue, G., and Zaret, K.S. (2012). Facilitators and impediments of the pluripotency reprogramming factors' initial engagement with the genome. *Cell* 151, 994-1004.
- Sperling, R.A., Dickerson, B.C., Pihlajamaki, M., Vannini, P., LaViolette, P.S., Vitolo, O.V., Hedden, T., Becker, J.A., Rentz, D.M., Selkoe, D.J., *et al.* (2010). Functional alterations in memory networks in early Alzheimer's disease. *Neuromolecular Med* 12, 27-43.

Stephan, A.H., Barres, B.A., and Stevens, B. (2012). The complement system: an unexpected role in synaptic pruning during development and disease. *Annu Rev Neurosci* 35, 369-389.

Stevens, B., Allen, N.J., Vazquez, L.E., Howell, G.R., Christopherson, K.S., Nouri, N., Micheva, K.D., Mehalow, A.K., Huberman, A.D., Stafford, B., *et al.* (2007). The classical complement cascade mediates CNS synapse elimination. *Cell* 131, 1164-1178.

Su, S.T., Ying, H.Y., Chiu, Y.K., Lin, F.R., Chen, M.Y., and Lin, K.I. (2009). Involvement of histone demethylase LSD1 in Blimp-1-mediated gene repression during plasma cell differentiation. *Molecular and cellular biology* 29, 1421-1431.

Subramanian, A., Tamayo, P., Mootha, V.K., Mukherjee, S., Ebert, B.L., Gillette, M.A., Paulovich, A., Pomeroy, S.L., Golub, T.R., Lander, E.S., *et al.* (2005). Gene set enrichment analysis: a knowledge-based approach for interpreting genome-wide expression profiles. *Proceedings of the National Academy of Sciences of the United States of America* 102, 15545-15550.

Suzuki, R., and Shimodaira, H. (2006). Pvcust: an R package for assessing the uncertainty in hierarchical clustering. *Bioinformatics* 22, 1540-1542.

Tachibana, M., Sugimoto, K., Nozaki, M., Ueda, J., Ohta, T., Ohki, M., Fukuda, M., Takeda, N., Niida, H., Kato, H., *et al.* (2002). G9a histone methyltransferase plays a dominant role in euchromatic histone H3 lysine 9 methylation and is essential for early embryogenesis. *Genes & development* 16, 1779-1791.

Tahiliani, M., Koh, K.P., Shen, Y., Pastor, W.A., Bandukwala, H., Brudno, Y., Agarwal, S., Iyer, L.M., Liu, D.R., Aravind, L., *et al.* (2009). Conversion of 5-methylcytosine to 5-hydroxymethylcytosine in mammalian DNA by MLL partner TET1. *Science* 324, 930-935.

Takahashi, K., and Yamanaka, S. (2006). Induction of pluripotent stem cells from mouse embryonic and adult fibroblast cultures by defined factors. *Cell* 126, 663-676.

Thomas, S.N., Funk, K.E., Wan, Y., Liao, Z., Davies, P., Kuret, J., and Yang, A.J. (2012). Dual modification of Alzheimer's disease PHF-tau protein by lysine methylation and ubiquitylation: a mass spectrometry approach. *Acta Neuropathol* 123, 105-117.

Trapnell, C., Williams, B.A., Pertea, G., Mortazavi, A., Kwan, G., van Baren, M.J., Salzberg, S.L., Wold, B.J., and Pachter, L. (2010). Transcript assembly and quantification by RNA-Seq reveals unannotated transcripts and isoform switching during cell differentiation. *Nature biotechnology* 28, 511-515.

Tronche, F., Kellendonk, C., Kretz, O., Gass, P., Anlag, K., Orban, P.C., Bock, R., Klein, R., and Schutz, G. (1999). Disruption of the glucocorticoid receptor gene in the nervous system results in reduced anxiety. *Nature genetics* 23, 99-103.

Tsai, M.C., Manor, O., Wan, Y., Mosammamarast, N., Wang, J.K., Lan, F., Shi, Y., Segal, E., and Chang, H.Y. (2010). Long noncoding RNA as modular scaffold of histone modification complexes. *Science* 329, 689-693.

Vassar, R., Bennett, B.D., Babu-Khan, S., Kahn, S., Mendiaz, E.A., Denis, P., Teplow, D.B., Ross, S., Amarante, P., Loeloff, R., *et al.* (1999). Beta-secretase cleavage of Alzheimer's amyloid precursor protein by the transmembrane aspartic protease BACE. *Science* 286, 735-741.

Verheij, C., Bakker, C.E., de Graaff, E., Keulemans, J., Willemsen, R., Verkerk, A.J., Galjaard, H., Reuser, A.J., Hoogeveen, A.T., and Oostra, B.A. (1993). Characterization and localization of the FMR-1 gene product associated with fragile X syndrome. *Nature* 363, 722-724.

- Vetrivel, K.S., Zhang, Y.W., Xu, H., and Thinakaran, G. (2006). Pathological and physiological functions of presenilins. *Molecular neurodegeneration* 1, 4.
- Wang, J., Hevi, S., Kurash, J.K., Lei, H., Gay, F., Bajko, J., Su, H., Sun, W., Chang, H., Xu, G., *et al.* (2009). The lysine demethylase LSD1 (KDM1) is required for maintenance of global DNA methylation. *Nature genetics* 41, 125-129.
- Wang, J., Scully, K., Zhu, X., Cai, L., Zhang, J., Prefontaine, G.G., Krones, A., Ohgi, K.A., Zhu, P., Garcia-Bassets, I., *et al.* (2007). Opposing LSD1 complexes function in developmental gene activation and repression programmes. *Nature* 446, 882-887.
- Wang, J., Telese, F., Tan, Y., Li, W., Jin, C., He, X., Basnet, H., Ma, Q., Merkurjev, D., Zhu, X., *et al.* (2015). LSD1n is an H4K20 demethylase regulating memory formation via transcriptional elongation control. *Nat Neurosci* 18, 1256-1264.
- Wasson, J.A., Simon, A.K., Myrick, D.A., Wolf, G., Driscoll, S., Pfaff, S.L., Macfarlan, T.S., and Katz, D.J. (2016). Maternally provided LSD1/KDM1A enables the maternal-to-zygotic transition and prevents defects that manifest postnatally. *eLife* 5.
- Weick, E.M., and Miska, E.A. (2014). piRNAs: from biogenesis to function. *Development* 141, 3458-3471.
- Wheeler, D.L., Church, D.M., Lash, A.E., Leipe, D.D., Madden, T.L., Pontius, J.U., Schuler, G.D., Schriml, L.M., Tatusova, T.A., Wagner, L., *et al.* (2001). Database resources of the National Center for Biotechnology Information. *Nucleic acids research* 29, 11-16.
- Whitlock, J.P., Jr., and Simpson, R.T. (1977). Localization of the sites along nucleosome DNA which interact with NH₂-terminal histone regions. *The Journal of biological chemistry* 252, 6516-6520.

Whyte, W.A., Bilodeau, S., Orlando, D.A., Hoke, H.A., Frampton, G.M., Foster, C.T., Cowley, S.M., and Young, R.A. (2012). Enhancer decommissioning by LSD1 during embryonic stem cell differentiation. *Nature* 482, 221-225.

Wisniewski, H.M., and Wegiel, J. (1991). Spatial relationships between astrocytes and classical plaque components. *Neurobiol Aging* 12, 593-600.

Wolfe, M.S., Xia, W., Ostaszewski, B.L., Diehl, T.S., Kimberly, W.T., and Selkoe, D.J. (1999). Two transmembrane aspartates in presenilin-1 required for presenilin endoproteolysis and gamma-secretase activity. *Nature* 398, 513-517.

Xiang, Y., Zhu, Z., Han, G., Lin, H., Xu, L., and Chen, C.D. (2007a). JMJD3 is a histone H3K27 demethylase. *Cell research* 17, 850-857.

Xiang, Y., Zhu, Z., Han, G., Ye, X., Xu, B., Peng, Z., Ma, Y., Yu, Y., Lin, H., Chen, A.P., *et al.* (2007b). JARID1B is a histone H3 lysine 4 demethylase up-regulated in prostate cancer. *Proceedings of the National Academy of Sciences of the United States of America* 104, 19226-19231.

Yamane, K., Toumazou, C., Tsukada, Y., Erdjument-Bromage, H., Tempst, P., Wong, J., and Zhang, Y. (2006). JHDM2A, a JmjC-containing H3K9 demethylase, facilitates transcription activation by androgen receptor. *Cell* 125, 483-495.

Yauch, R.L., Gould, S.E., Scales, S.J., Tang, T., Tian, H., Ahn, C.P., Marshall, D., Fu, L., Januario, T., Kallop, D., *et al.* (2008). A paracrine requirement for hedgehog signalling in cancer. *Nature* 455, 406-410.

Yoshiyama, Y., Higuchi, M., Zhang, B., Huang, S.M., Iwata, N., Saido, T.C., Maeda, J., Suhara, T., Trojanowski, J.Q., and Lee, V.M. (2007). Synapse loss and microglial activation precede tangles in a P301S tauopathy mouse model. *Neuron* 53, 337-351.

You, A., Tong, J.K., Grozinger, C.M., and Schreiber, S.L. (2001). CoREST is an integral component of the CoREST- human histone deacetylase complex. *Proceedings of the National Academy of Sciences of the United States of America* 98, 1454-1458.

Zhang, B., Gaiteri, C., Bodea, L.G., Wang, Z., McElwee, J., Podtelezchnikov, A.A., Zhang, C., Xie, T., Tran, L., Dobrin, R., *et al.* (2013). Integrated systems approach identifies genetic nodes and networks in late-onset Alzheimer's disease. *Cell* 153, 707-720.

Zhang, Y., James, M., Middleton, F.A., and Davis, R.L. (2005). Transcriptional analysis of multiple brain regions in Parkinson's disease supports the involvement of specific protein processing, energy metabolism, and signaling pathways, and suggests novel disease mechanisms. *American journal of medical genetics Part B, Neuropsychiatric genetics : the official publication of the International Society of Psychiatric Genetics* 137B, 5-16.

Zhao, J., Sun, B.K., Erwin, J.A., Song, J.J., and Lee, J.T. (2008). Polycomb proteins targeted by a short repeat RNA to the mouse X chromosome. *Science* 322, 750-756.

Zhu, D., Holz, S., Metzger, E., Pavlovic, M., Jandausch, A., Jilg, C., Galgoczy, P., Herz, C., Moser, M., Metzger, D., *et al.* (2014). Lysine-specific demethylase 1 regulates differentiation onset and migration of trophoblast stem cells. *Nat Commun* 5, 3174.